



**T.C.**

**ÇANAKKALE ONSEKİZ MART UNIVERSITY  
SCHOOL OF GRADUATE STUDIES**

**DEPARTMENT OF MOLECULAR BIOLOGY AND GENETIC**

**INVESTIGATE OF THE GENETIC PROCESSES THAT CONTROL THE  
ADVENTITIOUS ROOTING OF OLIVE (*OLEA EUROPAEA* L.) CUTTINGS.**

**MASTER OF SCIENCE THESIS**

**Cansu KARAKURT**

**Thesis Supervisor**

**Prof. Dr. Kemal Melih TAŞKIN**

**ÇANAKKALE – 2023**





T.C.

ÇANAKKALE ONSEKİZ MART UNIVERSITY  
SCHOOL OF GRADUATE STUDIES

DEPARTMENT OF MOLECULAR BIOLOGY AND GENETIC

**Investigate of the Genetic Processes that Control the Adventitious Rooting of Olive  
(*Olea europaea* L.) Cuttings.**

MASTER OF SCIENCE THESIS

Cansu KARAKURT

Thesis Supervisor

Prof. Dr. Kemal Melih TAŞKIN

This study has been supported by The Scientific and Technological Research Council of  
Türkiye

Project No:119Z924

ÇANAKKALE – 2023

## ETİK BEYAN

Çanakkale Onsekiz Mart Üniversitesi Lisansüstü Eğitim Enstitüsü Tez Yazım Kuralları'na uygun olarak hazırladığım bu tez çalışmada; tez içinde sunduğum verileri, bilgileri ve dokümanları akademik ve etik kurallar çerçevesinde elde ettiğimi, tüm bilgi, belge, değerlendirme ve sonuçları bilimsel etik ve ahlak kurallarına uygun olarak sunduğumu, tez çalışmada yararlandığım eserlerin tümüne uygun atıfta bulunarak kaynak gösterdiğimi, kullanılan verilerde herhangi bir değişiklik yapmadığımı, bu tezde sunduğum çalışmanın özgün olduğunu, bildirir, aksi bir durumda aleyhime doğabilecek tüm hak kayıplarını kabullendiğimi taahhüt ve beyan ederim.

I declare that all the information and results offered in visual, audio, and written form are obtained by myself observing the academic and ethical rules. Moreover, all other results and information referred in the thesis but not specific to this study are cited.

Cansu KARAKURT

19/07/2023

## ACKNOWLEDGEMENTS

I would like to express my sincere gratitude to my supervisor, Prof. Dr. Kemal Melih TAŞKIN, for guidance and support throughout my thesis. Expertise and mentorship have been invaluable and I am grateful for the opportunity to work under your supervision.

I would like to thank Dr. Fatih SEZER and Dr. Aslıhan ÖZBİLEN, who patiently taught me everything and encouraged me to study.

I would like to extend my sincere gratitude to the thesis committee and the members of the jury for their attention and time.

I would like to thank my lovely friends Kübra ÖZTÜRK, Buket ÜNER, and Göktuğ SERBEZLER for their unwavering support, belief in me, and ability to enjoy my day. I would also like to KMTLAB team Ali, İrem, Ezgi and Hasan, Doğukan, Celal who never stop helping me during my thesis.

I would like to express my sincere gratitude to my parents, Erdinç and Nalan Karakurt, for always believing in and supporting me. I would also like to thank my brother Mümin KARAKURT and my cousin Emine KARAKURT for supporting me and for having faith in me during my thesis.

I would like to thank The Scientific and Technological Research Council of Turkey for their financial support (Project No: 119Z924).

Cansu KARAKURT  
Çanakkale, Temmuz 2023

## ÖZET

### ZEYTİN (*OLEA EUROPAEA* L.) ÇELİKLERİNİN ADVENTİF KÖK OLUŞUMUNU KONTROL EDEN GENETİK SÜREÇLERİN ARAŞTIRILMASI

Cansu KARAKURT

Çanakkale Onsekiz Mart Üniversitesi

Lisansüstü Eğitim Enstitüsü

Moleküler Biyoloji ve Genetik Anabilim Dalı Yüksek Lisans Yeterlik Tezi

Danışman: Prof. Dr. Kemal Melih TAŞKIN

19/07/2023, 70

Ekonomik olarak önemli bir tarım ürünü olan zeytin (*Olea europaea* L.), seksüel ve aseksüel yöntemlerle çoğaltılmıştır. Günümüzde zeytin genellikle çelik ile üretilmektedir ancak bu yöntemin başarısı micro-çeliklerin adventif kök oluşturma kapasitesine bağlıdır. Adventif kök (AR) oluşumu çelikle vejetatif üremede önemli bir yere sahiptir. AR, gövdeler, yapraklar ve hatta kotiledonlar gibi çeşitli kök dışı dokulardan yeni kök oluşumunu içermektedir. Farklı zeytin çeşitleri, vejetatif çoğaltmada farklı derecelerde köklenme yetisine sahip olabilir. Domat gibi ekonomik önemi olan bazı çeşitler köklenme oranlarının düşük olması sebebiyle çelik ile üretilmemektedir. Bu nedenle bu çalışmada zeytinin çelikle üretiminde standart olarak kullanılan oksin uygulamasına zeytin çeşitlerinin neden farklı cevaplar verdiği ile ilgili genlerden bazıları araştırılmıştır. Bu amaçla, kolay köklenen Gemlik ve zor köklenen Domat çeşitlerinde adventif kök oluşumunda görev alan bazı genlerin (*AOX2*, *IBR1*, *IBR3*, *IBR10* ve *PtAIL1*) karakterizasyonu, IBA, NAA ve IBA+NAA uygulanmış mikro çeliklerinde gen anlatım çalışmaları yapılmış ve transkript dizileri biyoinformatik olarak karşılaştırılmıştır. Çalışmada *A. thaliana* türünden alınan referans protein dizileri, gen ortologlarını tanımlamak için kullanılmıştır. Protein dizileri TAIR veri tabanından indirilerek Geneious yazılımında zeytin protein veri tabanına karşı Blastp analizinde kullanılmıştır. Blast analizi sonucunda elde edilen diziler Geneious yazılımında hizalanmış ve filogenetik ağaçlar oluşturulmuştur. hormon uygulaması sonrasında kolay köklenen ve zor köklenen zeytin çeşitlerinde farklı gen anlatım profilleri gözlemlenmiştir. Çalışmada elde edilen sonuçlar her iki çeşitte de IBA uygulaması sonucu *OeIBR10* geninin anlatımının ilk 24 saate arttığını gösterirken, 15. günde kolay köklenen çeşitle gen

anlatımının durduğunu göstermiştir. NAA uygulamasının *OeIBR10*, *OeIBR1* ve *OePTAIL* genlerinin anlatımını baskıladığı gözlemlenmiştir. Elde ettiğimiz bulgular zeytin çeşitlerinde köklenme sürecinin anlaşılmasında önemli veriler ortaya çıkarmıştır.

**Anahtar Kelimeler:** Adventif kök, Gen anlatımı, IBA, NAA, Zeytin



## ABSTRACT

### INVESTIGATE OF THE GENETIC PROCESSES THAT CONTROL THE ADVENTITIOUS ROOTING OF OLIVE (*OLEA EUROPAEA L.*) CUTTINGS

Cansu KARAKURT

Çanakkale Onsekiz Mart University

School of Graduate Studies

Master of Science Thesis in Animal Science

(Supervisor: Prof. Dr. Kemal Melih TAŞKIN)

19/07/2023, 70

This ancient and valuable crop, known as the Olive (*Olea europaea L.*), has been reproduced both sexually and asexually. Olive (*Olea europaea L.*) is one of the species routinely propagated by cuttings and the success of this method depends on the ability of microcuttings to form adventitious roots. Adventitious rooting is the ability to produce true-to-type clones in large quantities through rapid and effective vegetative propagation. Through this process, roots are created from a variety of non-root tissues, including stems, leaves, and even cotyledons. Different olive cuttings may have various degrees of rooting effectiveness depending on the propagation cultivars employed. Some economically significant types, such as Domat, cannot be generated from cuttings due to their low rooting capacities. For this reason, in this research, it has been investigated why olive varieties give different responses to the hormone treatment such as IBA, NAA and the combination of IBA and NAA. In this study, gene expression levels were assessed in IBA, NAA and IBA+NAA-treated micro cuttings, and transcript sequence analyses were compared bioinformatically to identify some genes (*AOX2*, *IBR1*, *IBR3*, *IBR10*, and *PtAIL1*) that are responsible for adventitious rooting in the Gemlik (easy to root) and Domat (hard to root) olive cultivars. The reference protein sequences from the *A. thaliana* species were used to identify gene. Protein sequences were downloaded from TAIR database and used in Blastp analysis against olive protein database in Geneious software. It was noted that different gene expression profiles were observed in the easy-root and hard-root olive cultivars after the hormone treatment. The results showed that the expression of the OeIBR10 gene increased during the



24 hours in both cultivars as a result of IBA treatment. On the 15th day after IBA treatment, gene expression stopped in the easy-to-root olive cultivar (Gemlik). *OeIBR10*, *OeIBR1* and *OePTAIL* genes expressions were suppressed after NAA treatment. The study's findings produced significant information that can be used to comprehend how olive varieties root.

**Keywords:** Adventitious root, Gene expression, IBA, NAA, Olive



## TABLE OF CONTENTS

	Page No
JÜRİ ONAY SAYFASI.....	i
ETİK BEYAN.....	ii
ACKNOWLEDGEMENTS.....	iii
ÖZET .....	iv
ABSTRACT .....	v
TABLE OF CONTENTS .....	vi
ABBREVIATIONS.....	vii
LIST OF TABLES.....	ix
LIST OF FIGURES.....	x
CHAPTER 1	
INTRODUCTION	
1.1. Adventitious Root Formation.....	2
1.2. Adventitious Root Formation and Phytohormone Relationship.....	3
1.2.1. Auxin.....	4
1.2.2. The Role of Auxin in AR .....	5
CHAPTER 2	
PREVIOUS STUDIES	
CHAPTER 3	
MATERIALS AND METHODS	
3.1. Plant Materials .....	14
3.2. Determination of Genes.....	14
3.2.1. Primer Design.....	15
3.3. Preparation of Olive Cuttings and Hormone Treatment.....	16

3.4. RNA Isolation.....	17
3.5. cDNA Synthesis .....	18
3.6. Agarose Gel Electrophoresis and Buffers.....	19
3.6.1. Agarose Gel Electrophoresis.....	19
3.6.2. 10X TAE Buffer Preparation.....	20
3.6.3. Ethidium Bromide Stock Solution.....	20
3.7. Quantitative Real Time PCR (qPCR) Analysis.....	21
3.7.1. Determination of Primer Efficiency.....	22
3.7.2. Identification of Reference Genes.....	22
3.7.3. The Expression Profiles of the Genes in Various Olive Tissues .....	22
3.8. Sequence Analysis of Gene.....	22
3.8.1. RNA Isolation and cDNA Synthesis.....	22
3.8.2. PCR Studies.....	24
3.8.3. Bioinformatic Studies.....	25
3.9. Statistical Analysis.....	25

## CHAPTER 4

27

### RESULTS AND DISCUSSION

4.1. Bioinformatic Analysis.....	27
4.2. Preparing cuttings and Hormone Treatment.....	29
4.3. Gene Expression Analysis.....	29
4.3.1. RNA Isolation.....	29
4.3.2. PCR Determination of Gene Expressions.....	33
4.3.2.1. Gene Expression Analysis After IBA treatment.....	38
4.3.2.2. Gene Expression Analysis After IBA and NAA treatment.....	42
4.3.2.3. Gene Expression Analysis After NAA treatment.....	46
4.4. Gene Sequence Analysis.....	49
4.4.1. Plant Materials and RNA Isolation.....	49
4.4.2. PCR Studies for Sequencing.....	50
4.4.3. Bioinformatic Analysis.....	54
4.5. Discussion.....	61

CHAPTER 5  
CONCLUSION

67

REFERENCES.....

69

APPENDIX .....

I

ÖZGEÇMİŞ .....

IV



## ABBREVIATIONS

AR	Adventitious root
TUBITAK	The Scientific and Technological Research Council Of Türkiye
IBA	Indole-3-butyric acid
aa	Amino Acid
IAA	Indole-3-acetic acid
ABA	Abscisic acid
NAA	1-naphthaleneacetic acid
cDNA	Complementary DNA
PCR	Polymerase chain reaction
Bp	Base pair
TAIR	The Arabidopsis Information Resource
Kb	Kilobase
UV	Ultraviolet
PGR	Plant growth regulator
SHAM	Salicylhydroxamic acid
M	Molarity (Molar concentration)
mL	Milliliter
$\mu$ L	Microliter
BLAST	Basic Local Alignment Search Tool

## LIST OF TABLES

Table 1. Components of DNase reaction	19
Table 2. Components of High-Capacity cDNA Reverse Transcription Kits	20
Table 3. Thermal cycler program for High-Capacity cDNA Reverse Transcription Kits	20
Table 4. The reaction componenets of RT-PCR.	22
Table 5: The settlings of RT-PCR.	23
Table 6. Components of DNase reaction	24
Table 7. Thermal cycler program for High-Capacity cDNA Reverse Transcription Kits	25
Table 8. The components of Phusion High Fidelity DNA Polymerase	26
Table 9. Thermal cycler program for Phusion High Fidelity DNA Polymerase	26
Table 10. Primers used in gene expression analysis.	29
Table 11. Qubit results of the treated with the IBA samples	31
Table 12. Qubit results of the treated with NAA and IBA samples	32
Table 13. Qubit results of the treated with NAA samples	33
Table 14. Qubit-measured RNA concentrations obtained for sequence analysis	51
Table 15. Primer sequences for the PCR	51

## LIST OF FIGURES

Figure 1. Adventitious root formation in cuttings from woody plants is shown schematically.	2
Figure 2. Chemically structure of endogenous (IAA, IBA) and synthetic (NAA) auxins molecules.	5
Figure 3. Expression patterns of the genes that code for IBR and fatty acid $\beta$ -oxidation enzymes. A formula for changing IBA into IAA. To the right of the arrows, general enzymatic needs are displayed along with potential locations for IBR3, IBR10, and IBR1 activity	7
Figure 4. BLAST analysis results of AOX2, IBR1, IBR3, IBR10, and PTAIL1 genes a) blastp results of gene protein sequences of <i>A. thailiana</i> against <i>Olea europaea</i> proteome b) tblastn results of gene protein sequences of <i>Olea europaea</i> against <i>Olea europaea</i> transcriptome c) blastn results of gene transcript sequence of <i>olea europaea</i> against <i>Olea europaea</i> genome	16
Figure 5. Schematic representation of the 1st group.	17
Figure 6. Schematic representation of the 2nd group.	18
Figure 7. Schematic representation of the 3rd group.	18
Figure 8. The ladder is composed of 14 distinct DNA fragments (in base pairs) that have undergone chromatographic purification.	21
Figure 9. Phylogenetic (UPGMA) tree with sequences from the blastp and reference protein sequences ( <i>AtAOX2</i> , <i>AtAOX1</i> , <i>AtIBR1</i> , <i>AtIBR3</i> , <i>AtIBR10</i> , <i>AtPtAIL1</i> ).	29
Figure 10. Visulized of isolated RNAs under UV light.	30
Figure 11. Results of standard curve experiments of the <i>OeAOX2</i> gene.	35
Figure 12. Results of standard curve experiments of the <i>OeIBR3</i> gene.	36
Figure 13. Results of standard curve experiments of the <i>OeIBR10</i> gene.	37
Figure 14. Results of standard curve experiments of the <i>OePtAIL1</i> gene.	38
Figure 15. Results of standard curve experiments of the <i>OeIBR1</i> gene.	39
Figure 16. Gene expression results of <i>OeAOX2</i> . (Error bars represent standard error)	40
Figure 17. Gene expression results of <i>OeIBR10</i> . (Error bars represent standard error)	41

Figure 18. Gene expression results of OeIBR3. (Error bars represent standard error)	41
Figure 19. Gene expression results of OeIBR1. (Error bars represent standard error)	42
Figure 20. Gene expression results of OePTAIL1. (Error bars represent standard error)	43
Figure 21. Gene expression results of OeAOX2. (Error bars represent standard error)	44
Figure 22. Gene expression results of OeIBR3. (Error bars represent standard error)	44
Figure 23. Gene expression results of OeIBR10. (Error bars represent standard error)	45
Figure 24. Gene expression results of OePTAIL1. (Error bars represent standard error)	46
Figure 25. Gene expression results of OeIBR1. (Error bars represent standard error)	46
Figure 26. Gene expression results of OeAOX2. (Error bars represent standard error)	47
Figure 27. Gene expression results of OeIBR1. (Error bars represent standard error)	48
Figure 28. Gene expression results of OeIBR10. (Error bars represent standard error)	49
Figure 29. Gene expression results of OeIBR3. (Error bars represent standard error)	49
Figure 30. Gene expression results of OePTAIL1. (Error bars represent standard error)	50
Figure 31. Agarose gel electrophoresis images of Gemlik variety PCR products (1 kb DNA Ladder (Thermo Scientific - SM0311))	53
Figure 32. Agarose gel electrophoresis images of Gemlik variety PCR products (1 kb DNA Ladder (Thermo Scientific - SM0311))	54
Figure 33. Agarose gel electrophoresis images of Domat variety PCR products (1 kb DNA Ladder (Thermo Scientific - SM0311))	55
Figure 34. Agarose gel electrophoresis images of Domat variety PCR products (1 kb DNA Ladder (Thermo Scientific - SM0311))	56
Figure 35. Blastn analysis results of obtained sequences	57
Figure 36. Alignment of OeIBR3 sequences from easy (Gemlik) and hard (Domat) to root olive cultivars	58
Figure 37. Alignment of OeIBR10 sequences from easy (Gemlik) and hard (Domat) to root olive cultivars	58
Figure 38. Alignment of OeAOX2 sequences from easy (Gemlik) and hard (Domat) to root olive cultivars	59
Figure 39. Phylogenetic tree obtained using protein sequences of olive and various plant IBR3 genes.	60
Figure 40. Phylogenetic tree obtained using protein sequences of olive and various plant IBR10 genes.	61
Figure 41. Phylogenetic tree obtained using protein sequences of olive and various plant	



AOX2 genes.	62
Figure 42. Gene expression results of OeAOX2 in all treatment groups. (Error bars represent standard error)	64
Figure 43. Gene expression results of OeIBR3 in all treatment groups. (Error bars represent standard error).	65
Figure 44. Gene expression results of OeIBR10 in all treatment groups. (Error bars represent standard error).	66
Figure 45. Gene expression results of OeIBR1 in all treatment groups. (Error bars represent standard error).	67
Figure 46. Gene expression results of OePTAIL in all treatment groups. (Error bars represent standard error).	68



## CHAPTER 1

### INTRODUCTION

Many woody plant species such as olive are successfully propagated vegetatively. A technique of plant reproduction known as vegetative propagation allows the growth of new plants without the use of seeds from the vegetative parts of the parent plant, such as stems, roots, or leaves. Using this technique, genetically identical clones of parent plants can be produced. Vegetative propagation has been accomplished using various methods. Taking a portion of the stem with leaf nodes and allowing it to root in a suitable medium is known as cutting. When layering, a parent plant's branch or stem is bent, partially buried in the soil or rooting medium until the roots grow, and then split off to become a separate plant. The parent plant is divided into smaller pieces, each with its own roots and shoots, to produce divisions. A scion or bud from a desirable plant is joined to or inserted into a compatible rootstock via grafting and budding, which causes the fusion of tissues and the creation of a new plant. Vegetative propagation is frequently used in horticulture, agriculture, and forestry for the propagation of plants with desirable qualities, maintenance of genetic consistency, and preservation of rare types. It offers a quick and effective way to grow plants that might not set seeds, or whose progeny might not always look like the parent plant (Bonga et. al. 1987). The success rate of this method is constrained by the capacity of the adventitious root development of cuttings. The olive (*Olea europaea* L.), which belongs to the Oleaceae family is native to in the Mediterranean countries, such as Spain, Italy, Greece, Israel, Morocco, Tunisia, and Turkey. There are various ways to propagate olive trees, each with advantages and suitability for specific uses. Olive seeds are utilized in seed propagation, although they are rarely employed for commercial purposes because of their extended fruiting times and potential for trait diversity. Cutting propagation, which involves taking cuttings from mature olive wood and treating them with hormones to promote root growth, is a frequently used technique. New olive trees were created by planting the cuttings in an appropriate rooting medium. Another popular technique is grafting, which is used to increase disease resistance or to propagate certain cultivars. This entails fusing an appropriate rootstock with the desired olive cultivar. When budding, a type of grafting, a desirable cultivar bud, is inserted into the bark of the rootstock tree. For olives with low rooting capacity, air layering was used, in which a portion of the bark was removed and coated with moist rooting solution until roots appeared. Small pieces of plant tissue can be used in tissue

culture, which is a laboratory-based method, to produce large quantities of olive plants. Each approach has its own advantages and disadvantages, and the choice is based on the desired cultivar, accessible resources, and specific goals (Farabbi, et.al. 2004, n.d.). Olive is mostly propagated using semi-hardwood cutting and conventional techniques. However, the adventitious root (AR) formation success of cuttings of cultivated olive varieties is different. Some economically significant olive varieties, including Domat, are not vegetatively propagated. Therefore, in this study, we investigated why olive cuttings respond differently to auxin treatment, which is generally used in olives.

### 1.1 Adventitious Root Formation

AR growth can be observed from the main stem, a branch, or other tissues after a plant receives a damage. ARs can develop from either the premade root primordia or the induced primordia via the division of parenchyma cells. Before they emerge from the parent root, ARs can be identified with their apical meristem, a root cap, and the start of a vascular cylinder (Steffens et al., 2016). Additionally, ARs are produced, mostly in response to particular stresses conditions such as waterlogging and wounding, the latter of which is typically applied during stem cutting propagation (Druege et al., 2019). Numerous exogenous and endogenous factors, including hormone crosstalk and nutrient concentration in soil, have an impact on AR production in cuttings (Druege et al., 2016) (Figure 1).

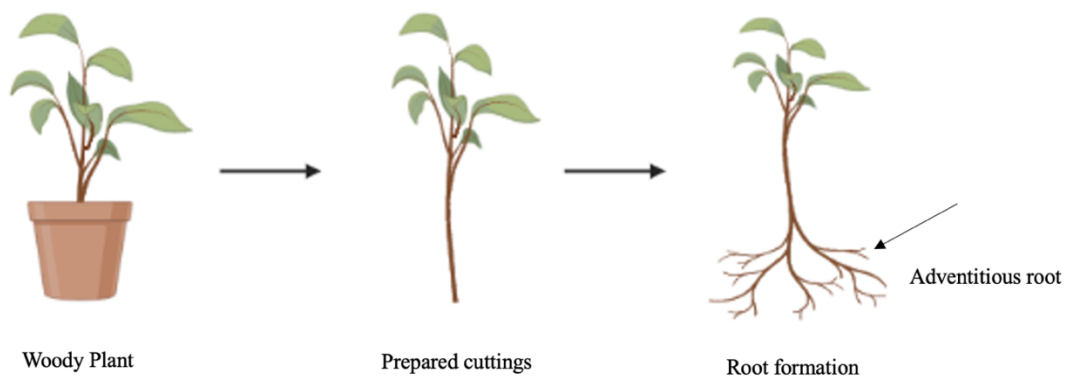


Figure 1. Adventitious root formation in cuttings from woody plants is shown schematically.

AR root formation occurs in three consecutive developmental stages.

- a. Induction: AR development is stimulated in plant tissues during the induction stage. Many factors, including hormonal balance, the environment, and the physiological state of the plant, affect this stage. Auxins, particularly indole-3-butyric acid (IBA) and naphthaleneacetic acid (NAA), are essential for olive cuttings to generate adventitious roots. Auxin treatment stimulates cell division and elongation in the stem tissue, which initiates the roots. According to Jasik and De Klerk (1999), several starch grains appear in the cells that form the root primordia at this early stage of development. These starch granules are connected to the accumulation of carbohydrate and auxin at the stem base in cuttings (Agulló-Antón et al., 2014).
- b. Initiation: The actual development of root primordia, which are condensed clusters of cells that eventually become roots, occurs during the initiation stage. Once the plant tissue has been stimulated, the cells in the cambium layer of the stem begin to divide and differentiate into root primordia. The quantity and location of auxins in stem tissue have an impact on this process. Auxins cause the production of particular genes involved in root growth, which initiate the process of AR (Itoh et al., 2005).
- c. Extension; ARs grow longer and become completely functional during the expression stage of root primordia. Cell elongation and maturation of root primordia cause visible roots to emerge from stem tissue. Freshly created roots continue to expand and establish a vascular link with the surroundings to absorb water and nutrients. For adventitious roots to continue to grow and develop at this stage, the environment must be favorable, including the appropriate moisture levels, temperature, and substrate makeup (Vidoz et al., 2010).

## **1.2 Adventitious root formation and phytohormone relationship**

Plant growth regulators (PGRs) affect AR development. Auxins, which are one of these hormones, are crucial for stimulating root growth. Synthetic auxins, such as IBA and

NAA, and natural auxins, such as IAA, stimulate cell elongation and division, which promotes AR synthesis (Pacurar et al., 2014). In contrast, the production of adventitious roots is inhibited by cytokinins. Cytokinins generally stimulate cell division and shoot development, which inhibits root formation. However, an appropriate ratio of auxins to cytokinins is essential. A higher auxin-to-cytokinin ratio must be maintained to encourage root development, while limiting excessive shoot growth. In general, adventitious root development is inhibited by Abscisic acid (ABA). Auxins promote cell proliferation and elongation, whereas ABA inhibits these processes. Additionally, ABA can cause the development of a barrier that limits water loss and prevents pathogen damage at the base of the cuts. Another factor in the development of adventitious roots is the gaseous plant hormone, ethylene. Its impact on the roots depends on its concentration. High ethylene concentrations may inhibit root production, whereas low ethylene concentrations can promote root production (Lakehal & Bellini, 2019).

### **1.2.1. Auxin**

One of the hormones which play a role in plant growth and development is auxin. Auxins are a group of plant hormones the density and the types of it highly affects the early stages of embryogenesis, the organization of the apical meristem and branching of the plant's aerial parts, the formation of the main root along with the initiation of lateral and adventitious roots (Went et al., 1937). Indole-3-acetic acid (IAA) and indole-3-butyric acid (IBA) are the main endogenous auxins in plants. IBA was originally synthetically synthesized, and it was only later discovered that it had its endogenous presence in plants (Korasick et al., 2013), and is, in fact, the second most relevant natural auxin. There are also some synthetic auxins such as 1-naphthaleneacetic acid (NAA) and 2,4-dichlorophenoxyacetic acid (2,4D), and many others (Figure 3). Zimmerman and Wilcoxon, 1935, showed that IBA and NAA also induced AR formation, similar to IAA.

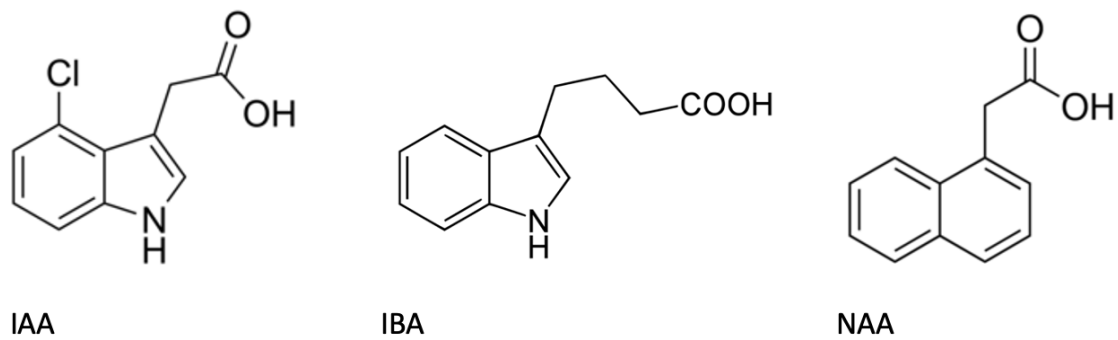


Figure 2. Chemically structure of endogenous (IAA, IBA) and synthetic (NAA) auxins molecules.

### 1.2.1 The role of auxin in AR

IBA, NAA, IAA, and commercialized root promoters are the most popular sources of PGRs for rooted cuttings. In many woody plants, the successful production of adventitious roots is necessary the presence of auxin (Botanicae et al., n.d.). Previously, to stimulate root formation the cuttings were treated with IAA (Cooper, 1935) and soon after, IBA, which promoted rooting similarly but was thought to be even more effective, was discovered. IBA is now more effective than IAA and is used commercially to root microcuttings (Kreiser et al., 2016). Changes in auxin concentration have been related to both the interdependent phases of the process and the rooting capacity of a species or cultivar; however, genotype seems to have a greater impact on rooting performance. (Ayoub & Qrunfleh, 2006). The high auxin concentrations required for the induction phase's success become inhibitory during root expression, presumably because they prevent root elongation and stimulate cellular differentiation (Li et al., 2009). IBA is the most frequently utilized auxin when using semi-hardwood cuttings because, with a few exceptions, it frequently stimulates roots more effectively than NAA (İsfendiyaroğlu & Özeker, 2008). However, in some circumstances, the combination of both auxins leads to greater rooting rates, but genotype appears to be a significant factor (Denaxa et al., n.d.). There isn't a single IBA concentration that will cause rooting in all cultivars, despite the fact that several concentrations have been tested (Aziz Kurd et al., 2010). According to the previous studies for the olive cultivars optimum IBA concentration was determined 4000 ppm (Iljazi et al., 2014).

Conversion of IBA to IAA plays a critical role in AR formation. This transformation accelerates the development of root primordia. The initial production of root primordia depends on cell division and differentiation, both of which are stimulated by IAA, an active form of auxin. The transformation of IBA to IAA results in a greater rate of root primordia initiation, laying the groundwork for effective root development by increasing the concentration of active auxin in plant tissue (Porfirio et al., 2016). Epstein and Lavee (1984) have described IBA-IAA conversion in olive. After treating "Kalamata" (hard-to-root) and "Koroneiki" (easy-to-root) cuttings with radioactive IBA-14C, most of the recovered radioactivity was found at the base of the cuttings in the form of IAA-14C. The "Koroneiki" cuttings exhibited higher conversion rates. Strangely, the procedure moved more quickly in cultivars that were difficult to root (Epstein & Lavee, 1984). In the peroxisome, IBA is converted to IAA (Zolman et al., 2007). IBA  $\beta$ -oxidation appears to be the primary function of several peroxisomal enzymes, such as INDOLE-3-BUTYRIC ACID RESPONSE1 (IBR1(Zolman et al., 2008)), IBR3 (Zolman et al., 2007), and IBR10 (Zolman et al., 2008). *IBR3*, which catalyzes the  $\alpha,\beta$ -oxidation of acyl-CoA esters, is comparable to acyl-CoA dehydrogenases. It is believed that *IBR3* is responsible for the second stage of an IBA metabolic pathway in Arabidopsis that resembles  $\beta$ -oxidation (Zolman et al., 2007) A peroxisomal member of the short-chain dehydrogenase/reductase (SDR) family of enzymes is encoded by the gene *IBR1*. This enzyme may be in charge of catalyzing a dehydrogenation step in the conversion of IBA to IAA, which is similar to  $\beta$ -oxidation. *IBR10* codes for a peroxisomal delta3, delta2-enoyl CoA isomerase that is involved in the breakdown of unsaturated fatty acids. This enzyme may also play a role in an alternative route that turns IBA into IAA (Figure 4) (Zolman et al., 2008).

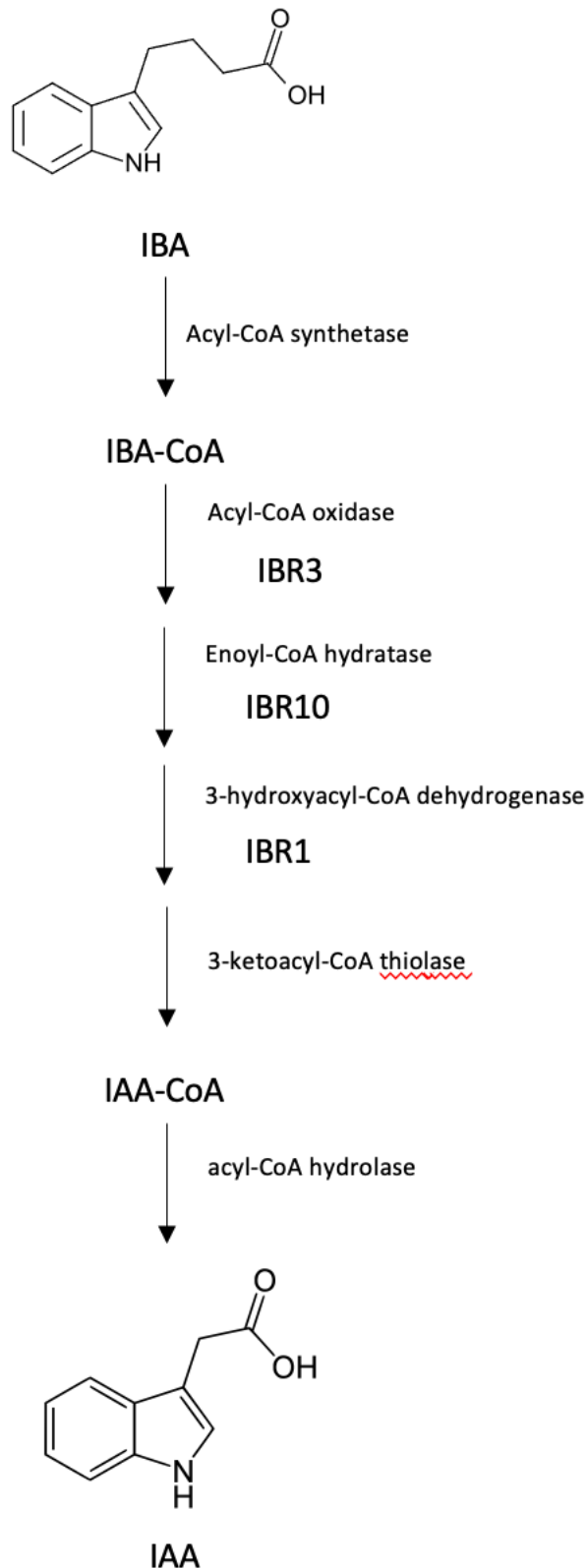


Figure 3. Expression patterns of the genes that code for IBR and fatty acid  $\beta$ -oxidation enzymes. A formula for changing IBA into IAA. To the right of the arrows, general enzymatic needs are displayed along with potential locations for IBR3, IBR10, and IBR1 activity



Studies on AR formation in olive species place a significant focus on alternate oxidase (AOX) genes, according to a review of the literature (Arnholdt-Schmitt et al., 2006; Hedayati et al., 2015; Santos MacEdo et al., 2009; Santos Macedo et al., 2012; Velada et al., 2018). Plants have AOX genes, which are involved in the electron transport system and play crucial roles in the stress response (Arnholdt-Schmitt et al., 2006). It is well known that the mechanisms that constitute the abiotic stress response are directly related to the AR formation in plant species (da Costa et al., 2013; Santos MacEdo et al., 2009). The AOX gene, one of the stress response genes, has been suggested as a marker for adventitious rooting in olive plants. Agogia x Leccino hybrids have been used to determine the molecular characterisation of AOX genes (Hedayati et al., 2015a) in olive species, gene expressions under IBA treatment, and AOX gene expressions by determining easy and difficult to root varieties. SNPs on AOX genes associated with rooting ability may represent functional markers for assessing rooting ability (Santos Macedo et al., 2012; Velada et al., 2018).

Transcription factors affects AR formation as well. Studies on woody species, with the exception of *Populus*, are scarce, despite the fact that numerous transcription factor families have been shown to be involved in this process in model species such as *Arabidopsis*. *PtAIL1* has been discovered to be a gene related to adventitious roots in the *Populus* species, a model organism for trees. *PtAIL1* belongs to the AP2 transcription factor family. The *PtAIL1* gene, among those under investigation, caught the attention of researchers due to its high expression in root primordia. The *PtAIL1* gene expression was increased (overexpressed) in the same study, and a decrease in adventitious rooting was seen when it was suppressed by RNAi technology. RNAi silences adventitious rooting, but it does not totally reset it, indicating that adventitious rooting is a complex process influenced by a variety of variables (Rigal et al., 2012).

In this thesis, we aimed to determine the molecular basis of the different responses to IBA and NAA treatments in easy-to-root (Gemlik) and hard-to-root (Domat) olive varieties. With this thesis;

1. Bioinformatics analysis of the structures of AOX2, IBR1, IBR3, IBR10, and PtAIL1 genes in olive genome.
2. Determination of expression of AOX2, IBR1, IBR3, IBR10 and PtAIL1 genes in easy (Gemlik) and hard (Domat) rooting olive cultivars after IBA and NAA treatment

3. PCR amplification of the transcript sequences of genes with significant differences in gene expression in easy (Gemlik) and hard (Domat) rooted olive cultivars and comparative bioinformatics analysis were performed as a result of sequence analysis.



## CHAPTER 2

### PREVIOUS STUDIES

New roots produced from cells of non-root tissues post-embryonically are known as adventitious root. A postembryonic organogenesis process involve adventitious root development is triggered by differentiated cells other than those designated to create roots. A vital stage in vegetative propagation via stem cuttings, adventitious root development has been used in horticulture, agriculture, and forestry. (Bonga, t.y.). Numerous external and endogenous factors have an impact on AR development in cuttings. Plant hormones are one of the factors affecting the development of AR. Particular emphasis was placed on auxin in earlier research (Druege et al., 2016b). IBA, which is the commercial auxin, is used generally to induce root formation. De Klerk et al. (1995) found that in the apple micro cuttings high auxin concentrations required for the induction phase's success turn inhibitory during root expression, necessitating IAA catabolism to prevent root development from being stifled because high auxin concentrations inhibit root elongation and promote cellular differentiation (De Klerk et al., 1995; Li et al., 2009). Various IBA concentrations and polyamine and auxin combinations were also tested on the two Türkiye olive cultivars Gemlik and Domat. It was found that the easy-to-root (Gemlik) cultivar was rooted at any concentration and combination, but the hard-to-root (Domat) cultivar produced only calluses and no root formation (Özkaya et al, 1994). During the two seasons of rooting the Gemlik and Domat cultivars, IBA, NAA, and a combination of IBA and NAA applications were used for microcutting, and it was found that a mix of 5:2 g/L (IBA:NAA) gave the finest rooting results, also in the difficult-to-root Domat, where the rooting percentage was increased to 60%. The timing of the IBA application and the 5-day IBA treatment induced more root formation than the 0-day application, which was also investigated in the same study (İsfendiyaroğlu, 2016). In another study of hormone treatment on the olive cultivar *Galega vulgar*, the liquid form of IBA and powder form of NAA and IAA were tested, and it was discovered that the powder form of NAA treatment resulted in the greatest root formation (Fernandes Serrano & Serrano Amaral, n.d.). In a separate study, they tested eight different IBA concentrations and four different microcutting sizes in olive of the "Dolce Agagia" cultivar and discovered that tetranodal microcuttings with 1.25 mg/L-1 IBA provide the best rooting, root length, and survival percentage (Haq et al., 2009). The hormone concentrations (IBA and NAA) were also investigated in the Moraiolo olive cultivar.

Cuttings were placed in rooting medium OM supplemented with six different concentrations of IBA and NAA. The optimum concentration for rooting olive cuttings is 1.5 mg/L for IBA and 1.0 mg/L for NAA. They also observed that higher concentrations of both hormones negatively affected the rooting (Ali & Abbasi, 2009). In a different study, the carbohydrate content, C/N ratio, and three different IBA concentrations (0, 2000, 3000, and 4000 mg/L-1) were examined in cuttings taken between 1st February and 1st April from two different olive cultivars, Gordal Sevillano and Tanche. The researcher found that the Gordal Sevillano cultivar cutting collected on March 1 and treated with 4000 ppm IBA gave the maximum rooting percentage and carbohydrate content. When comparing the two olive cultivars, Gordal Sevillona showed higher rooting and carbohydrate contents than Tanche.

The first study of the effect of IBA-IAA conversion on AR development belongs to Epstein and Lavee (1984). Two different olive cultivars, Kalamata (difficult to root) and Koroneiki (easy to root), were treated with the radioactive IBA-<sup>14</sup>C. After three days, 20–30% of the recovered label from both cultivars was discovered in IAA, and a month later, around 70% of the radioactivity was in IAA. Only 10% of the recovered radioactivity in Koroneiki was still in IBA-<sup>14</sup>C two months after it was applied; 90% of it had been transformed into IAA-<sup>14</sup>C. The difficult-to-root cv. Kalamata converted IBA to IAA a little more quickly than Koroneiki. In the same study, IBA-IAA conversion also investigated on the grapevine cuttings and similar results were obtained (Epstein & Lavee, 1984). In another study, apple microcuttings were grown in MS medium supplemented with [4-<sup>3</sup>H] IBA or [5-<sup>n</sup>-<sup>3</sup>H] IAA, and root formation was related to the amount of IAA or IBA; the maximum yield was obtained at 3.2–10 µM of hormone concentration. The highest content of IBA<sup>int</sup> and IAA<sup>int</sup> (derived from IBA) was found in the root emerge part of the stem. The content of IAA<sup>int</sup> after IAA treatment is exactly the same as that derived from IBA. Furthermore, it demonstrates that the IBA is converted into the IAA but not the other way around; the IAA is not converted into the IBA (Van Der Krieken et al., 1992). In another study in the IBA to IAA conversion that a novel peroxisomal enzyme, *IBR3*, which is involved, firstly identified in the *ibr3* mutants in *Arabidopsis thaliana*. The *ibr3* mutant, which is defective in root elongation inhibition and lateral root promotion in response to IBA, normally responds to other auxins, including IAA. The mutant phenotypes were then rescued in the *ibr3* mutants, and the transformed plants displayed wild-type responses in root elongation and lateral root assays in the presence of IBA. This was accomplished by transforming the *ibr3* mutants with

a construct expressing a full-length IBR3 cDNA driven by the cauliflower mosaic virus 35S promoter. This demonstrates that IBR3 flaws specifically interfere with IBA answers (Zolman et al., 2007). In the following research on the IBA to IAA conversion, the *ibr1* and *ibr10* mutants, which are defective in their response to IBA, a precursor to the active plant hormone IAA. The mutants exhibit reduced lateral root initiation, decreased inhibition of root extension, and decreased expression of IBA-responsive genes. These defects resemble those seen in the *ibr3* mutant, which damages a putative peroxisomal acyl-CoA oxidase or dehydrogenase that was previously identified. Novel peroxisomal enzymes involved in IBA metabolism and provides genetic evidence that peroxisomes are involved in this process. Accordingly, it is hypothesized that *IBR1* and *IBR10* participate in the conversion of IBA into IAA by eliminating two side-chain methylene units in a method resembling fatty acid beta-oxidation (Zolman et al., 2008). The study describing the biochemical processes that take place following IBA treatment in cuttings is another significant investigation on adventitious rooting in olive species. In this research, IBA and IAA levels were measured after cuttings were treated with IBA at various phases of adventitious rooting. The highest level of IAA was reached after the IBA treatment on the easy-to-root cultivar at 24 hours, and the level of IAA was reduced after 96 hours, which is the initiation stage of the AR, according to the results. During the initiation phase, the IAA concentration was low. Despite this, the hard-rooted cultivar's IAA levels increased at the 24th hour but were unable to match those of the easy-rooted cultivar, and there was no IAA level decrease after the 96th hour as was observed in the other cultivars. High auxin levels may restrict rooting in the initial phase of cutting rooting even when they promote rooting during the induction phase (Porfirio et al., 2016).

When we looked at the effect of stress on AR formation, we encountered AOX genes. The potential of olive alternative oxidase as a source of effective AR induction markers is discussed in this study, which demonstrates the first signs of a significant link between AOX activity and differential adventitious rooting in semi-hardwood cuttings. When the easy-to-root Portuguese cultivar 'Cobrançosa' was treated with salicyl-hydroxamic acid, which is an inhibitor of AOX, the root induction could be significantly reduced; however, when treated with H<sub>2</sub>O<sub>2</sub> or pyruvate, both known to induce AOX activity, the degree of rooting increased. This result show that the AOX gene activity affect the AR in olive cuttings (Santos MacEdo et al., 2009). In a separate investigation, researchers looked at the role of AOX in the rooting

process and how it relates to the olive micro cuttings '*Galega vulgar*' adaptive phenylpropanoid and lignin metabolism. The study examined the function of AOX in olive rooting using an in vitro system for microshoot propagation. The researchers observed that salicylhydroxamic acid (SHAM) had no inhibitory effect on calli production but that it inhibited roots, which led to AR in olive microshoots. Since phenylpropanoid and lignin accumulation were suppressed by SHAM treatment, it may be hypothesized that AOX control of root formation is connected to changes in phenylpropanoid and lignin metabolism, which in turn interact with meristematic growth. Considering that, AOX genes may be crucial for the process of adaptive cell reprogramming during rooting (Santos Macedo et al., 2012). The transcript accumulation of the OeAOX1a and OeAOX1d genes and the three different phases of the adventitious rooting process were shown to be correlated in the investigation of the expression of AOX1 subfamily genes during IBA-induced adventitious rooting in the olive tree, which is *Galgea vulgar*. In the early stages of rooting, the expression of the OeAOX1a and OeAOX1d genes was significantly elevated, with the largest peak of transcript accumulation occurring 8 hours after IBA treatment. The rooting assay revealed a consistent expression pattern for both genes, with the greatest peak of up-regulation occurring 8 hours after IBA application. However, when compared to the levels seen at the equivalent controls, OeAOX1a displayed higher levels of expression than OeAOX1d at this time point. This result shows that the AOX1 genes are generally active in the induction phase of adventitious rooting in olive (Velada et al., 2018). Another study discovered a link between the AOX2 gene and olive cuttings' capacity to root. The Leccino x Dolce Agogia progeny was used in the study to evaluate various candidate genes, and it showed that only the AOX2 gene was significantly upregulated and linked with phenotypic traits. In the study, four different alleles were found in the two parental varieties, which were distinguished by several SNPs, and when they looked at the expression analysis of six gene transcripts at five different times after cutting preparation for high-rooting and low-rooting genotypes, they found that there were differences in the expression of the six gene transcripts between high- and low-rooting genotypes. The expression of the AOX2 gene was significantly higher in high-rooting genotypes carrying alleles 1 and 4 compared to low-rooting genotypes carrying alleles 1 and 3. These results show that some polymorphism on AOX2 genes effect the AR on olive cuttings (Hedayati et al., 2015a).

Transcription factors also have an impact on adventitious rooting. Investigations into the influence of transcription factors on adventitious roots in tree species including *Pinus taeda* and *Populus* sp. led to the identification of gene expression patterns linked to various stages of AR development and significant TFs. These TFs control hormone signaling pathways that support AR formation as well as the regulation of genes involved in cell division, differentiation, and elongation. TFs are complicated to regulate because of interactions with other proteins and signaling cascades. The production of AR in poplar has been hypothesized to be inhibited by gibberellins, whereas cytokinins may interact with the auxin and ethylene pathways. The AP2/ERF protein family of transcription factors also regulates two crucial plant functions, how plants respond to stress and how they govern growth, and it plays a role in the development of AR in trees. (Legué et al., 2014). Researchers discovered that the level of *PtAIL1* transcript rises during the initial stages of adventitious rooting in their study on the AINTEGUMENTA LIKE1 homeotic transcription factor *PtAIL1* and its function in regulating the production of adventitious root primordia in poplar. When *PtAIL1* was overexpressed, adventitious roots formed more slowly than when *PtAIL1* was downexpressed. In addition, 15 genes were found to be overexpressed in stem tissues in *PtAIL1*-overexpressing plants, resulting in the development of root primordia. (Rigal et al., 2012).

## CHAPTER 3

### MATERIALS AND METHODS

In this study, *AOX2*, *IBR1*, *IBR3*, *IBR10*, and *PtAIL1*, a transcription factor, were identified in the olive genome by bioinformatic approaches, and expression analyses were carried out following IBA treatment in two different olive cultivars. These genes are known to be significant in adventitious rooting.

#### 3.1. Plant Materials

Microcuttings of Gemlik and Domat cultivars used in this study were obtained from 1-year-old trees. Saplings of related varieties were purchased from the Edremit Olive Production Station Directorate. Short cuttings containing four nodes for each variety were cut from young boughs and prepared in the laboratory.

#### 3.2. Determination of genes

The genomic and transcript sequences of olive *AOX2*, *IBR1*, *IBR3*, *IBR10*, and *PtAIL1* were obtained using the Sylvestris genome. (Unver et al., 2017). A local BLAST database was established in Geneious (Kearse et al., 2012) software by downloading the whole genome, transcriptome and proteome data of Sylvestris from the NCBI database (Genome ID: 10724). Afterwards, the protein sequences of the *AOX2* (AT5G64210), *IBR1* (AT4G05530), *IBR3* (AT3G06810), *IBR10* (AT4G14430) and *PtAIL1* (AT4G37750) genes were downloaded from the TAIR ([arabidopsis.org](http://arabidopsis.org)) database and then used as query in BLASTP analysis against olive database in Geneious software. The sequences obtained from the BLAST were aligned in Geneious, and phylogenetic trees were created with Arabidopsis reference sequences and examined using the Tree builder of Geneious software. The most similar olive sequences to the reference sequences were chosen for the study because they were grouped with the reference sequences in the phylogenetic trees and shared the same conserved domain. Selected protein sequences were compared against the existing olive transcriptome by translated BLASTN and transcript sequences encoding the relevant proteins were found. Primers were selected from these transcripts (Figure 4).



IBR1						
a	Name	E Value $\Delta$	% Identical Sites	Query coverage	% Pairwise Identity	Sequence Length
	Oeu016255.1	0	72.3%	99.64%	72.3%	833
	Oeu031983.1	9.45e-173	59.0%	51.21%	59.0%	398
	Oeu059100.1	3.77e-19	25.7%	34.71%	25.7%	412
b	Name	E Value $\Delta$	% Identical Sites	Query coverage	% Pairwise Identity	Sequence Length
	Oeu007162.2	0	100.0%	100.00%	100.0%	759
	Oeu002754.1	6.77e-157	83.9%	100.00%	83.9%	762
	Oeu019723.1	4.22e-29	36.6%	95.26%	36.6%	894
	Oeu026089.1	6.75e-28	31.5%	96.84%	31.5%	882
	Oeu030909.1	8.15e-28	34.3%	93.28%	34.3%	747
c	Name	E Value $\Delta$	% Identical Sites	Query coverage	% Pairwise Identity	Sequence Length
	chr13	4.40e-73	99.4%	20.42%	99.4%	2,154
	chr13	2.06e-66	100.0%	18.31%	100.0%	2,139
	chr13	1.60e-62	100.0%	17.39%	100.0%	2,132
	chr13	1.25e-58	99.2%	16.86%	99.2%	2,128
	chr13	3.50e-54	100.0%	15.42%	100.0%	2,117

IBR3						
a	Name	E Value $\Delta$	% Identical Sites	Query coverage	% Pairwise Identity	Sequence Length
	Oeu016255.1	0	72.3%	99.64%	72.3%	833
	Oeu031983.1	9.45e-173	59.0%	51.21%	59.0%	398
	Oeu059100.1	3.77e-19	25.7%	34.71%	25.7%	412
b	Name	E Value $\Delta$	% Identical Sites	Query coverage	% Pairwise Identity	Sequence Length
	Oeu016255.1	0	100.0%	100.00%	100.0%	2,499
	Oeu031983.1	0	70.9%	51.74%	70.9%	1,194
	Oeu059100.1	6.01e-16	23.0%	42.78%	23.0%	1,236
	Oeu031983.1	6.03e-10	81.1%	4.44%	81.1%	1,194
c	Name	E Value $\Delta$	% Identical Sites	Query coverage	% Pairwise Identity	Sequence Length
	scaffold1656	1.75e-136	100.0%	10.64%	100.0%	2,266
	scaffold1656	1.83e-106	100.0%	8.48%	100.0%	2,212
	scaffold1656	1.65e-96	100.0%	7.70%	100.0%	2,194
	scaffold1656	1.11e-93	100.0%	7.56%	100.0%	2,189
	scaffold1656	5.20e-92	100.0%	7.44%	100.0%	2,186

IBR10						
a	Name	E Value $\Delta$	% Identical Sites	Query coverage	% Pairwise Identity	Sequence Length
	Oeu058881.1	1.89e-88	58.9%	100.00%	58.9%	246
	Oeu058884.1	6.94e-80	57.6%	87.92%	57.6%	417
	Oeu037888.1	2.41e-70	47.9%	97.80%	47.9%	253
	Oeu021557.1	3.76e-21	40.3%	46.25%	40.3%	129
	Oeu037887.1	3.78e-17	36.8%	40.83%	36.8%	157
b	Name	E Value $\Delta$	% Identical Sites	Query coverage	% Pairwise Identity	Sequence Length
	Oeu058881.1	3.87e-180	100.0%	100.00%	100.0%	738
	Oeu058884.1	2.09e-149	96.8%	87.80%	96.8%	1,251
	Oeu037888.1	1.83e-77	52.9%	97.56%	52.9%	739
	Oeu021557.1	1.49e-27	50.5%	45.12%	50.5%	287
	Oeu037887.1	1.40e-17	40.2%	39.43%	40.2%	471
c	Name	E Value $\Delta$	% Identical Sites	Query coverage	% Pairwise Identity	Sequence Length
	chr18	0	100.0%	100.00%	100.0%	2,738
	chr18	0	97.7%	100.00%	97.7%	2,738
	scaffold45511	1.41e-132	89.2%	51.63%	89.2%	2,381

AOX						
a	Name	E Value $\Delta$	% Identical Sites	Query coverage	% Pairwise Identity	Sequence Length
	Oeu019227.1	2.96e-166	80.1%	79.04%	80.1%	346
	Oeu046793.1	1.46e-135	63.2%	81.30%	63.2%	308
	Oeu019995.2	8.44e-102	77.7%	49.58%	77.7%	176
	Oeu015530.1	6.11e-28	69.0%	20.11%	69.0%	184
	Oeu046792.1	6.29e-16	58.3%	13.60%	58.3%	72
b	Name	E Value $\Delta$	% Identical Sites	Query coverage	% Pairwise Identity	Sequence Length
	Oeu019227.1	0	100.0%	100.00%	100.0%	1,038
	Oeu046793.1	3.43e-142	71.3%	74.57%	71.3%	924
	Oeu019995.2	1.16e-104	80.1%	50.87%	80.1%	528
	Oeu015530.1	2.49e-33	53.2%	32.88%	53.2%	352
	Oeu046792.1	2.48e-17	68.8%	13.87%	68.8%	216
c	Name	E Value $\Delta$	% Identical Sites	Query coverage	% Pairwise Identity	Sequence Length
	scaffold1815	0	99.6%	48.17%	99.6%	371,659
	scaffold1815	0	100.0%	100.00%	100.0%	371,659
	scaffold1815	2.87e-61	100.0%	12.52%	100.0%	371,659
	scaffold1815	2.35e-22	100.0%	5.78%	100.0%	371,659

PTAIL1						
a	Name	E Value $\Delta$	% Identical Sites	Query coverage	% Pairwise Identity	Sequence Length
	Oeu034344.1	4.25e-171	56.2%	87.93%	56.2%	497
	Oeu032654.1	4.07e-161	62.1%	71.89%	62.1%	613
	Oeu034990.1	1.99e-147	47.0%	89.01%	47.0%	487
	Oeu022008.1	2.30e-123	79.5%	38.74%	79.5%	353
	Oeu000419.1	2.64e-123	49.2%	74.77%	49.2%	552
b	Name	E Value $\Delta$	% Identical Sites	Query coverage	% Pairwise Identity	Sequence Length
	Oeu034344.1	0	100.0%	100.00%	100.0%	1,491
	Oeu032654.1	0	63.2%	89.34%	63.2%	1,839
	Oeu034990.1	2.06e-174	55.3%	91.95%	55.3%	1,461
	Oeu022008.1	5.70e-141	60.2%	61.97%	60.2%	1,059
	Oeu000419.1	1.35e-127	54.3%	74.85%	54.3%	1,656
c	Name	E Value $\Delta$	% Identical Sites	Query coverage	% Pairwise Identity	Sequence Length
	scaffold2896	7.91e-148	99.7%	19.38%	99.7%	2,290
	scaffold2896	1.34e-135	100.0%	17.71%	100.0%	2,264
	scaffold2896	6.52e-104	100.0%	13.88%	100.0%	2,207
	scaffold2896	2.34e-103	100.0%	13.82%	100.0%	2,206
	chr18	1.41e-100	90.5%	18.85%	90.5%	2,284

Figure 4. BLAST analysis results of AOX2, IBR1, IBR3, IBR10, and PTAIL1 genes a) blastp results of gene protein sequences of *A. thaliana* against *Olea europaea* proteome b) tblastn results of gene protein sequences of *Olea europaea* against *Olea europaea* transcriptome c) blastn results of gene transcript sequence of *Olea europaea* against *Olea europaea* genome

### 3.2.1. Primer design

Quantitative real-time PCR primers based on exon junctions were selected using Geneious software. The primers were chosen to bind to two separate exons and have an intron region of at least 1000 base pairs between them in the genome if suitable primers cannot be chosen from the exon junction or if the efficiency analysis is poor. To avoid genomic DNA contamination that could still happen despite applying DNase before cDNA synthesis. The genes, that have one exon, they do not meet all the requirements. For the inside of the exons, primers were chosen.

### 3.3. Preparation of olive cuttings and IBA treatment

Micro-cuttings were obtained from 1-year-old trees. Plants were purchased from Edremit Olive Production Station Directorate. Cuttings with four nodes were prepared from sapling and all leaves, except from the upper four, were removed.

Three treatment groups were tested. There were three biological replicates in each group, and each replicate had at least ten cuttings.

For the first group each cutting, approximately 1 cm, was immersed for 5 s in a 4000 ppm IBA solution. The cuttings were then placed in perlite-filled pots and kept in plant development cabinets at a temperature of 25 °C and high humidity (>90 percent). After the treatments, following the 24 hours, 7th, and 15th days, the IBA-treated tissues of the cuttings were cut to a length of about 1 cm, immediately frozen in liquid nitrogen, and stored at -80 °C for RNA isolation (Figure 5).

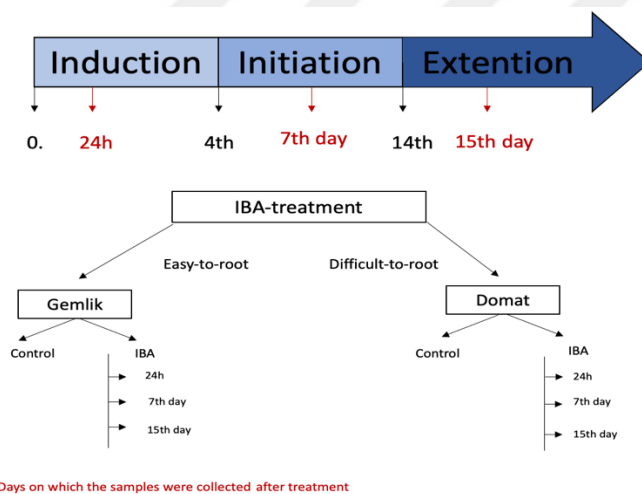


Figure 5. Schematic representation of the 1st group.

For the second group, prepared cuttings were submerged 5 s in a solution containing 5000 ppm IBA and 2000 ppm NAA. After that, the cuttings were put in pots filled with perlite and kept in plant growth cabinets at a temperature of 25 °C and a high humidity level (>90 percent). The IBA-NAA treated cuttings were collected on the 24-hour, 7th, and 15th days and instantly frozen in liquid nitrogen, and kept at -80 °C (Figure 6).

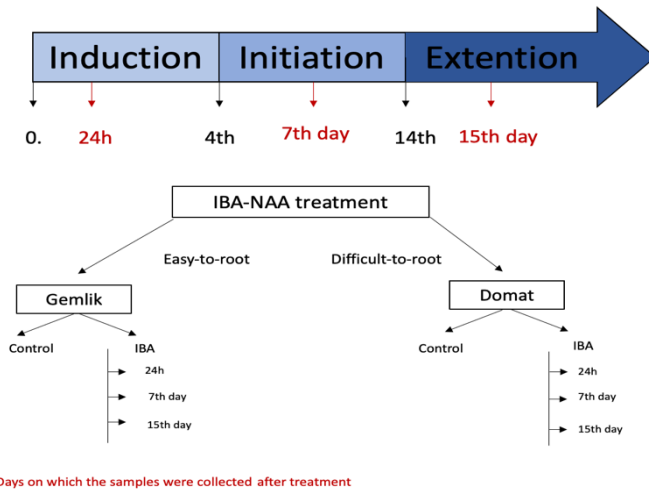


Figure 6. Schematic representation of the 2nd group.

In the third group, each cutting (approximately 1,0 cm) was subjected to a quick-deep treatment for 5 s in a 2000 ppm NAA solution. After that, the cuttings were planted in pots filled with perlite and kept in cabinets at a temperature of 25 °C and a high humidity level (>90 percent) to promote plant growth. Cuttings that had been exposed to NAA were collected on the 24-hour, 7th, and 15th days. They were then immediately frozen in liquid nitrogen and kept at -80 °C (Figure 7).

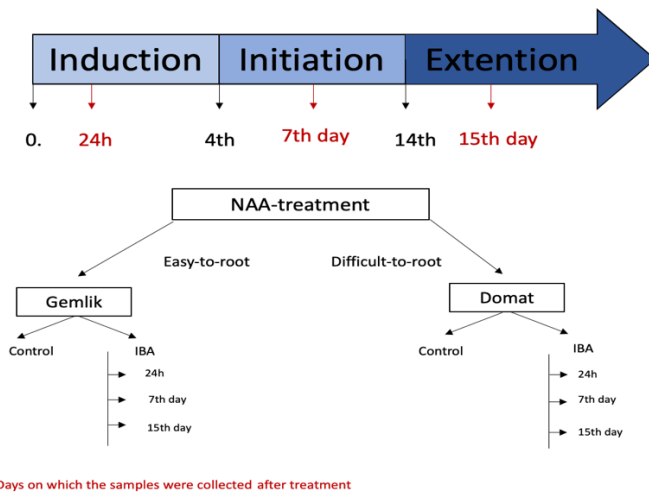


Figure 7. Schematic representation of the 3rd group.

### 3.4. RNA isolation

For samples obtained for 24 hours, the isolation materials were maintained in 1% DEPC (Applichem-A0881,0100). It was sterilized the following day for 15 minutes at 121 °C in an autoclave. The tissues were removed from -80 °C, submerged in liquid nitrogen, and homogenized using a mortar. Homogenized tissues (100 mg) were transferred to Eppendorf tubes and RNA isolation was performed using the PureLink RNA mini kit (Invitrogen 12183018A) and Trizol (Ambion–15596018). After the isolation, the quality of the RNAs was determined by agarose gel electrophoresis.

The amount of isolated RNAs was determined with Qubit® 2.0 (Invitrogen, Q32866). 1 µl of RNA Reagent (Invitrogen, Q10210) and 199 µl of reaction buffer were added to the tubes and mixed by vortexing. Then, 1 µl of the prepared solution was discarded and 1 µl of the RNA sample was added to the final volume to make 200 µl. After the tubes were left for 2 minutes, the amounts were determined with the help of the Qubit® 2.0 fluorometer.

### 3.5. cDNA synthesis

cDNA synthesis was performed with the kit (4368814; Applied Biosystems). DNase was applied to remove DNA residues from isolated total RNA samples. Using PCR, the tubes were then maintained at 37°C for 30 minutes. (Table 1)

Table 1

Components of DNase reaction

<b>Components</b>	<b>Amount</b>	<b>Final concentration</b>
10X DNase buffer	1 µl	1X
RNA	1000 ng	100 ng / µl
DNase I (1 u/µl)	1 µl	0.1 u / µl
Nuclease-free water	Complete the final volume	-
Final volume	10 µl	-

Then, 1 µl of EDTA (50 mM), 2 µl of random primer, and 0.8 µl of dNTP mix were added to the reactions and DNase I was inactivated for 10 minutes at 65 °C. A High-

Capacity cDNA Reverse Transcription Kit (Applied Biosystems, Fisher Scientific, USA) was used to perform the synthesis as directed by the manufacturer. For this purpose, cDNA reaction components (Table 2) were added to RNA samples after DNase treatment.

Table 2

Components of High-Capacity cDNA Reverse Transcription Kits

<b>Components</b>	<b>Amount</b>
10X RT Buffer	2 $\mu$ l
Reverse transcriptase	1 unit
Nuclease free water	3.2 $\mu$ l
Final volume	6.2 $\mu$ l

The samples were incubated according to the protocol's instructions (Table 3), then kept at +4 °C until were used following cDNA synthesis.

Table 3

Thermal cycler program for High-Capacity cDNA Reverse Transcription Kits

<b>Settings</b>	<b>Temperature</b>	<b>Time</b>
1	25 °C	10 min
2	37 °C	120 min
3	85 °C	4 min
4	4 °C	$\infty$

### **3.6 Agarose gel electrophoresis and buffers**

#### **3.6.1 Agarose gel electrophoresis**

In the thesis study, PCR products, DNA samples, and RNA samples were all visualized using 1% agarose gel electrophoresis. Heating 50 ml of 1X TAE buffer with 0.5

g of agarose produced a homogenous solution. 3  $\mu$ l of EtBr were added to the prepared gel after it had cooled, and the gel was then poured.

After the gel solidified, the material to be loaded (PCR product, DNA or RNA) was mixed with ladder 6X loading dye and loaded into the wells in the specified order. Then, the first well of the gel was loaded with a 1 KB ladder (Fermentas DNA Ladder SM0633). The gel was then run for 45 minutes at 90 V/cm. PCR products were imaged using a Canon camera after being visualized under UV light. (Figure 5)

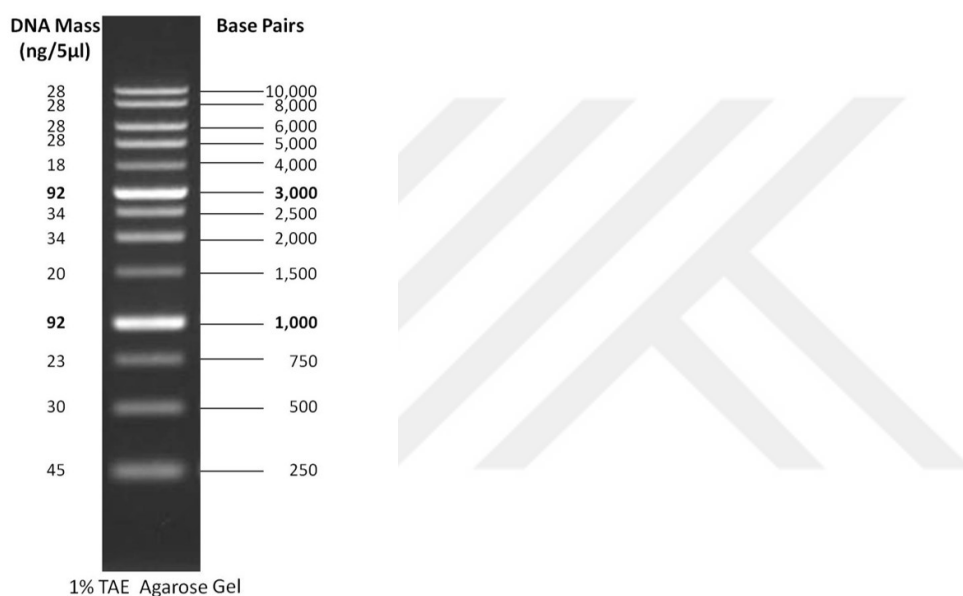


Figure 8. The ladder is composed of 14 distinct DNA fragments (in base pairs) that have undergone chromatographic purification.

### 3.6.2. 10X TAE buffer preparation

TRIS BASE (48.4 g) and EDTA (3.72 g), used to prepare 10X TAE buffer, were dissolved in 900 ml of dH<sub>2</sub>O. Then the pH was brought to 8.0 with acetic acid and made up to 1 liter with dH<sub>2</sub>O. It has been stored at room temperature. For the 1X TAE buffer, 100 ml of the previously prepared 10X TAE buffer was added into 900 ml of dH<sub>2</sub>O.

### 3.6.3. Ethidium Bromide Stock Solution

0.1 g of EtBr was dissolved in 10 ml of dH<sub>2</sub>O. The stock solution was covered with aluminum foil and stored at room temperature.

### 3.7. Quantitative Real Time PCR (qPCR) Analysis

qPCR reactions were prepared with 5 $\mu$ l SYBR Green PCR Master Mix (Applied Biosystems, USA) by mixing 0.3 $\mu$ l (200 nM) each primer and 1 $\mu$ l cDNA, making up the total reaction volume to 10 $\mu$ l with nuclease-free water. (Table 4)

Table 4

The reaction components of RT-PCR.

<b>Reaction components</b>	<b>Amount</b>	<b>Final concentrations</b>
2X Master mix	5 $\mu$ l	1X
cDNA	1 $\mu$ l	-
10 $\mu$ M Forward Primer	0,3 $\mu$ l	300 nM
10 $\mu$ M Reverse Primer	0,3 $\mu$ l	300 nM
Nuclease-free water	0,4 $\mu$ l	-

In a 96-well plate, the Step One Plus (Applied Biosystems, USA) instrument was utilized for RT-PCR. (Table 5)

Table 5

The settlings of RT-PCR.

Step	Temperature	Time	Cycle
Initial Denaturation	95 °C	10 min	1
Denaturation	95 °C	15 sec	
Annealing	55 °C	30 sec	40
Extention	72 °C	1 min	

### 3.7.1. Determination of Primer Efficiency

The amount of cDNA used as a template in the qPCR reaction was diluted up to  $10^6$ , 10 times each, for the qPCR experiments used to test the efficiency of the primers. Using Step One Plus Software V2.0.6 (Applied Biosystems, USA), the  $\Delta\Delta CT$  approach was used to identify the threshold cycle. The mean Ct values of all three replicates were used to calculate the standard curve, slope, and correlation coefficient ( $R^2$ ). The efficiency value was determined using the following formula:

$$\text{Efficiency} = 10(-1/\text{slope}) - 1$$

Only primer pairs having an  $R^2$  value greater than 0.98, a single peak in melt curve analysis, and an efficiency value of 90–110% in gene expression analysis were used.

### 3.7.2. Identification of Reference Genes

Candidate reference genes were identified by first using the work of (Noceda et al., 2022) as a reference in the selection of the reference genes used in the thesis. The OUB2 and ACT7a genes were chosen as reference genes after considering the efficiency and  $R^2$  values revealed in the analysis of these candidate genes (Hürkan et al., 2018).



### 3.7.3. The expression profiles of the genes in various olive tissues

In gene expression studies, experiments were performed with 3 biological replicates and 3 technical replicates. For the experiments performed with the SYBR Green method, the efficiency was determined by standard curve experiments for each primer pair, and only primers with efficiency values in the range of 90–110% were used. The data was analyzed by the  $\Delta\Delta C_t$  method. During the analysis, the reference genes determined as a result of the reference gene study were chosen as endogenous controls.

### 3.8. Sequence analysis of genes

#### 3.8.1. RNA isolation and cDNA synthesis

Cuttings of the shoots, stems, and leaves of the Gemlik and Domat cultivars were frozen in liquid nitrogen and kept at  $-80^\circ\text{C}$  until RNA isolation. The Purelink RNA Mini Kit (Invitrogen- 12183-018A) and TRIzol (Thermo Fischer-15596026) were used to isolate total RNA. Following its isolation, total RNA was quantified using Qubit 2.0 (Invitrogen-Q32866) and examined on an agarose gel to assess its quantity. RNAs were kept until usage at  $-80^\circ\text{C}$ .

In the study, cDNA synthesis was carried out with the help of a kit (4368814; Applied Biosystems). DNase was applied to remove DNA fragments from isolated total RNA samples. Afterwards, the tubes were kept at  $37^\circ\text{C}$  for 30 minutes. (Table 5)

Table 6

Components of DNase reaction

Components	Amount	Final concentration
10X DNase buffer	1 $\mu\text{l}$	1X
RNA	1000 ng	100 ng / $\mu\text{l}$
DNase I (1 u/ $\mu\text{l}$ )	1 $\mu\text{l}$	0.1 u / $\mu\text{l}$
Nuclease-free water	Complete the final volume	-
Final volume	10 $\mu\text{l}$	-

After incubation, the components required for the cDNA reaction were added to the tubes. The DNase enzyme was inhibited at 65°C for 10 minutes. As a next step, 10X reaction buffer (2 µl), nuclease-free water (3.2 µl), and reverse transcriptase enzyme (1 µl) were added to the tubes. The final volume was 20 µl and the tubes were incubated in the thermal cycler. (Table 6)

Table 7

Thermal cycler program for High-Capacity cDNA Reverse Transcription Kits

Settings	Temperature	Time
1	25 °C	10 min
2	37 °C	120 min
3	85 °C	4 min
4	4 °C	∞

### 3.8.2. PCR studies

The gene of interest was amplified by PCR utilizing the synthesized cDNAs as templates (Table 7). To test various primer annealing temperatures, PCR experiments were run as a gradient. In these PCR experiments, a Phusion High Fidelity DNA Polymerase enzyme (Thermo Scientific, F530L) with a proofreading feature was used. The program used for PCR is shown below (Table 8).

Table 8

The components of Phusion High Fidelity DNA Polymerase

<b>Components</b>	<b>Amounts (µl)</b>	<b>Final concentration</b>
5X High Fidelity PCR Buffer	5	1X
10mM dNTP mix	0,5	200 µl
10µM Reverse Primer	1	0,4 µl
10µM Forward Primer	1	0,4 µl
cDNA	1	-
Nuclease-free water	16,25	-
Phusion	0,25	0.02 u/µl
<b>Final volume</b>	<b>25</b>	

Table 9

Thermal cycler program for Phusion High Fidelity DNA Polymerase

<b>Temperature</b>	<b>Time</b>	<b>Cycle</b>
98 °C	3 min	1
98 °C	30 sec	36
55°C-60°C	30 sec	
72°C	2 min	
72°C	10 min	1
4 °C	30 min	1

1% agarose gel electrophoresis was used to evaluate these PCR results. Utilizing the PCR Purification Kit (Invitrogen, K310001), non-specific PCR findings that did not produce growth were purified. In the event that PCR produced additional bands next to the desired product, these PCR products were extracted from the gel using the PureLink® Quick Gel Extraction Kit (Invitrogen, K2100-12). After that, sequence analysis was carried out using a service (Medsantek, Turkey).

### 3.8.3. Bioinformatic studies

As a result of PCR and sequence analysis studies, transcript sequences of OeAOX2, OeIBR3 and OeIBR10 genes of both cultivars were obtained. The sequence analysis

findings' ab1 extension files were uploaded to the Geneious software, where analyses were done. In order to achieve this, bad readings were filtered out, reads from the same gene and variety were combined, and consensus sequences were obtained, each with a 0.05 margin of error value. Blastn analysis with the obtained consensus sequences was performed against the NCBI non-redundant database using the Geneious software. Afterwards, the sequences were aligned with the default parameters using the “Muscle” algorithm (Edgar, 2004). in the Geneious program. Using this alignment file, phylogenetic trees were drawn with the UPGMA algorithm using the “Geneious Tree Builder” option in Geneious software.

### **3.9. Statistical Analysis**

Statistical Package for the Social Sciences (SPSS) version 26.0 was used for statistical analysis. According to Tukey’s HSD test, the data did not show a homogeneous distribution (Appendix1). Nested ANOVA was used to analyze the data by combining time, hormone treatment, gene, and variables. As a comparison was performed using the Nested ANOVA, between the variables hormone treatment variety and time, a significant relative gene expression difference has been deducted. (Appendix2,3).

## CHAPTER 4

### RESULTS AND DISCUSSION

#### 4.1. Bioinformatic analysis

The genomic and transcript sequences of the *AOX2*, *AOX1*, *IBR1*, *IBR3*, *IBR10*, and *PtAIL1* genes were obtained using the existing *Sylvestris* genome (Unver et al., 2017). The *Sylvestris* cultivar's whole genome, transcriptome, and proteome data were downloaded from the NCBI database (Genome ID: 10724), and a blast database was created in the Geneious software (Kearse et al., 2012). Subsequently, *AOX2* (AT5G64210, 353 a.a.), *AOX1* (AT3G22360, 353 a.a.), AT3G22370, 354 a.a.), AT3G27620, 329 a.a.), *IBR1* (AT4G05530, 254 a.a.), *IBR3* (AT3G06810, 824 a.a.), and *PtAIL1* (AT4G37750, 555 a.a.) genes were downloaded from the TAIR (arabidopsis.org) database and used in the Blastp analysis against *Sylvestris*'s protein database in Geneious software. By comparing protein sequences to the olive transcriptome using translated BLASTN, transcript sequences encoding similar proteins were identified. The obtained transcripts were used in the design of the primers. Primer sequences used in the thesis are listed in the (Table 9).

In the phylogenetic trees, the branches belonging to the genes of interest are indicated in different colors. Sequences grouped in the same branches as the reference *Arabidopsis* proteins in the phylogenetic trees were examined for further studies. In these sequences, the *OePtAIL*, *IBR1*, *IBR3*, and *IBR10* gene groups were found to have duplicates that produce the same protein (Figure 6). In these instances, primers were chosen to bind to all transcripts, taking into account the similarity of the transcript sequences. Blastp analyses of the *IBR1* group proteins, which are also included in the phylogenetic trees, in the olive database revealed the genes determined as "tropinone reductase 3" as the most similar result. This gene is encoded as AT2G29330 in the *Arabidopsis* genome and differs from the reference *IBR1* gene. In addition, *IBR* genes are in the "short-chain dehydrogenase/reductase (SDR)1" gene family. These results suggest that the functions of *IBR1* genes are carried out by *IBR3* and *IBR10* genes.

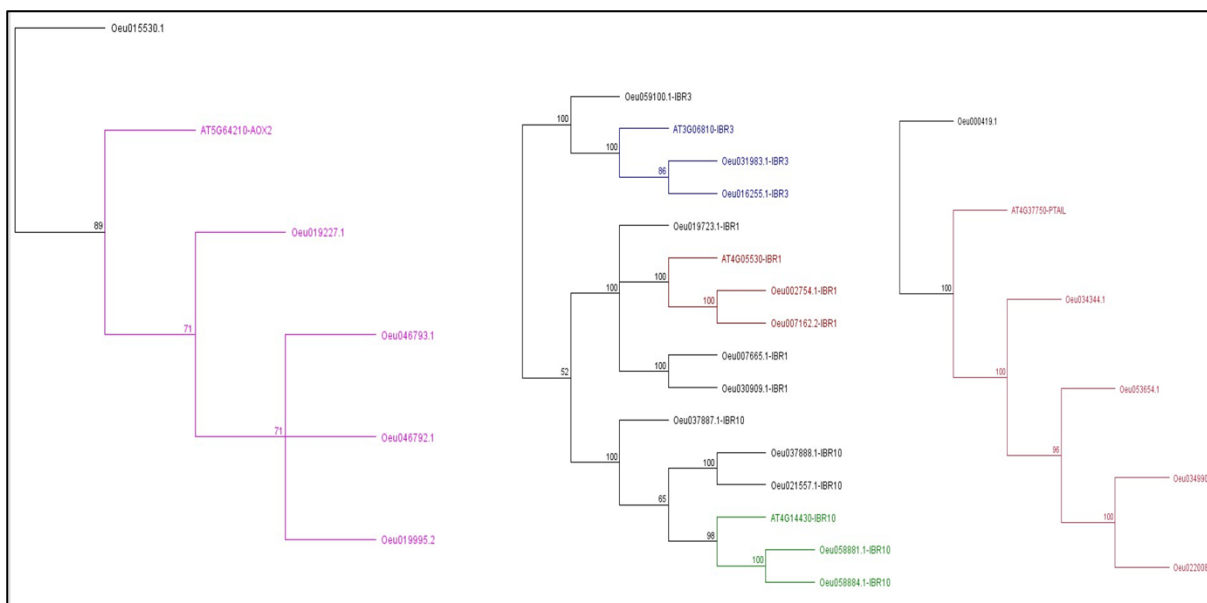


Figure 9. Phylogenetic (UPGMA) tree with sequences from the blastp and reference protein sequences (AtAOX2, AtAOX1, AtIBR1, AtIBR3, AtIBR10, AtPtAIL1).

Table 10

Primers used in gene expression analysis.

Gene	Primer's Name	Sequences of primers
<i>AOX2</i>	AOX2_R	5' CCGGTAAGTTTCCCAAGGCATA 3'
	AOX2_F	5' GTGGTGGCAGAGAAGAAGGT 3'
<i>IBR3</i>	IBR3_R	5' CACCTGCCGCTTACAGTAGT 3'
	IBR3_F	5' CCCAAAGCTCCCAGGTGTAG 3'
<i>PtAIL1</i>	PTAIL3_R	5' GTTTGGCGCCATAGCTTGTG 3'
	PTAIL3_F	5' ACGGAGTAGGTGAAATGGGTG 3'
<i>IBR10</i>	EC11_R	5' TAAGGGCAGTGGGTCCATA 3'
	EC11_F	5' ACCGGCTTAACCCGATTCTG 3'
<i>ACT7a</i>	ACT7a_R	5' TTGCTTACGTGGCACTTGAC 3'
	ACT7a_F	5' AACGGAATCTCTCAGCTCCA 3'
<i>OUB2</i>	OUB2_R	5' CCACGACTCAACAGAGACGA 3'
	OUB2_F	5' GCTGGAGGATGGAAGGACTC 3'
<i>IBR1</i>	IBR1_F	5'GGGAGATCTACAAGAGGCAGCT 3'
	IBR1_R	5'TGGTCACCCCATACATAGCCAA 3'

## 4.2. Preparing cuttings and IBA treatment

After receiving the IBA, NAA, and IBA-NAA treatments, cuttings were planted in pots containing perlite and placed in the appropriate settings. On days 24th hour, 7th day, and 15th day, RNA isolation was performed using the IBA-treated parts of the cuttings. (Figure 7)

## 4.3. Gene expression analysis

### 4.3.1 RNA isolation

Total RNA was isolated using the Purelink RNA Mini Kit (Invitrogen – 12183-018A) and TRIzol (Thermo Fischer-15596026). After total RNA was isolated, RNA concentrations were measured with Qubit 2.0 (Invitrogen-Q32866) (Table 11,12,13) and checked on an agarose gel (Figure 9). RNA were stored at -80°C until use. RNAs isolated for three periods determined from each treatment group were analyzed by agarose gel electrophoresis and when the rRNA bands were examined, it was observed that there was no degradation and no genomic DNA contamination.

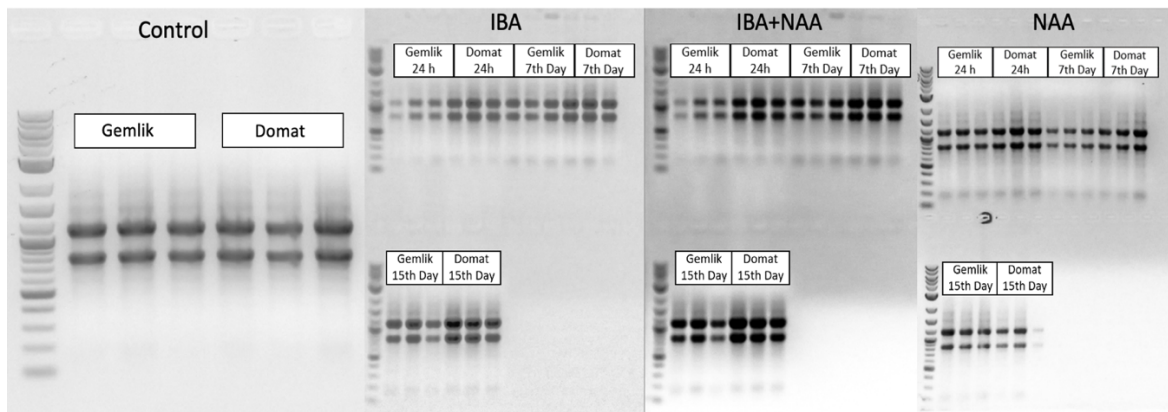


Figure 10. Visualized of isolated RNAs under UV light.

Table 11

Qubit results of the treated with the IBA samples

<b>Sample</b>	<b>Biological replicates</b>	<b>Concentration ng/μl</b>
Control (Domat)	1	466
	2	236
	3	430
Control (Gemlik)	1	670
	2	674
	3	462
24. Hour (Domat)	1	356
	2	496
	3	386
24. Hour (Gemlik)	1	226
	2	210
	3	170
7th Day (Domat)	1	306
	2	394
	3	346
7th Day (Gemlik)	1	310
	2	288
	3	300
15th Days (Domat)	1	264
	2	240
	3	216
15. Days (Gemlik)	1	894
	2	766
	3	474



Table 12

Qubit results of the treated with NAA and IBA samples

<b>Sample</b>	<b>Biological replicates</b>	<b>Concentration ng/<math>\mu</math>l</b>
Control (Domat)	1	466
	2	236
	3	430
Control (Gemlik)	1	670
	2	674
	3	462
24. Hour (Domat)	1	310
	2	186
	3	354
24. Hour (Gemlik)	1	218
	2	290
	3	276
7. Days (Domat)	1	522
	2	366
	3	680
7. Days (Gemlik)	1	260
	2	334
	3	270
15. Days (Domat)	1	514
	2	668
	3	802
15. Days (Gemlik)	1	358
	2	388
	3	448

Table 13

Qubit results of the treated with NAA samples

<b>Sample</b>	<b>Biological replicates</b>	<b>Concentration ng/<math>\mu</math>l</b>
Control (Domat)	1	466
	2	236
	3	430
Control (Gemlik)	1	670
	2	674
	3	462
24. Hour (Domat)	1	520
	2	800
	3	498
24. Hour (Gemlik)	1	364
	2	374
	3	292
7. Days (Domat)	1	518
	2	514
	3	720
7. Days (Gemlik)	1	184
	2	214
	3	228
15. Days (Domat)	1	280
	2	328
	3	492
15. Days (Gemlik)	1	582
	2	318
	3	554

### 4.3.2 Determination of gene expressions

The gene expression analyses were studied, which genes were responsible for adventitious rooting, from the tissues collected on the days (24th hour, 7th, and 15th days) coinciding with the different stages of AR (Pacurar et al., 2014) from IBA and NAA treated cuttings of Gemlik (easy to root) and Domat (difficult to root) cultivars. For this purpose, the efficiencies of the primers were calculated by standard curve studies, and only primer pairs with 90–100% results were used. In addition, only primers with  $R^2$  values that showed the linearity of the standard curve above 0.98 were used.

Primers AOX2\_F 5'GTGGTGGCAGAGAAGAAGGT3' and AOX2\_R 5'CCGGTAAGTTTCCAAGGCATA3' were used for the *OeAOX2* gene. These primers' efficiency curves demonstrated that the reaction was efficient with a 95.8% yield (Figure 8). The curve was found to be sufficiently linear with an  $R^2$  value of 0.9965. After considering these findings, it was determined that the primers suitable for gene expression studies.

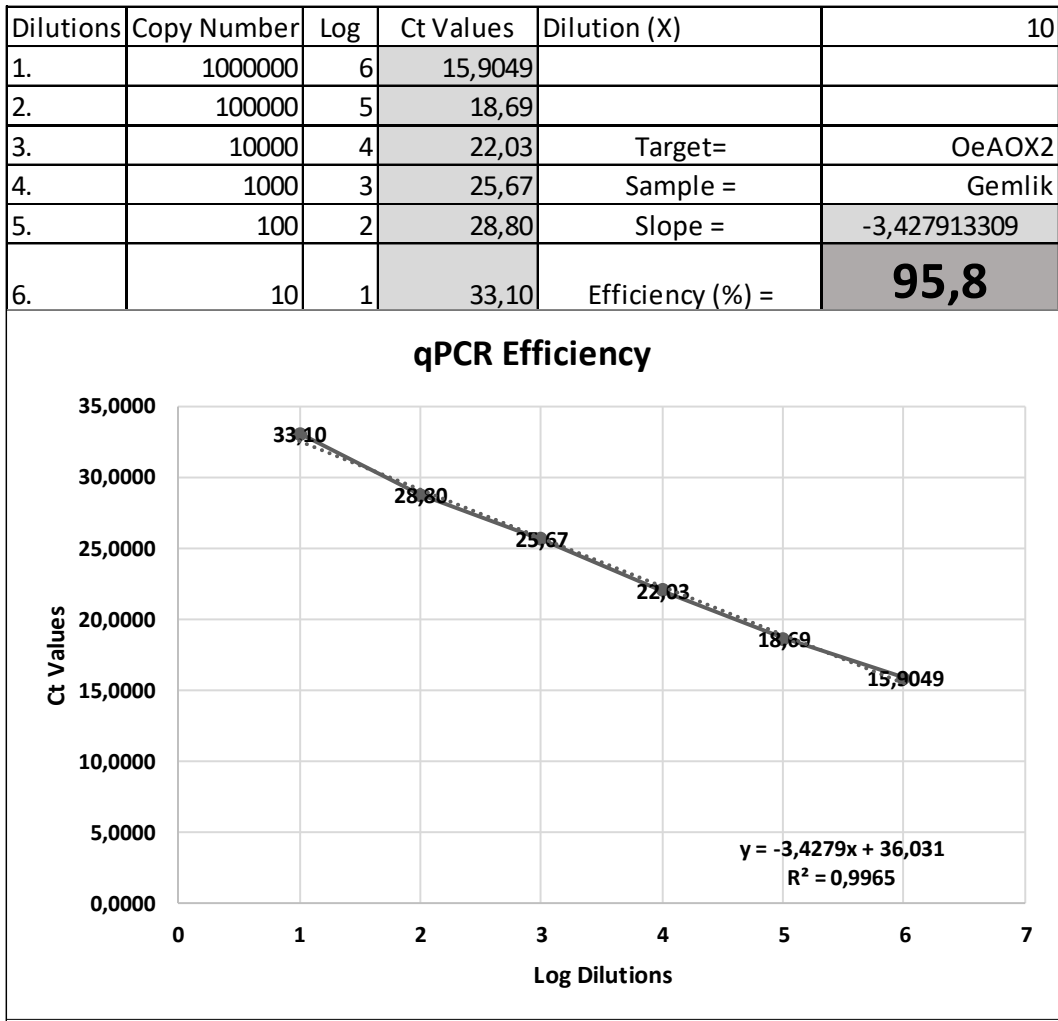


Figure 11. Results of standard curve experiments of the *OeAOX2* gene.

Primers IBR3\_F 5'CCCAAAGCTCCCAGGTGTAG3' and IBR3\_R 5'CACCTGCCGCTTACAGTAGT3' were used for the *OeIBR3* gene. These primers' efficiency curves demonstrated that the reaction was efficient with a 95.9% yield (Figure 9). The curve was found to be sufficiently linear with an R<sup>2</sup> value of 0.999. After considering these findings, it was determined that the primers suitable for gene expression studies.

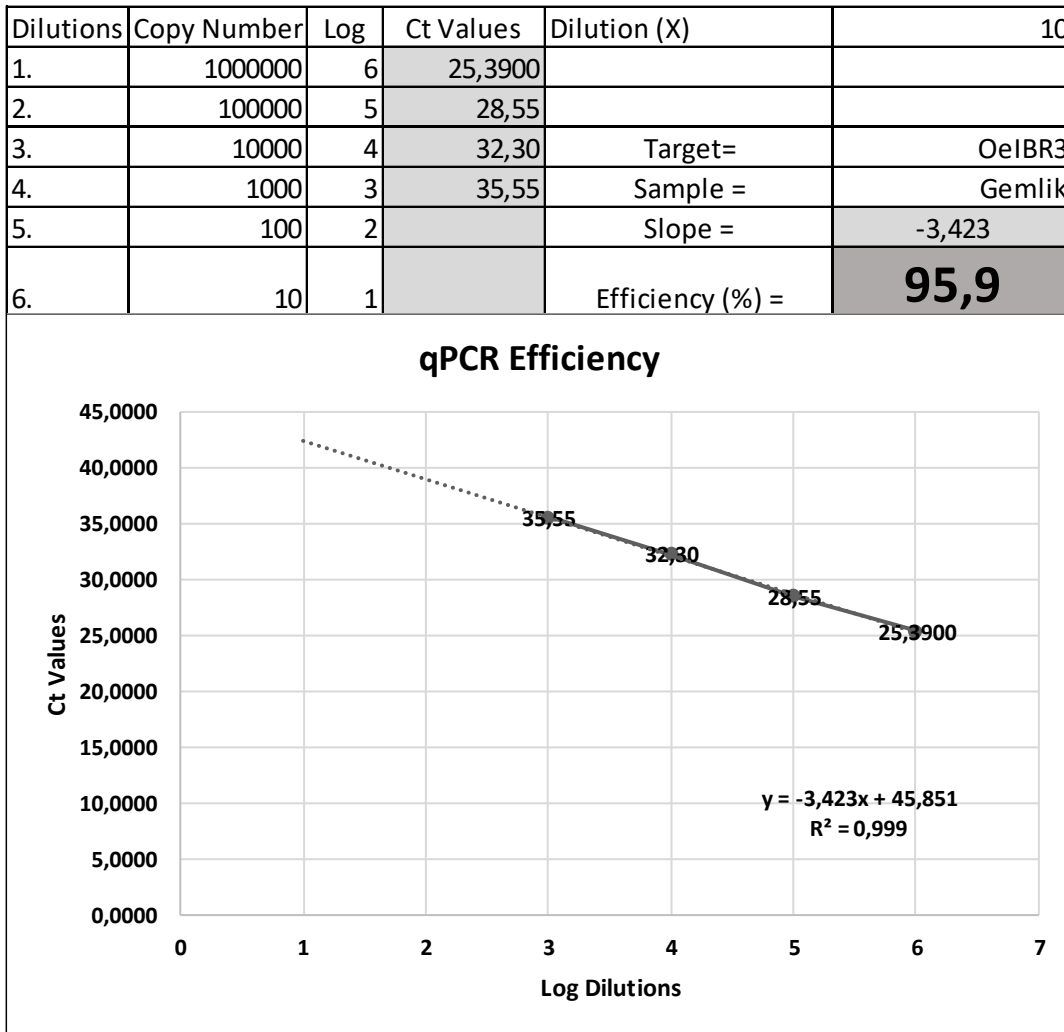


Figure 12. Results of standard curve experiments of the *OeIBR3* gene.

Primers IBR10\_R ‘TAAGGGCAGTGGGTCCCATA’ and IBR10\_F ‘ACCGGCTTAACCCGATTCTG’ were used for the *OeIBR10* gene. These primers' efficiency curves demonstrated that the reaction was efficient with a 100.3% yield (Figure 10). The curve was found to be sufficiently linear with an  $R^2$  value of 0.9966. After considering these findings, it was determined that the primers suitable for gene expression studies.

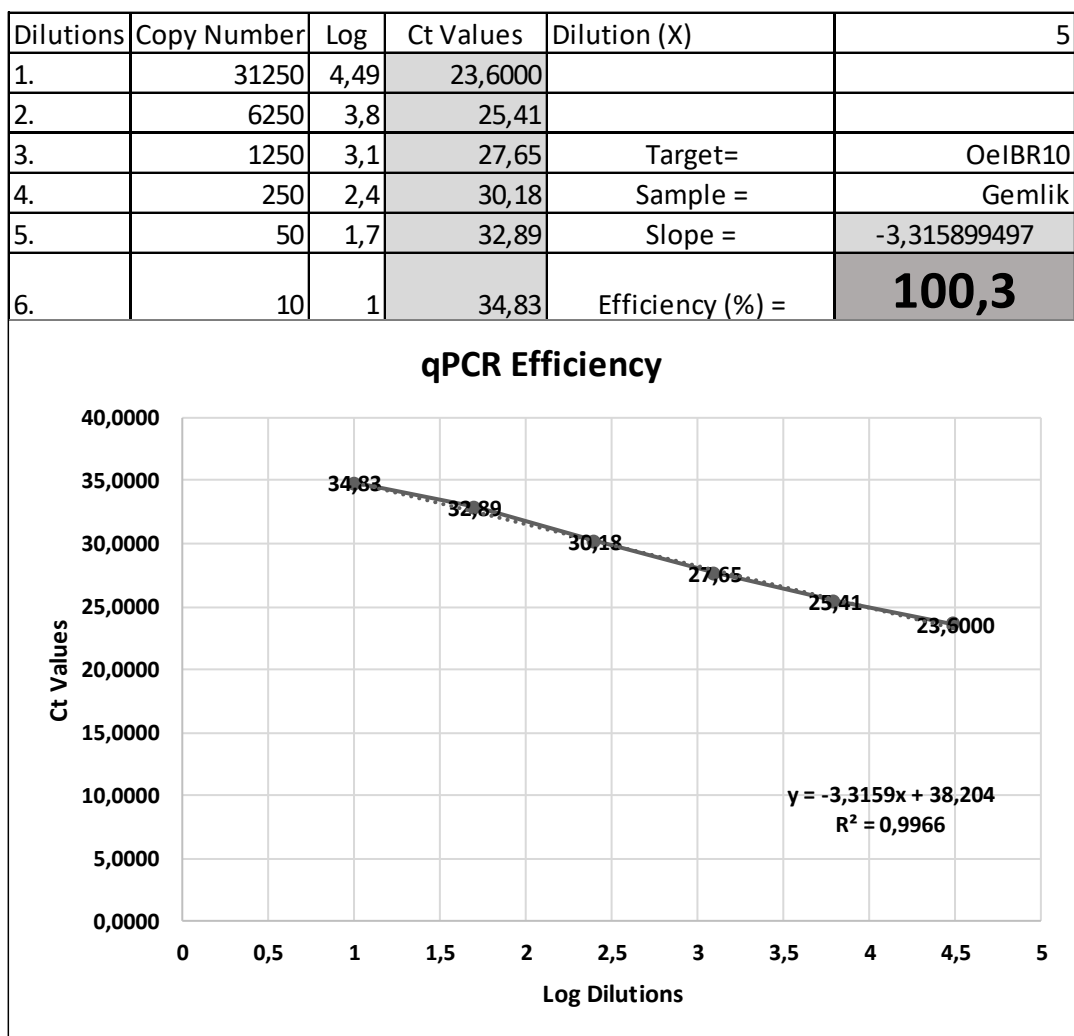


Figure 13. Results of standard curve experiments of the *OeIBR10* gene.

Primers PtAIL1\_F 5'ACGGAGTAGGTTGAAATGGGTG3' and PtAIL1\_R 5'GTTTGGCGCCATAGCTTGTG3' were used for the *OePtAIL1* gene. These primers' efficiency curves demonstrated that the reaction was efficient with a 92.1% yield (Figure 11). The curve was found to be sufficiently linear with an  $R^2$  value of 0.9953. After considering these findings, it was determined that the primers suitable for gene expression studies.

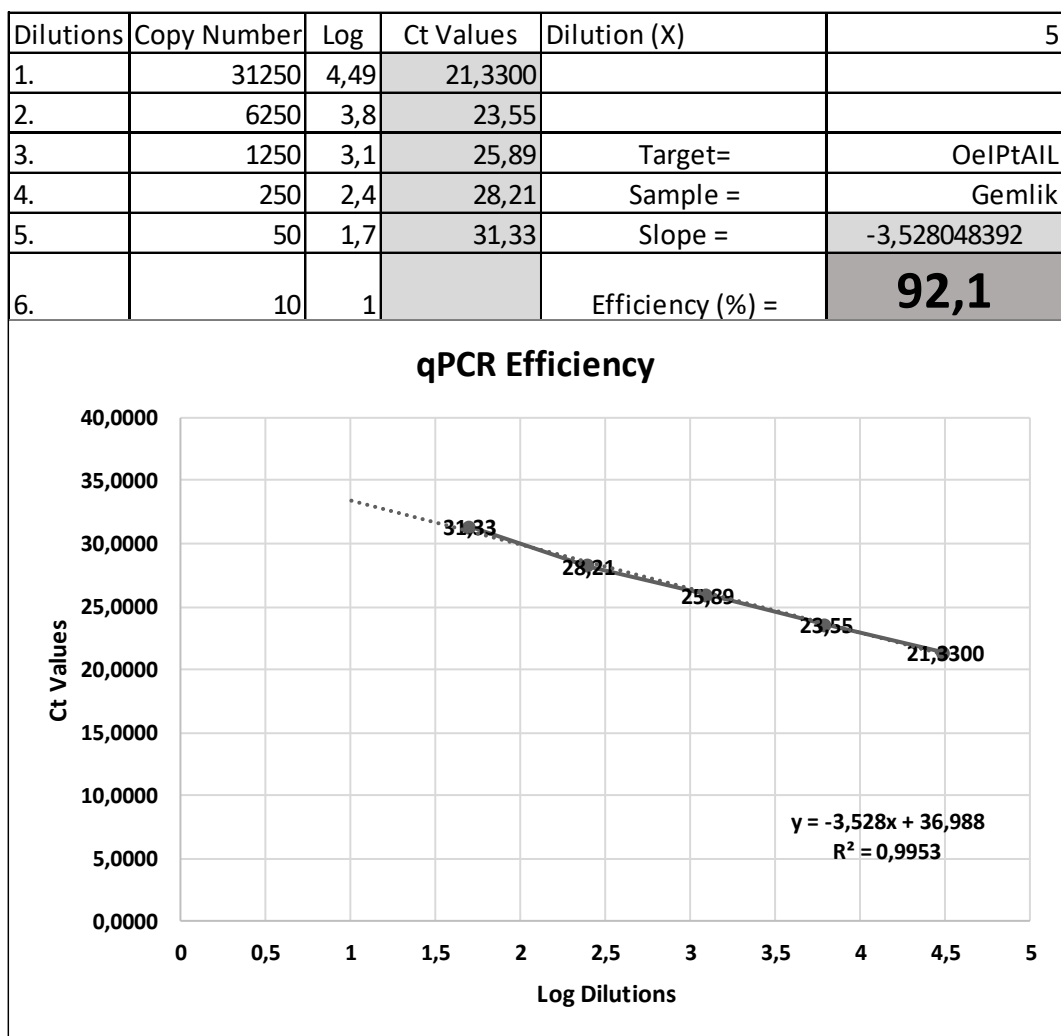


Figure 14. Results of standard curve experiments of the *OePtAIL1* gene.

Primers IBR1\_F 5'GGGAGATCTACAAGAGGCAGCT 3' and IBR1\_R 5'TGGTCACCCCATACATAGCCAA 3' were used for the *OeIBR1* gene. These primers' efficiency curves demonstrated that the reaction was efficient with a 95.2 % yield (Figure 12). The curve was found to be sufficiently linear with an  $R^2$  value of 0.9992. After considering these findings, it was determined that the primers suitable for gene expression studies.

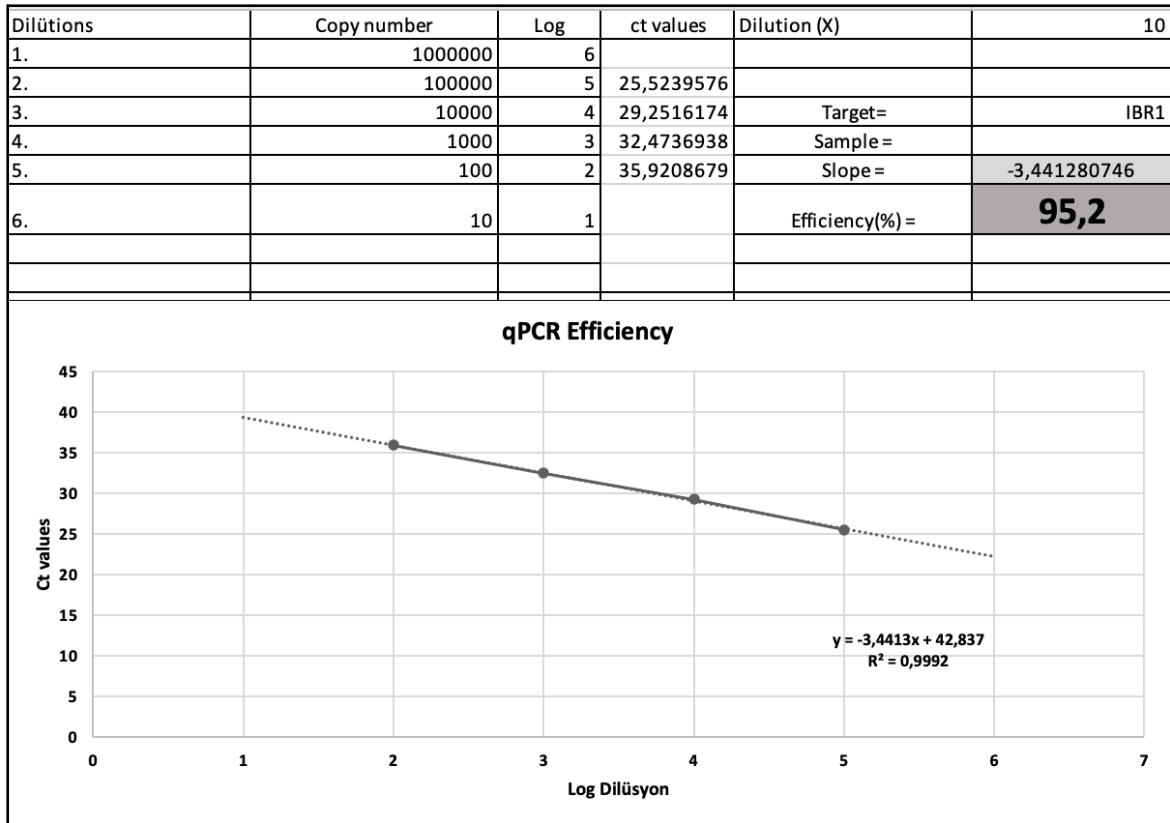


Figure 15. Results of standard curve experiments of the *OeIBR1* gene.

#### 4.3.2.1. Gene expression analysis after IBA treatment

*OeAOX2*, had higher expression in Gemlik than Domat within the control groups. After the initial 24 hours, the expression level of this gene in Gemlik cuttings decreased by half and then ceased. In the study, *OeAOX2* gene expression in the Domat cultivar was either low or not influenced by IBA treatment. These results suggest that regardless of IBA treatment, the *OeAOX2* gene expression is regulated differentially in hard-to-root olive cultivars. On the other side, it can be claimed that IBA suppresses the gene expression of *OeAOX2* in cultivars that are easy-to-root (Figure 13).



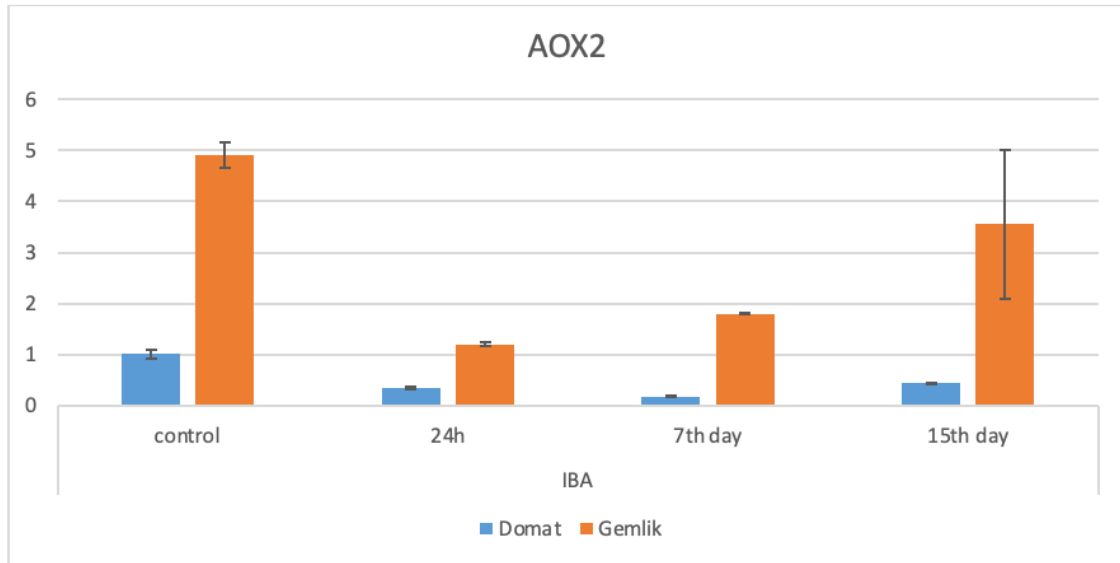


Figure 16. Gene expression results of *OeAOX2*. (Error bars represent standard error)

The *OeIBR10* gene, which is assumed to be in the role of converting IBA to IAA, showed the same levels of expression in both cultivars in the control groups that received no treatment, according to analysis of its expression results. Despite this, samples obtained 24 hours after IBA treatment showed a seven-fold increase in gene expression; however, this level did not persist over the course of the following days, and decreased. On the 7 days after the application of the IBA, an increase in the Gemlik cultivar was noted; however, gene expression stopped on the 15th day (Figure 14).

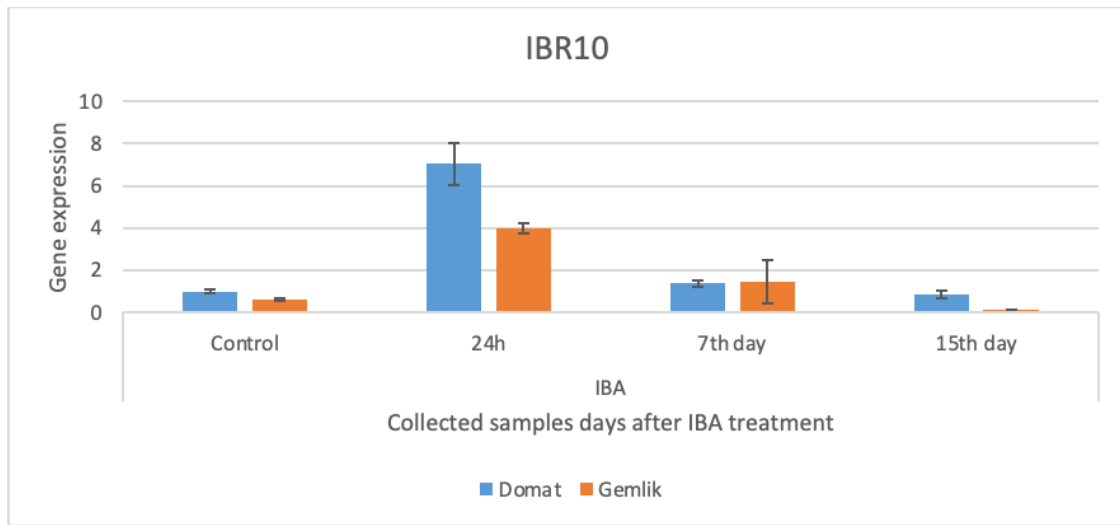


Figure 17. Gene expression results of *OeIBR10*. (Error bars represent standard error)

The *OeIBR3* gene is one of the genes thought to be responsible for the conversion of IBA to IAA. (Frick et al., 2018). Similar results are observed in both cultivars for *IBR3* gene expression. Even though Domat's gene expression was higher than Gemlik's in the control groups, both cultivars' gene expression decreased during the next few days (Figure 15).

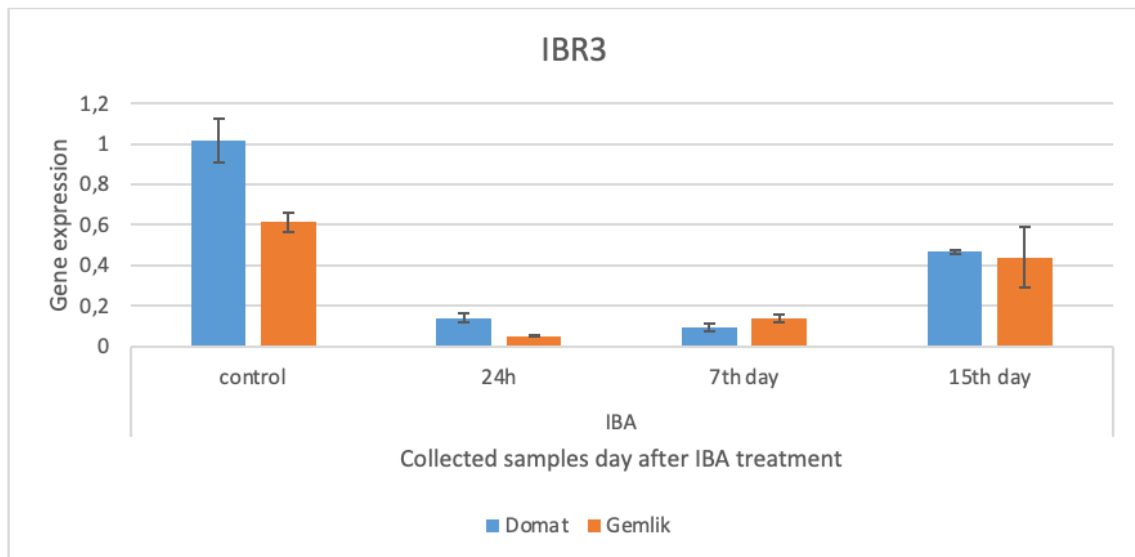


Figure 18. Gene expression results of *OeIBR3*. (Error bars represent standard error)

*OeIBR1* is a further gene that is believed to be involved in the conversion of IBA into IAA. both cultivars in the control groups that received no treatment had the same level of

gene expression. Gene expression was 4-fold higher in samples obtained 24 hours after IBA treatment, and this level persisted for the next few days. By the time samples were taken on the 15th day, however, gene expression had increased 10-fold compared to the control group. When examining the Gemlik variety, a 5-fold increase was seen in the 24th hour, but it decreased on the 7th day and stayed the same for the 15th day (Figure 16). These findings demonstrate that gene expression continues to increase in the difficult-to-root olive cultivar.

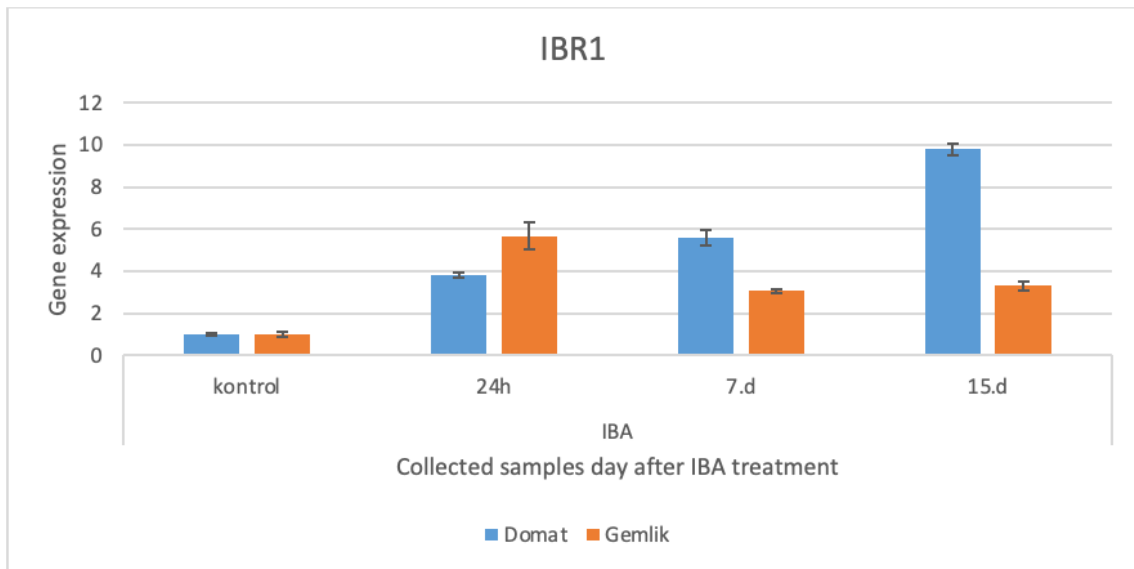


Figure 19. Gene expression results of *OeIBR1*. (Error bars represent standard error)

*OePTAIL1* is a transcription factor related to AR development. The expression in both groups was similar in the control and 24h. However, a significant decrease was observed at 7th days in Domat variety. In Gemlik, the expression level was close to one on the control, 24 h, and 7 days, but a significant decrease was observed on the 15th day.

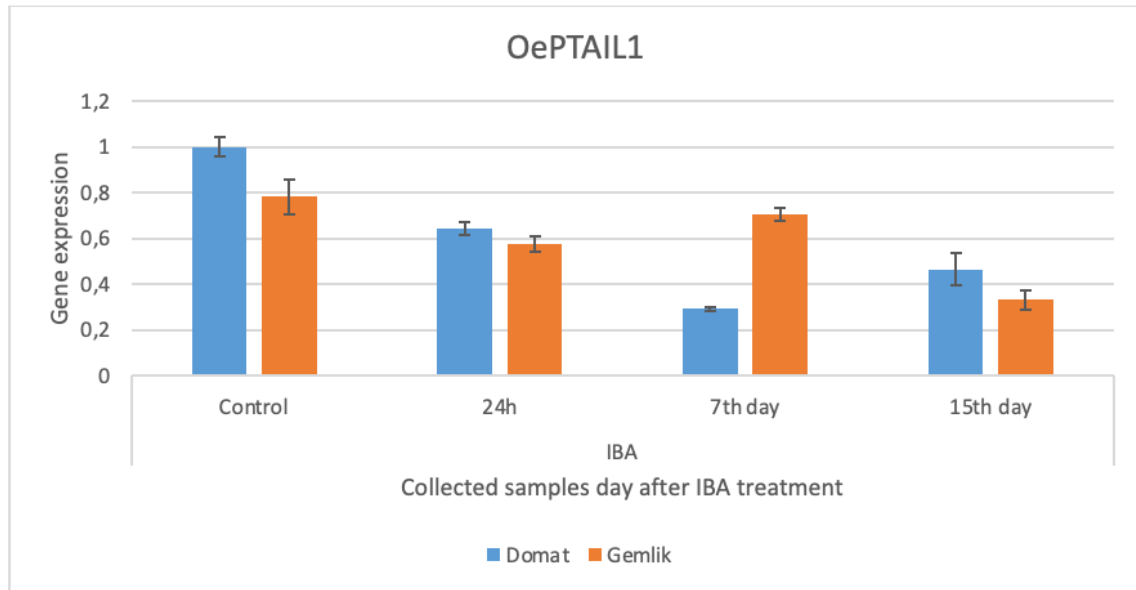


Figure 20. Gene expression results of *OePTAIL1*. (Error bars represent standard error)

#### 4.3.2.2. Gene expression analysis after IBA and NAA treatments

The expression of the *OeAOX2* gene in olive cuttings treated with two different auxin hormones. Compared to the easy-to-root "Gemlik" variety, there was a 5-fold increase in expression in the control groups from the difficult-to-root "Domat" variety. Although there was a decrease in gene expression in the Gemlik at the 24-hour mark, it increased over the next few days. When we examined the Domat variety, it became clear that the application had no effect on this gene's expression, which persisted at a low level (Figure 17).

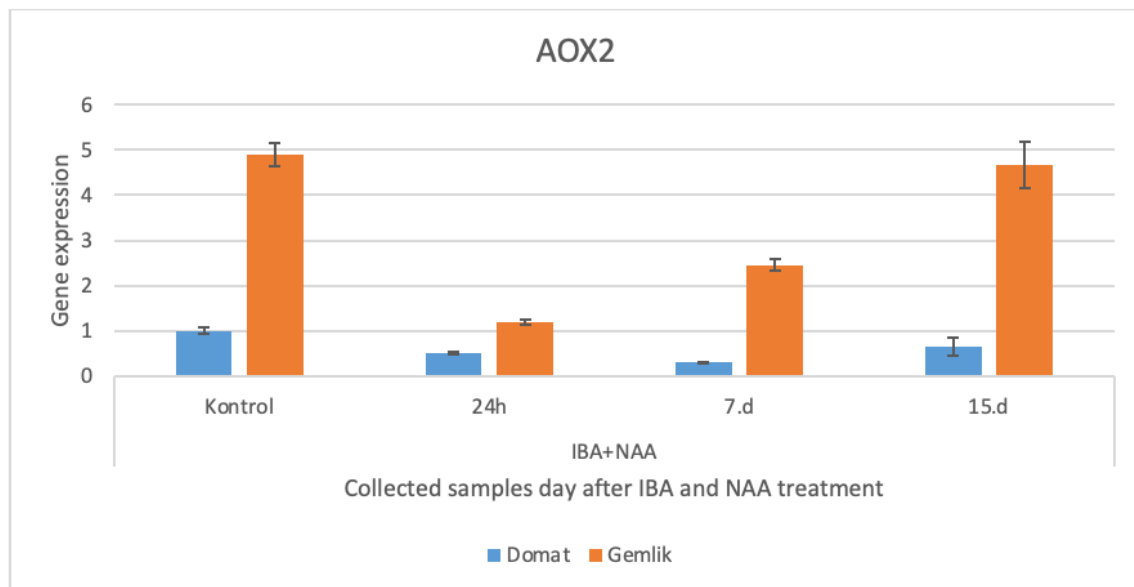


Figure 21. Gene expression results of *OeAOX2*. (Error bars represent standard error)

We noticed that the *OeIBR3* gene, which is assumed to be involved in the conversion of IBA into IAA, was expressed more in the Domat variety than in the Gemlik variety in the control groups when we looked at the gene expression results for this gene. Similar results were seen in both cultivars on the following days, with essentially no gene expression at the 24th hour and a slight increase in gene expression seen on days 7th and 15th (Figure 18).

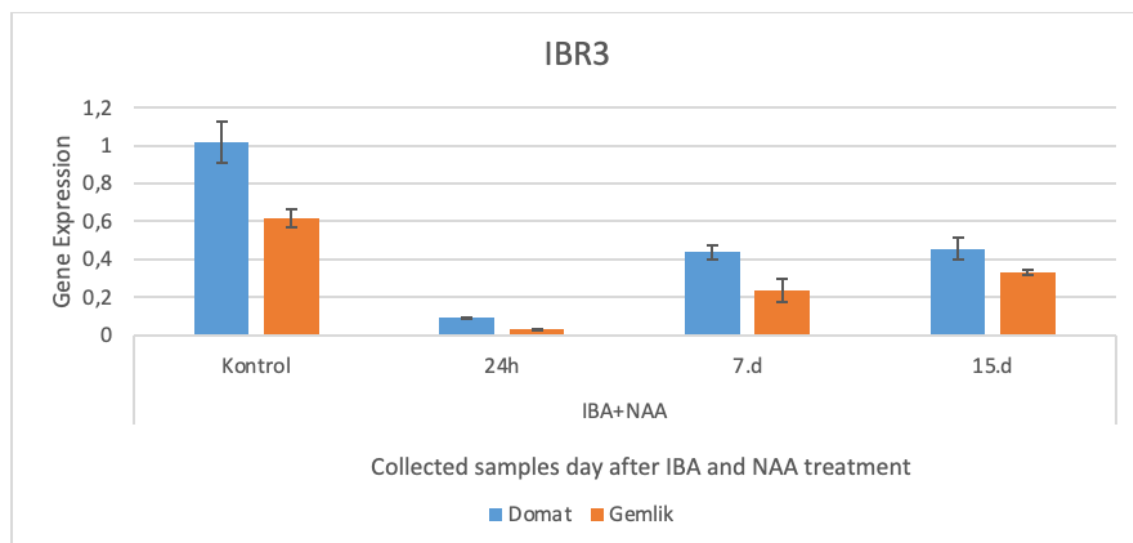


Figure 22. Gene expression results of *OeIBR3*. (Error bars represent standard error)

*OeIBR10* is another gene involved in the conversion of IBA into IAA. When we examined the gene expression data, we found that the gemlik cultivar's expression of this gene was low and even stopped entirely on the seventh day. It was noted that the gene expression in the Domat cultivar did not change until the 24th hour and then increased during the following days (Figure 19).

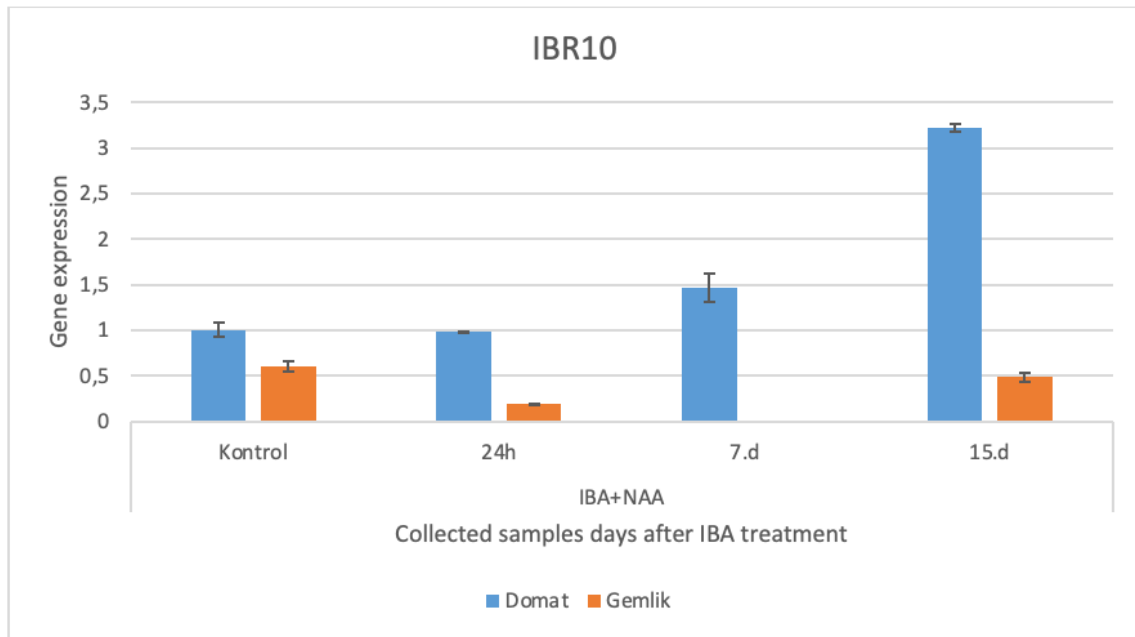


Figure 23. Gene expression results of *OeIBR10*. (Error bars represent standard error)

Examining the gene expression data for the *OePtAIL1* gene, which belongs to the AP2 transcription factor family and is related to adventitious roots, it was found that it was virtually at the same level in the control groups. At 24 hours, both varieties showed a decline, but the Gemlik cultivar's gene expression increased during the next few days (Figure 20).

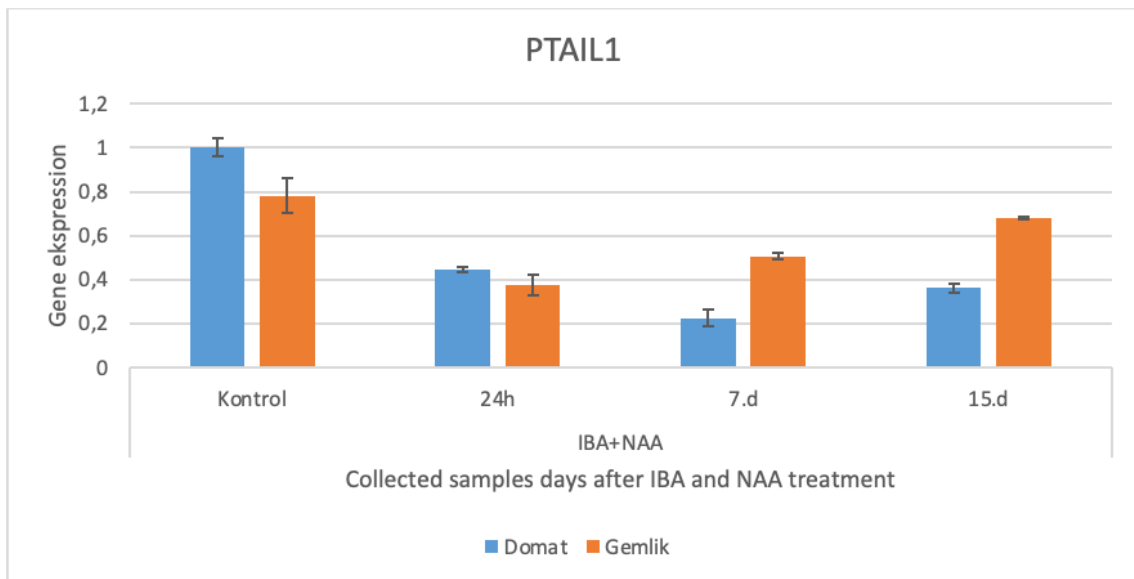


Figure 24. Gene expression results of *OePTAIL1*. (Error bars represent standard error)

*IBR1* plays a key role in the conversion of IBA to IAA. Gene expression results after the combination of IBA and NAA in the control groups were similar, but at 24h expressions was higher in both varieties and then decreased on the following days.

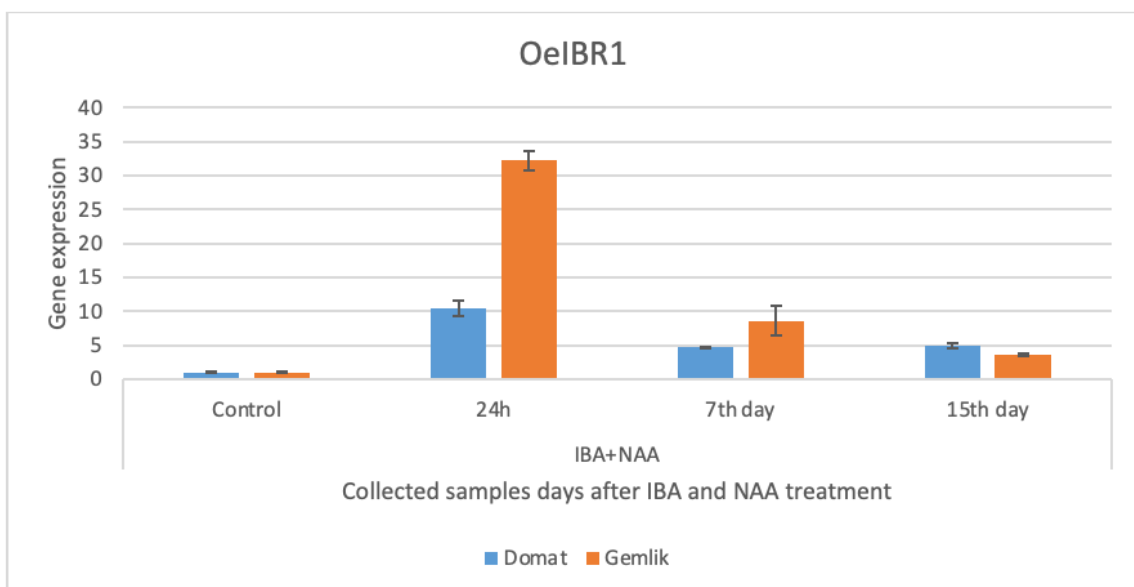


Figure 25. Gene expression results of *OeIBR1*. (Error bars represent standard error)

#### 4.3.2.3. Gene expression analysis after NAA treatment

In the gene expression studies performed as a result of the treatment of NAA, a synthetic plant hormone from the auxin family, to olive cuttings, it was observed that the *OeAOX2* gene was expressed 5-fold more in the Gemlik cultivar than in the control groups. At the 24th hour, the Gemlik cultivar showed a decrease, although gene expression increased over the next days. In the Domat variety, gene expression almost stopped at the 24th hour and 7th day, and increased on the 15th day (Figure 21).

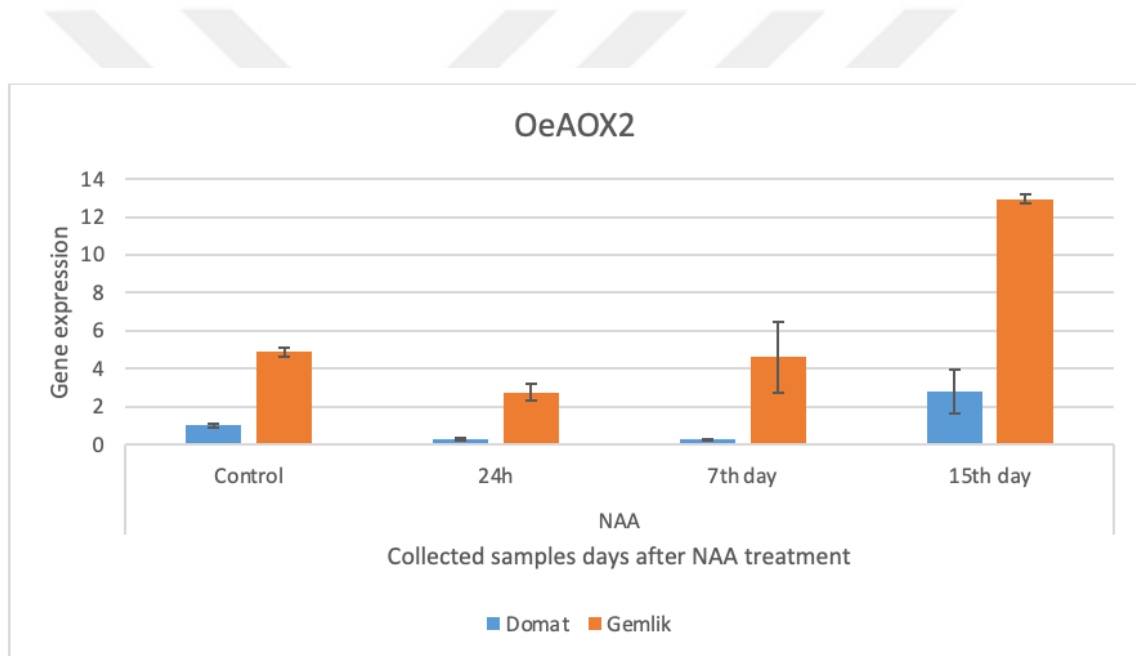


Figure 26. Gene expression results of *OeAOX2*. (Error bars represent standard error)

The *OeIBR1* gene expression levels in both cultivars in the control groups were the same level. Although there was a decrease in the Domat variety at the 24th hour, it was observed that the gene expression continued to increase in the following days. Following the application of NAA to the Gemlik cultivar, a decrease in gene expression was seen (Figure 22). Considering this result, it is believed that NAA treatment inhibits the expression of this gene.



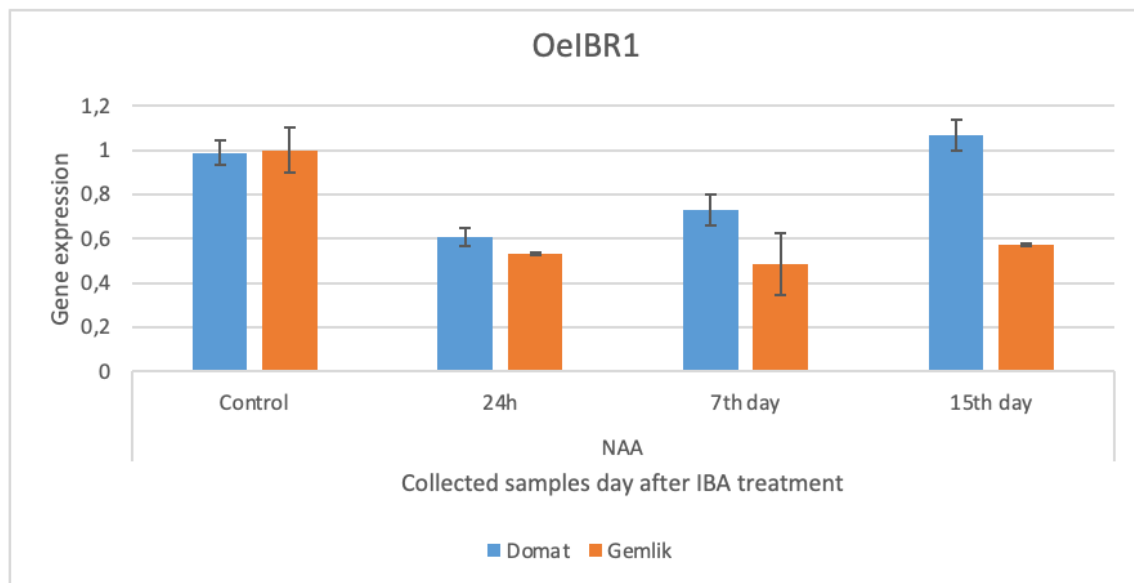


Figure 27. Gene expression results of OeIBR1. (Error bars represent standard error)

The *OeIBR10* gene's expression was found to be higher in the control groups in the Domat variety when it was examined following NAA treatment. Gene expression in the Gemlik cultivar did not change after 24 hours and stopped entirely after 7 days. Gene expression in the Domat cultivar increased in the 24th hour, decreased over the next days, but it never stopped (Figure 23).

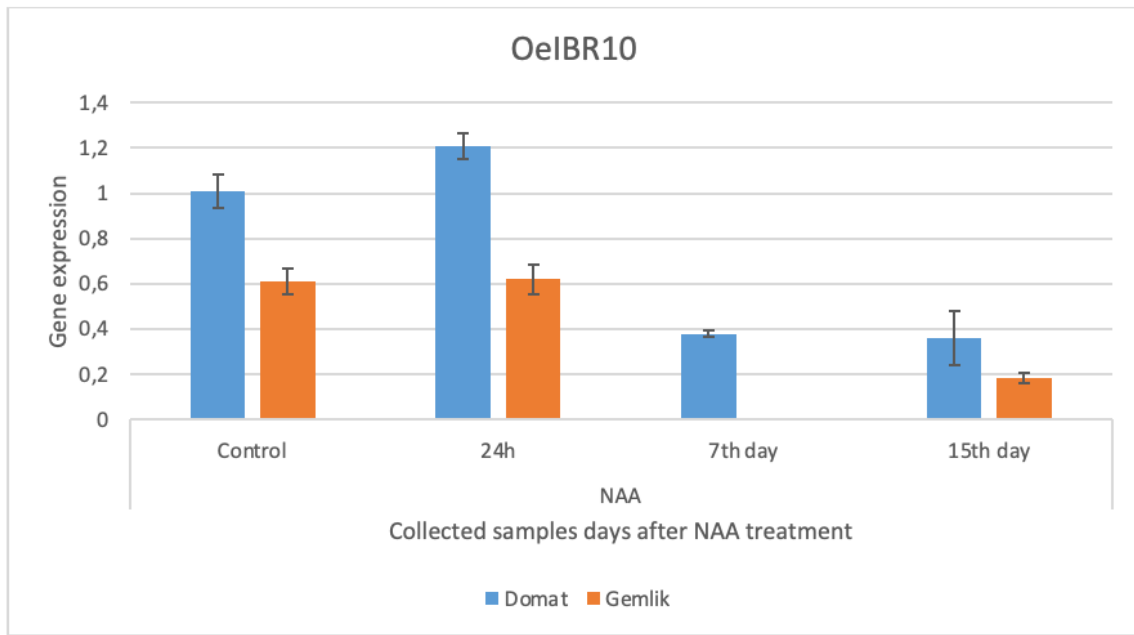


Figure 28. Gene expression results of OeIBR10. (Error bars represent standard error)

When the gene expression results of the OeIBR3 gene were examined, the gene expression in Domat cultivar almost stopped at the 24th hour compared to the control group, and then continued to increase. Similar results were observed in the gemlik cultivar (Figure 24). According to these results, it is thought that NAA treatment suppresses the expression of this gene.

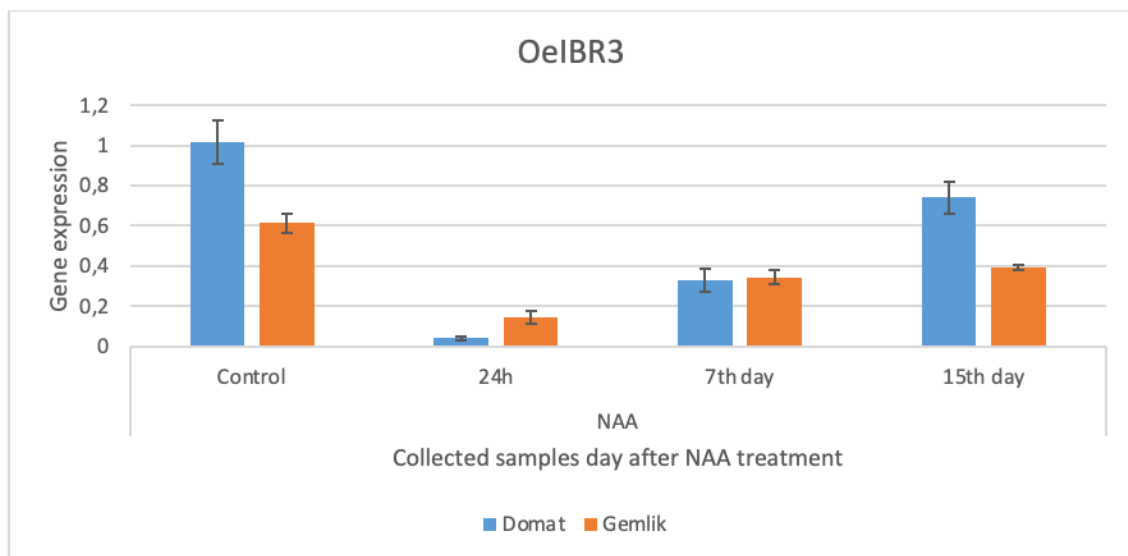


Figure 29. Gene expression results of OeIBR3. (Error bars represent standard error)

When the expression results of the transcription factor *OePTAIL1* were examined, it was determined that the expression levels were similar in the control groups of both cultivars. In both cultivars, it was observed that gene expression almost stopped on the 24th hour and 7th day. An increase was observed in the Gemlik variety on the 15th day (Figure 25). These results show that *OePtAIL1* gene expression levels in difficult and easily rooted olive cultivars decreased after NAA treatment.

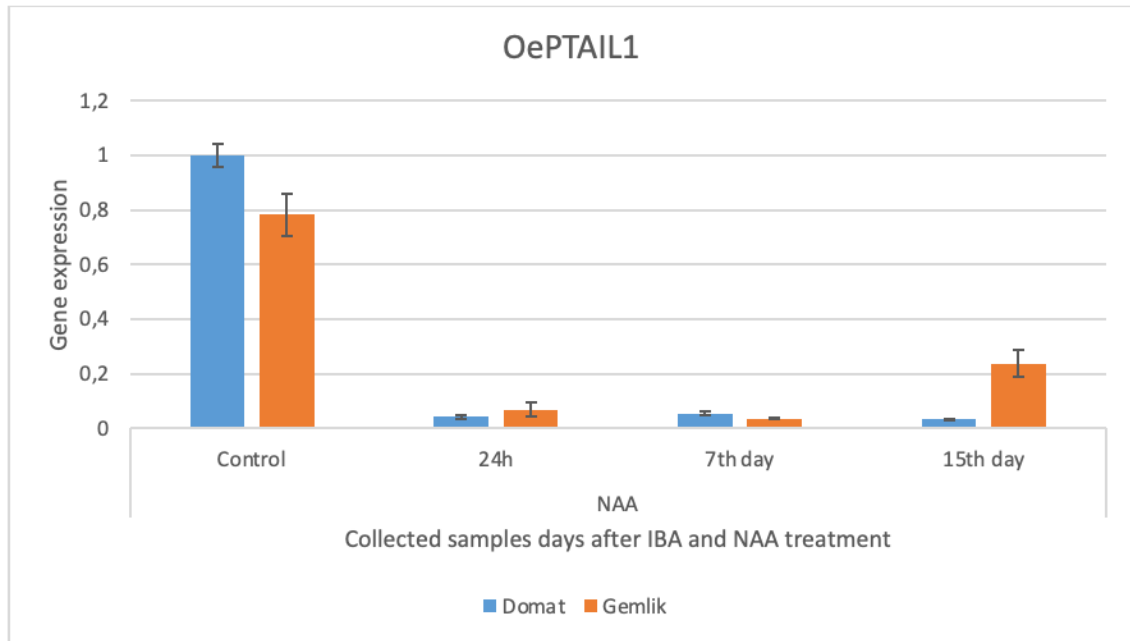


Figure 30. Gene expression results of *OePTAIL1*. (Error bars represent standard error)

### 4.3.3. Gene sequence analysis

#### 4.3.3.1 Plant materials and RNA isolations

From the shoot tips, stems, and leaves of the Domat and Gemlik cultivars, RNA was extracted. Following the isolation of total RNA, RNA concentrations (Table 14) were determined using Qubit 2.0 (Invitrogen-Q32866) and confirmed on an agarose gel. RNAs were stored at  $-80^{\circ}\text{C}$ . The extracted RNAs were found to have concentrations between 516 and 640  $\text{ng}/\mu\text{l}$  and were at a suitable level for later research in terms of degradation and DNA contamination.

Table 14

Qubit-measured RNA concentrations obtained for sequence analysis

Sample	Concentration ng/ $\mu$ l
Domat	516
Gemlik	640

#### 4.3.3.2. PCR studies for sequencing

In order to amplify the targeted gene region, PCR was performed and used the produced cDNAs as templates. To optimize the various binding temperatures of the primers for PCR studies, gradient PCR was done. The primers used for PCR are listed below. (Table 15)

Table 15

Primer sequences for the PCR

Gene	Primer name	Primer sequence	PCR product size
<i>AOX2</i>	OeAOX2_FL_R	5' AGGCACCGAAGAACAACCTT 3'	1200
	OeAOX2_FL_F	5' GTTTGATGAGGCGATGATTG 3'	
<i>IBR3</i>	IBR3_FL1_F	5' ATCGTGGCAGTATCCTATGC 3'	1584
	IBR3_FL3_R	5' ACAAGTCCACAGGCCTCC 3'	
	IBR3_FL2_F	5' TGCTTCAGGAGGACATCGTG 3'	1561
	IBR3_FL4_R	5' CATGCCGCCTTCACAACATG 3'	
<i>PtAIL1</i>	OePTAIL.1_FL_F	5' GGAATGCAGGAAGAATGCCC 3'	1201
	OePTAIL.1_FL_R1	5' TGAGCAACCTTCTCAGAATC 3'	
	OePTAIL.1_FL_F	5' GGAATGCAGGAAGAATGCCC 3'	2230
	OePTAIL.1_FL_R2	5' ACTTGAGACTTCATCTGGGC 3'	
<i>IBR10</i>	IBR10_BOTH_R	5' ACCCATAGCTGCCTCACAAAC 3'	748
	IBR10_BOTH_F	5'CGGCGACAACAAAGATGAGC 3'	
	IBR102.1_FL_F	5' ACCACCATGTGCACGTTAG 3'	902
	IBR102.1_FL_R	5' AAACCCTAATAAAGACGACC 3'	
	IBR102.2_FL_R	5' CCAAGAAACATTTGAGATTC 3'	834
	IBR102.2_FL_F	5' CGGCGACAACAAAGATGAGC 3'	

Agarose gel electrophoresis was used to evaluate the PCR results, and service procurement was used to execute sequence analyses on all products with expected sizes and sufficient concentrations.

Agarose gel electrophoresis was performed with a 1 kb DNA Ladder (Thermo Scientific - SM0311) and PCR products with sufficient concentration; if don't have any non-specific products, these were purified using the PCR Purification Kit (Invitrogen, K310001).

At the results of Gemlik variety, the *OeAOX2* gene was amplified using PCR, and the predicted product size (1200 base pairs) was obtained. 1201 and 2230 base pair products were expected from the PtAIL1\_R1 and PtAIL1\_R2 primer pairs. When the gel results were examined, it was seen that the products were of the expected size. The expected result of the OeIBR10 B, OeIBR10 2.1, and OeIBR10 2.2 primer pairs is 748, 902, and 834 base pairs, respectively. It was seen that the PCR products were of the expected size on the gel (Figure 26). The *OeAOX2*, *OeIBR10 B*, and *OeIBR10 2.2* genes had nonspecific products, therefore they were extracted from the gel and the sequencing analysis was performed with service procurement. For the *OeIBR3* gene, on the other hand, PCR was repeated with different primer pairs and confirmed by agarose gel electrophoresis because the expected size product could not be obtained (Figure 27).

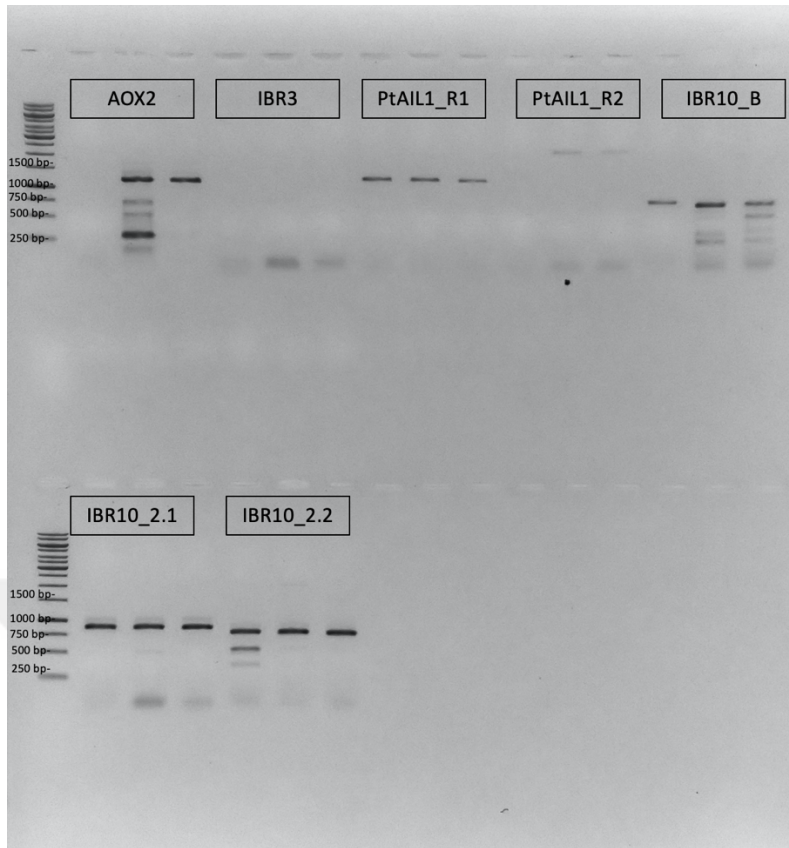


Figure 31. Agarose gel electrophoresis images of Gemlik variety PCR products (1 kb DNA Ladder (Thermo Scientific - SM0311))

The *OeIBR3* and *OePtAIL R2* primers produced products in the predicted sizes (1584 and 1561 base pairs), which were extracted from the gel. Using the Quick PCR Purification Kit, the products *OeAOX2*, *OePTAIL1*, and *IBR10* were purified (Invitrogen, K310001).



Figure 32. Agarose gel electrophoresis images of Gemlik variety PCR products (1 kb DNA Ladder (Thermo Scientific - SM0311))

PCR was performed using the same primer pairs from the cDNA templates of the Domat variety, and the PCR products obtained were visualized by agarose gel electrophoresis (Figure 28).

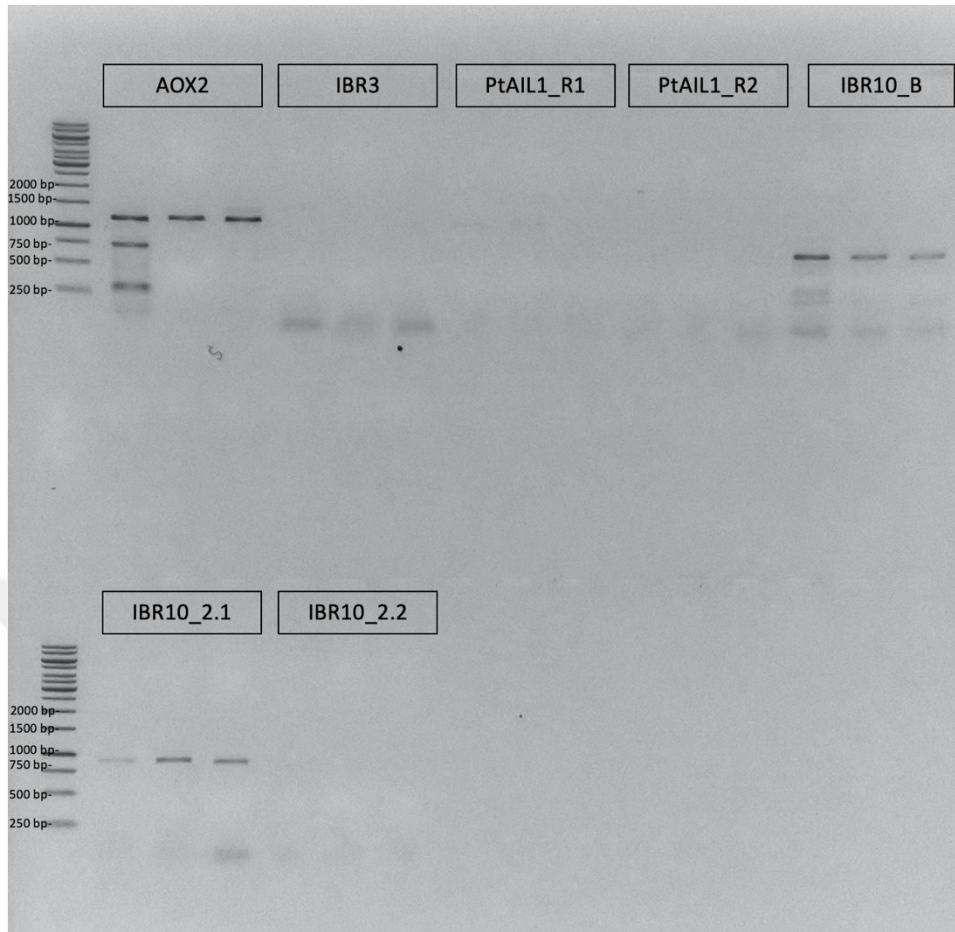


Figure 33. Agarose gel electrophoresis images of Domat variety PCR products (1 kb DNA Ladder (Thermo Scientific - SM0311))

When the PCR results were examined, it became clear that the PCR products for the *OeAOX2* and *OeIBR10* genes were as predicted. Sequence analysis was performed after products were purified using the Quick PCR Purification Kit (Invitrogen, K310001). Experiments were repeated with different combinations of primers IBR3\_FL1\_F, IBR3\_FL2\_F, IBR3\_FL3\_R, and IBR3\_FL4\_R for the *OeIBR3* gene that produced no product. (Figure 29).



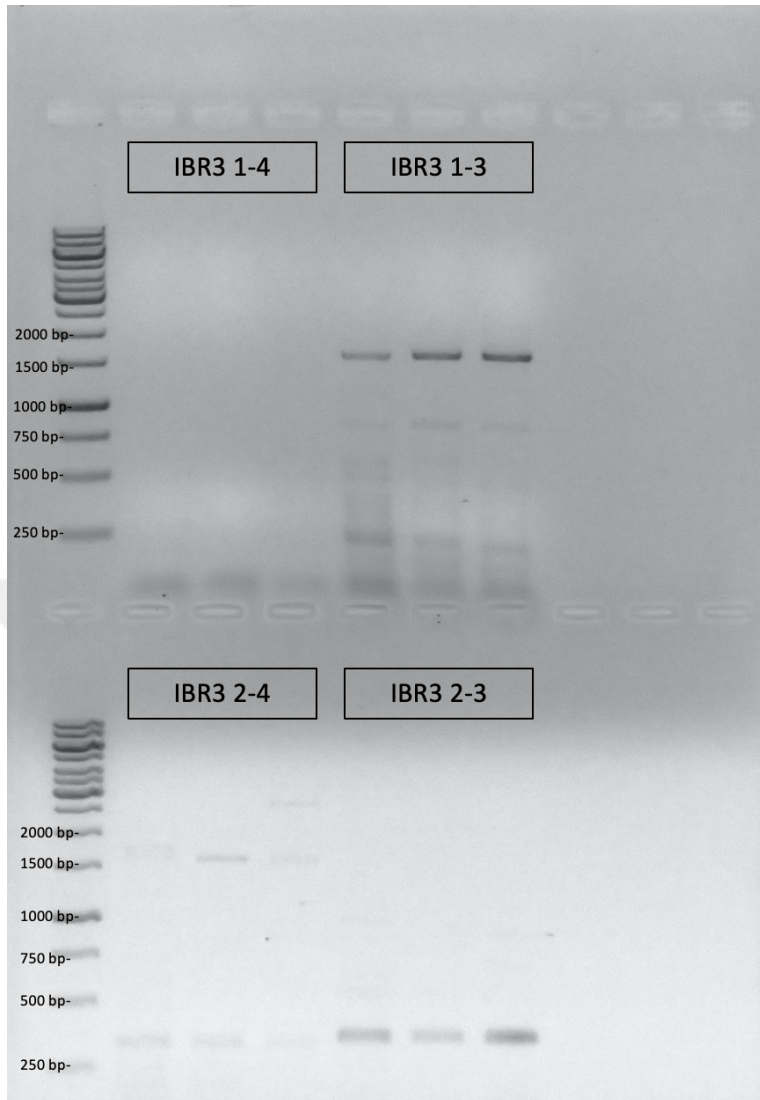


Figure 34. Agarose gel electrophoresis images of Domat variety PCR products (1 kb DNA Ladder (Thermo Scientific - SM0311))

When the PCR data were examined, it was found that using the IBR3\_FL1\_F and IBR3\_FL3\_R primer pairs products were the expected size. Following the extraction of PCR products from the gel, and the sequencing analysis was performed with service procurement.

#### 4.3.3.3. Bioinformatic analysis

After filtering the genes in terms of sequence analysis and quality scores, 600 base-pair products were obtained in the Domat and Gemlik cultivars of the *OeIBR3* gene. For the *OeIBR10* gene, 826 base-pair transcript products were obtained in the Domat cultivar and 843 base-pair products in the Gemlik cultivar. In the *OeAOX2* gene, a product with a length

of 1114 base pairs was obtained in the Domat cultivar and 1081 base pairs in the Gemlik cultivar. Blast analysis results confirmed that the correct products were amplified in PCR studies. The *OeAOX2* sequences obtained in our study are similar to the ubiquinol oxidase genes in the olive genome (Figure 30). For AOX2 genes, the names ubiquinol oxidase (NP\_0011312251.1) and alternative oxidase 2 (NP\_201226.2) are used in the literature. The Gemlik and Domat sequences show 94.5% and 93.6% similarity with the lowest E value (0) sequences. Similarly, *OeIBR3* sequences of PCR products performed with primers designed for *OeIBR3* showed high similarity (89.8% and 89.3%) to the *IBR3* gene in Gemlik and Domat cultivars. In the blast results of the products obtained with the *OeIBR10* primers, it was observed that there was high similarity (84.1%) with the enoyl-CoA delta isomerase gene.(Figure 35) Enoyl-CoA delta isomerase is another name for the *IBR10* gene (AT4G14430).

Query #	Name	Description	E Value	% Identical Sites	% Pairwise Identity	Query coverage
OeAOX2-DOMAT	XP_022857401.1	ubiquinol oxidase, mitochondrial-like [Olea europaea var. sylvestris]	0	94.2%	94.5%	79.25%
OeAOX2-DOMAT	XP_022881346.1	ubiquinol oxidase 2, mitochondrial-like isoform X1 [Olea europaea var. sylvestris]	2.39e-126	72.9%	72.9%	61.73%
OeAOX2-DOMAT	XP_022881347.1	ubiquinol oxidase 2, mitochondrial-like isoform X2 [Olea europaea var. sylvestris]	5.49e-137	72.2%	72.2%	66.85%
OeAOX2-DOMAT	XP_022881348.1	ubiquinol oxidase 2, mitochondrial-like isoform X2 [Olea europaea var. sylvestris]	5.49e-137	72.2%	72.2%	66.85%
OeAOX2-DOMAT	XP_022881349.1	ubiquinol oxidase 2, mitochondrial-like isoform X2 [Olea europaea var. sylvestris]	5.49e-137	72.2%	72.2%	66.85%
OeAOX2-GEMLIK	XP_022857401.1	ubiquinol oxidase, mitochondrial-like [Olea europaea var. sylvestris]	0	93.6%	93.9%	78.39%
OeAOX2-GEMLIK	XP_022881346.1	ubiquinol oxidase 2, mitochondrial-like isoform X1 [Olea europaea var. sylvestris]	1.34e-126	72.9%	72.9%	63.43%
OeAOX2-GEMLIK	XP_022881347.1	ubiquinol oxidase 2, mitochondrial-like isoform X2 [Olea europaea var. sylvestris]	4.68e-137	72.2%	72.2%	68.70%
OeAOX2-GEMLIK	XP_022881348.1	ubiquinol oxidase 2, mitochondrial-like isoform X2 [Olea europaea var. sylvestris]	4.68e-137	72.2%	72.2%	68.70%
OeAOX2-GEMLIK	XP_022881349.1	ubiquinol oxidase 2, mitochondrial-like isoform X2 [Olea europaea var. sylvestris]	4.68e-137	72.2%	72.2%	68.70%
OeIBR3-DOMAT	XP_022856292.1	probable acyl-CoA dehydrogenase IBR3 isoform X1 [Olea europaea var. sylvestris]	6.65e-124	89.3%	89.3%	98.00%
OeIBR3-DOMAT	XP_022856293.1	probable acyl-CoA dehydrogenase IBR3 isoform X2 [Olea europaea var. sylvestris]	1.02e-125	89.8%	89.8%	98.00%
OeIBR3-DOMAT	XP_022864244.1	transmembrane 9 superfamily member 1-like [Olea europaea var. sylvestris]	1.64e+00	44.1%	44.1%	15.00%
OeIBR3-DOMAT	XP_022865309.1	transcription repressor OFP6-like [Olea europaea var. sylvestris]	6.29e+00	30.6%	30.6%	23.50%
OeIBR3-DOMAT	XP_022883598.1	uncharacterized protein LOC111400411 [Olea europaea var. sylvestris]	4.10e+00	34.9%	34.9%	20.50%
OeIBR3-GEMLIK	XP_022841817.1	probable DNA helicase MCMB isoform X1 [Olea europaea var. sylvestris]	4.82e-01	27.3%	27.3%	42.00%
OeIBR3-GEMLIK	XP_022841818.1	probable DNA helicase MCMB isoform X2 [Olea europaea var. sylvestris]	4.77e-01	27.3%	27.3%	42.00%
OeIBR3-GEMLIK	XP_022856292.1	probable acyl-CoA dehydrogenase IBR3 isoform X1 [Olea europaea var. sylvestris]	3.74e-121	89.3%	89.3%	98.00%
OeIBR3-GEMLIK	XP_022856293.1	probable acyl-CoA dehydrogenase IBR3 isoform X2 [Olea europaea var. sylvestris]	6.44e-123	89.8%	89.8%	98.00%
OeIBR3-GEMLIK	XP_022879151.1	uncharacterized protein LOC111396842 [Olea europaea var. sylvestris]	3.83e+00	32.0%	32.0%	21.00%
OeIBR10-DOMAT	XP_022844139.1	enoyl-CoA delta isomerase 2, peroxisomal-like [Olea europaea var. sylvestris]	2.42e-141	84.1%	84.1%	86.80%
OeIBR10-DOMAT	XP_022844141.1	enoyl-CoA delta isomerase 2, peroxisomal-like [Olea europaea var. sylvestris]	3.22e-138	82.3%	82.9%	86.08%
OeIBR10-DOMAT	XP_022869640.1	enoyl-CoA delta isomerase 2, peroxisomal-like, partial [Olea europaea var. sylvestris]	6.12e-58	78.3%	78.8%	43.58%
OeIBR10-DOMAT	XP_022884391.1	enoyl-CoA delta isomerase 1, peroxisomal [Olea europaea var. sylvestris]	5.73e-51	42.9%	43.6%	83.90%
OeIBR10-Gemlik	XP_022844139.1	enoyl-CoA delta isomerase 2, peroxisomal-like [Olea europaea var. sylvestris]	2.26e-141	84.1%	84.7%	85.15%
OeIBR10-Gemlik	XP_022844141.1	enoyl-CoA delta isomerase 2, peroxisomal-like [Olea europaea var. sylvestris]	4.40e-138	82.3%	82.9%	84.44%
OeIBR10-Gemlik	XP_022869640.1	enoyl-CoA delta isomerase 2, peroxisomal-like, partial [Olea europaea var. sylvestris]	5.22e-58	78.3%	78.8%	42.76%
OeIBR10-Gemlik	XP_022884391.1	enoyl-CoA delta isomerase 1, peroxisomal [Olea europaea var. sylvestris]	5.10e-51	42.9%	43.6%	82.30%

Figure 35. Blastn analysis results of obtained sequences

When the *OeIBR3* transcript sequences obtained from easy (Gemlik) and hard (Domat) to root olive cultivars were analyzed comparatively, it was seen that they showed 96.6% similarity to each other. Geneious R8 software was used to translate the related sequences into possible protein sequences, and it was found that these sequences were 98.5% identical (Figure 31).

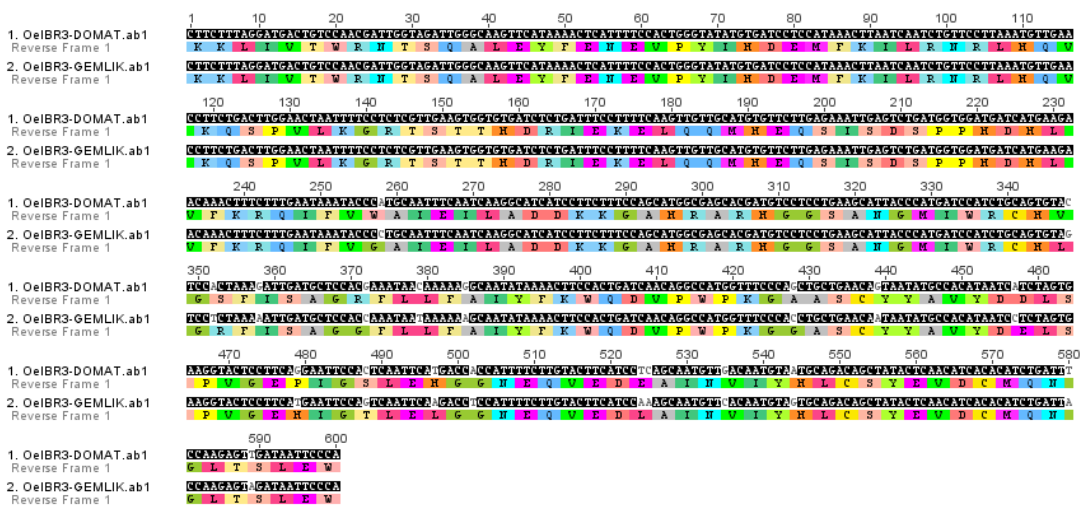


Figure 36. Alignment of *OeIBR3* sequences from easy (Gemlik) and hard (Domat) to root olive cultivars

When the *OeIBR10* transcript sequences obtained from easy (Gemlik) and hard (Domat) to root olive cultivars were analyzed comparatively, it was seen that they showed 99.7% similarity to each other. Geneious R8 software was used to translate the related sequences into possible protein sequences, and it was found that these sequences were 99.5% identical (Figure 32).



Figure 37. Alignment of *OeIBR10* sequences from easy (Gemlik) and hard (Domat) to root olive cultivars

When the *OeAOX2* transcript sequences obtained from easy (Gemlik) and hard (Domat) to root olive cultivars were analyzed comparatively, it was seen that they showed 100% similarity to each other. Geneious R8 software was used to translate the related sequences into possible protein sequences, and it was found that these sequences were 100% identical (Figure 33).



Figure 38. Alignment of *OeAOX2* sequences from easy (Gemlik) and hard (Domat) to root olive cultivars

The obtained *OeIBR3* sequences were clustered in the phylogenetic tree with other olive genome *IBR* genes. The species *Dorcoceras hygrometricum*, *Striga asiatica*, *Handroanthus impetiginosus*, *Sesamum indicum*, *Erythranthe guttata*, and *Salvia splendens* are in the closest group to the group with olive sequences (Figure 34).

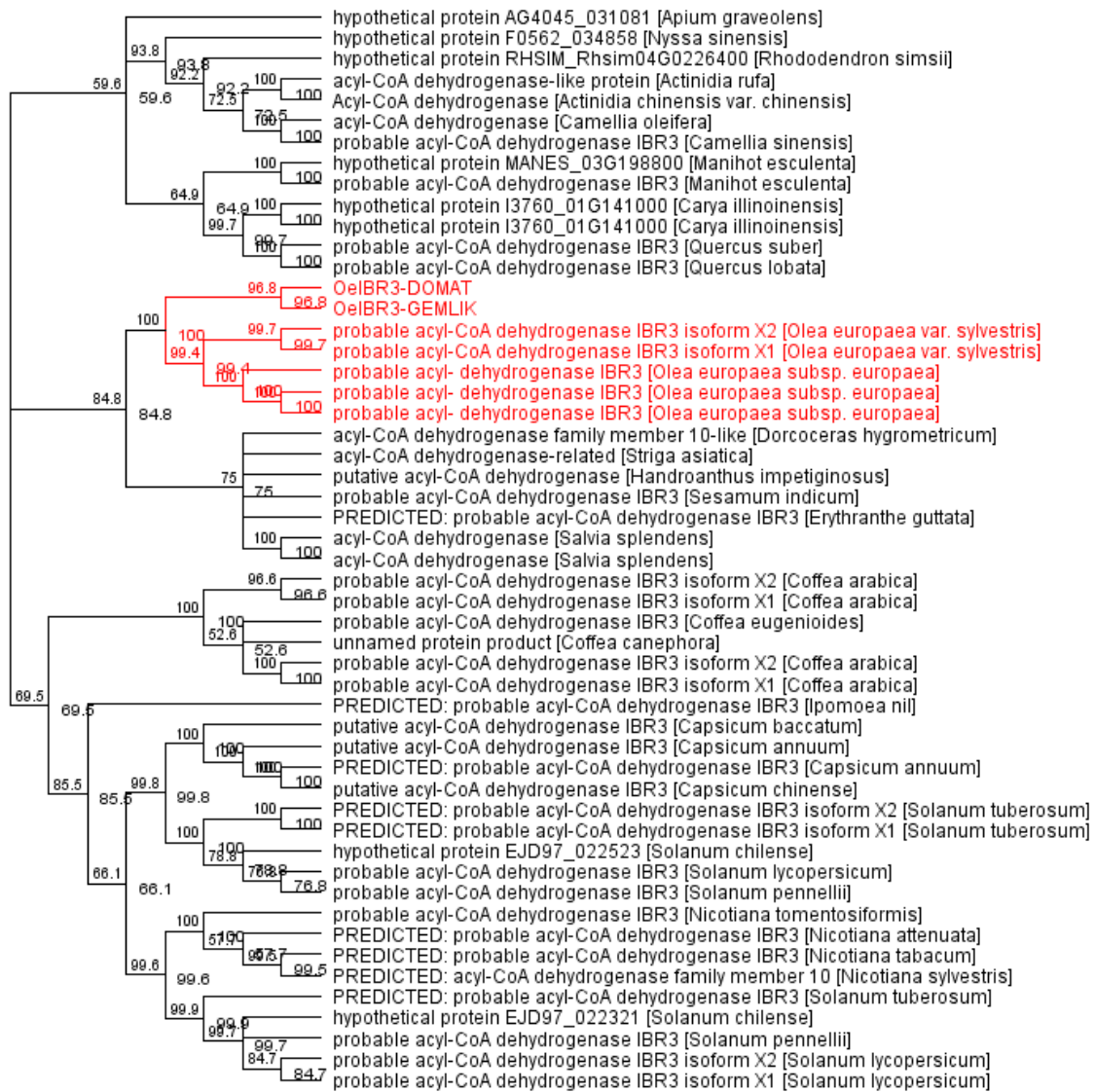


Figure 39. Phylogenetic tree obtained using protein sequences of olive and various plant *IBR3* gene.

In the constructed phylogenetic tree, the *OeIBR10* sequences were clustered with other olive genome *IBR* genes. *Genlisea aurea*, *Dorcoceras hygrometricum*, *Phtheriospermum japonicum*, *Striga asiatica*, *Handroanthus impetiginosus*, *Sesamum indicum*, *erythranthe guttata*, and *Salvia splendens* are among the species that are most closely related to the group with olive sequences (Figure 35).

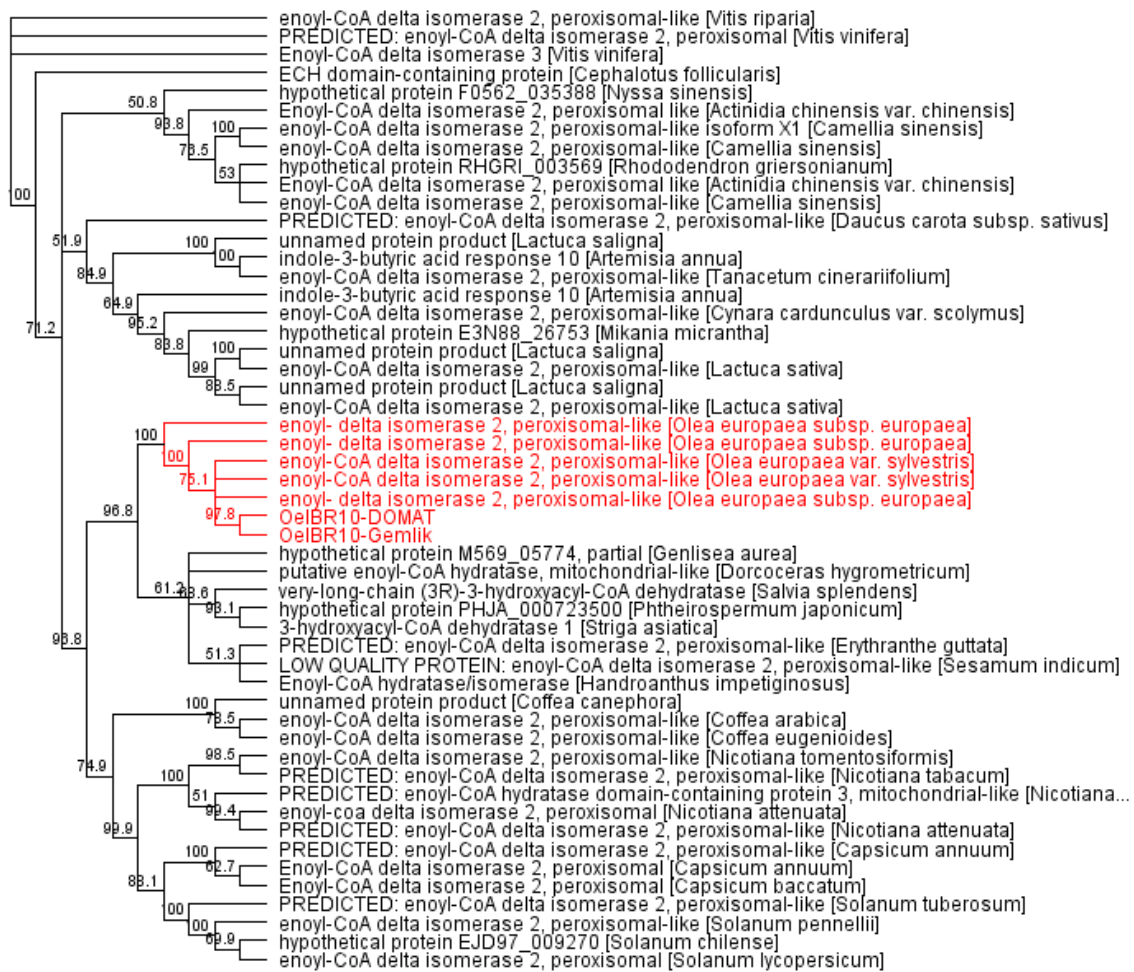


Figure 40. Phylogenetic tree obtained using protein sequences of olive and various plant *IBR10* gene.

In the phylogenetic tree, the acquired *OeAOX2* sequences were grouped with the *AOX2* (Alternative oxidase 2, Ubiquinol oxidase 2) genes from the other olive genome (Figure 36).

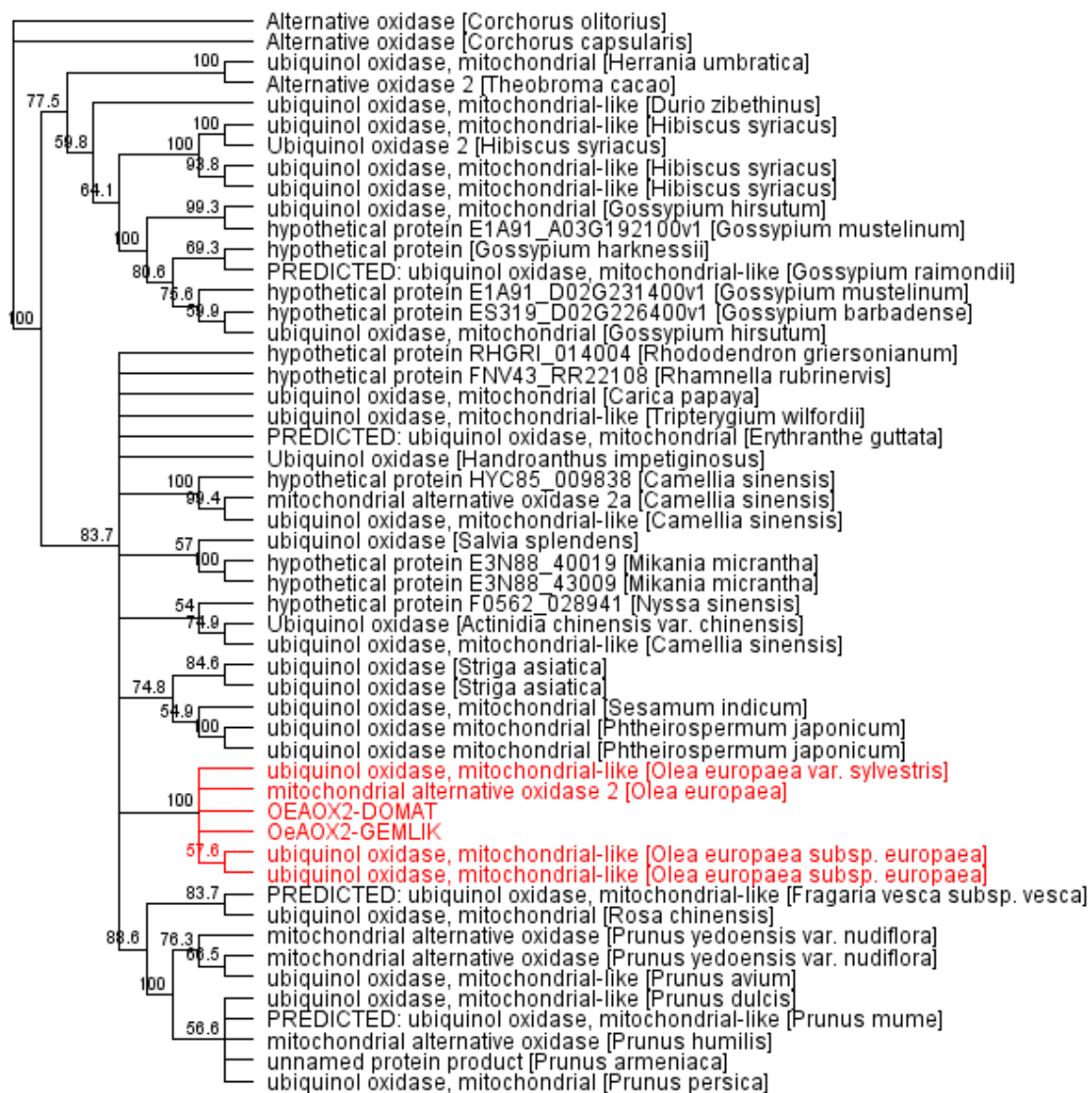


Figure 41. Phylogenetic tree obtained using protein sequences of olive and various plant AOX2 genes.

#### 4.4. Discussion

In this study, the structures of the genes AOX2, IBR, and PtAIL1 were determined in the olive genome and gene expression levels were analyzed in easy-to-root (Gemlik) and hard-to-root (Domat) olive cultivars, which are treated with auxins hormones like IBA, IBA+NAA, and NAA. These genes are known to play a role in adventitious rooting processes in some model plants. Using PCR, the nucleotide sequences of these genes' transcripts were amplified, allowing phylogenetic trees to be constructed.

The adventitious rooting process after IBA treatment on olive cuttings is divided into 3 stages; induction, initiation and expression stages (Pacurar et al., 2014). In the thesis, *Olea europaea* L. cv. gene expression studies of the genes were carried out from the tissues that collected from the treated with IBA, IBA+NAA and NAA Gemlik and Domat cuttings. Tissues were collected in the days leading up to the three stages of adventitious rooting in olives which are 24h, 7th day and 15th day.

Molecular characterization of AOX2 and AOX1 genes in olives was performed gene expression was determined under IBA treatment, and gene expression levels were compared in hard-to-rooted and easy-to-rooted Leccino x Dolce Agogia hybrids (Hedayati et al., 2015b). In this thesis, the expression of the AOX2 gene was investigated in 2 local cultivars. When the gene expression results were examined, it was determined that there was higher expression level after auxin treatment in the easy-to-root olive variety than the hard-to-root olive variety (Figure 39). A previous study had seen similar results in easy and hard rooting olive cultivars from a cross of Leccino x dolce Agogia.



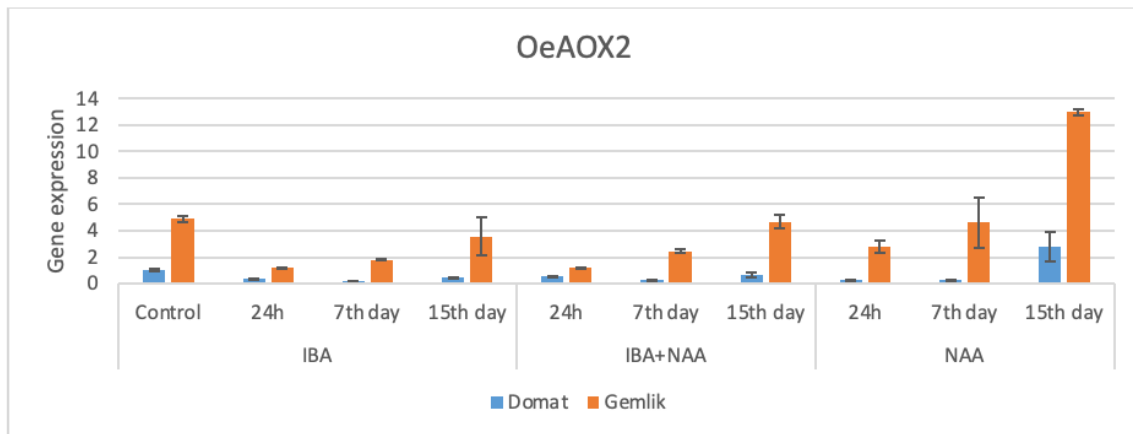


Figure 42. Gene expression results of *OeAOX2* in all treatment groups. (Error bars represent standard error)

High auxin levels can restrict rooting in the subsequent initial stage even while they stimulate rooted in the induction stage (Porfirio et al., 2016). Furthermore, research on several tree species has demonstrated the significance of IBA-IAA conversion (Alvarez et al., 2008; Kreiser et al., 2016b; Krieken et al., 2017). One of the genes believed to be involved in the conversion of IBA into IAA is the *OeIBR3* gene (Frick & Strader, 2018). Similar outcomes were found in the gene expression analyses for the cultivars Gemlik and Domat. According to the expression studies, all auxin treatments were found to be lower in the initial 24 hours compared to the control groups, and in the following days, Domat variety was found to be higher than Gemlik variety.

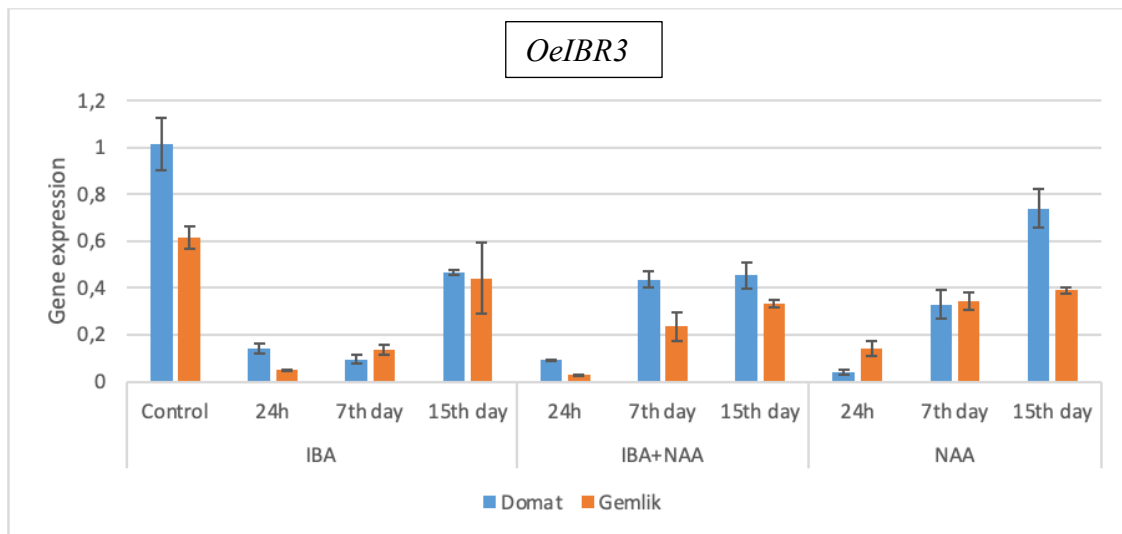


Figure 43. Gene expression results of *OeIBR3* in all treatment groups. (Error bars represent standard error).

When the gene expression results of *OeIBR10*, another gene thought to be responsible for the conversion of IBA to IAA (Zolman et al., 2008a), were examined, it was observed that there were similar results in the control groups, but there was an increase in gene expression in both cultivars after IBA treatment, but it did not continue in the following days. When examined in the groups treated with NAA, which is a synthetic auxin, gene expression were decreased in both cultivars and even in some samples of the Gemlik cultivar completely stopped (Figure 41). These results indicate that NAA treatment suppresses the expression of this gene.

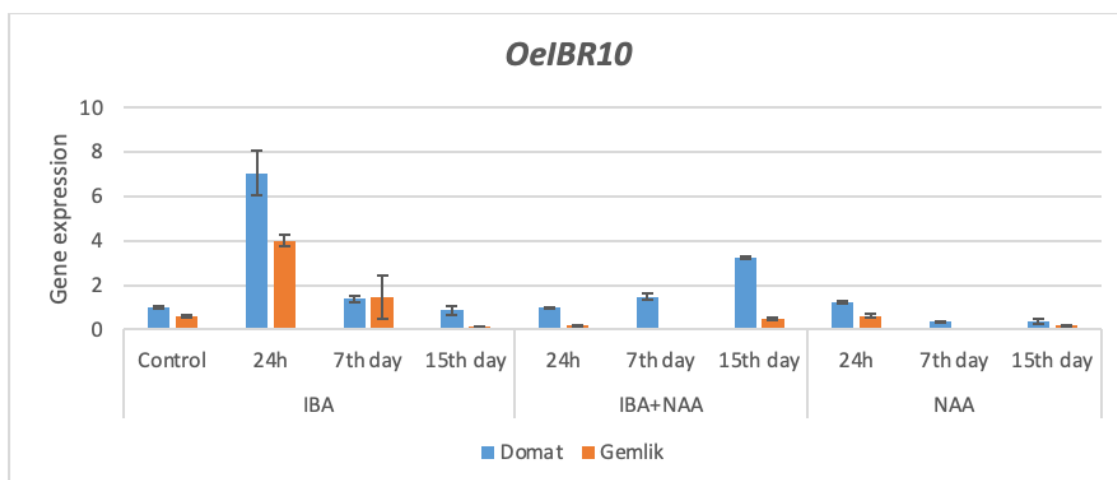


Figure 44. Gene expression results of *OeIBR10* in all treatment groups. (Error bars represent standard error).

An increase in gene expression level was seen in both varieties in the first 24 hours in the groups that were treated only with IBA and two auxin hormones—IBA and NAA—were treated together, according to the gene expression results of *OeIBR1*, another gene responsible for the conversion of IBA into IAA (Zolman et al., 2008a). In the days that followed, the IBA-treated group's gene expression level reduced in the Gemlik cultivar whereas it continued to increase in the Domat cultivar. Gene expression in both cultivars decreased in the group receiving both IBA and NAA at the same time. Gene expression is almost absent in both cultivars in the NAA-treated group (Figure 42). These findings demonstrate that NAA treatment inhibits *IBR1* gene expression.

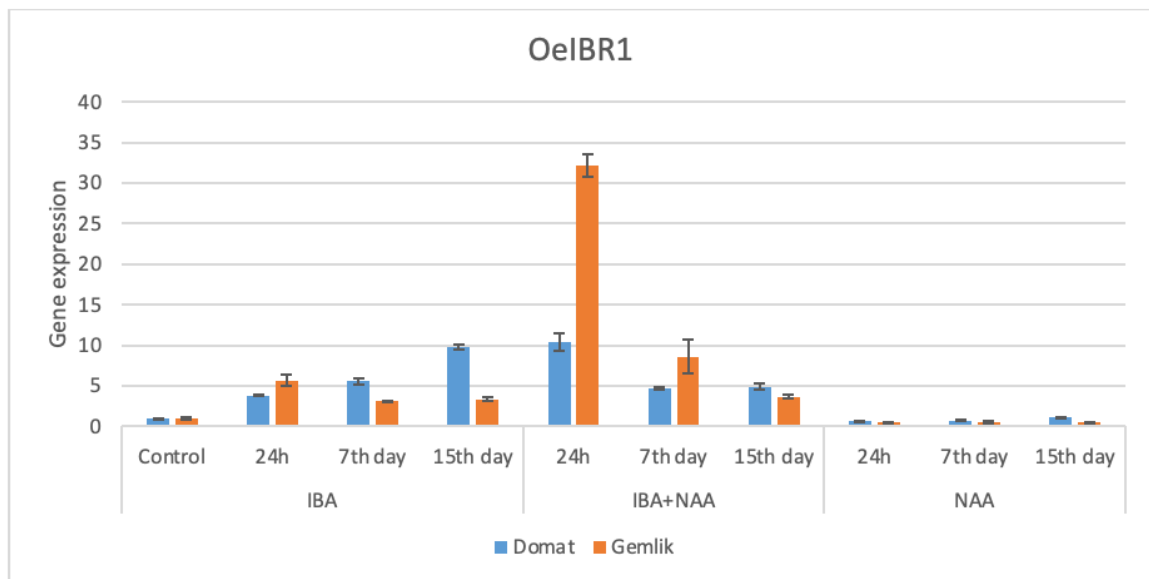


Figure 45. Gene expression results of OeIBR1 in all treatment groups. (Error bars represent standard error).

When the gene expression data for the AP2 transcription factor family member OePtAIL1, which has been related to adventitious rooting, were investigated, it was found that the expression levels in the control groups of both cultivars were similar. IBA-treated Gemlik cuttings' expression was seen to remain unchanged, however expression in Domat varieties dropped. The expression of this gene decreased or even nearly stopped in cultivars of Gemlik and Domat that had been treated with NAA. When the PtAIL1 gene's expression increased (overexpressed), adventitious rooting was seen to rise, whereas adventitious rooting was seen decrease when the gene was silenced using RNAi technology (Rigal et al., 2012b).

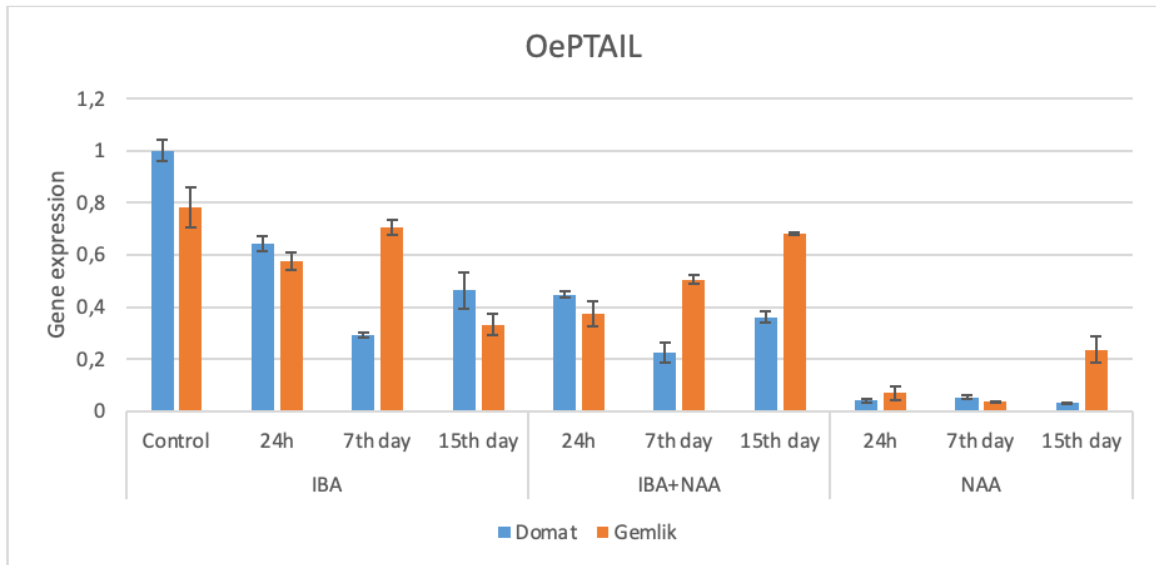


Figure 46. Gene expression results of OePTAIL in all treatment groups. (Error bars represent standard error).

## CHAPTER 5

### CONCLUSION

The objective of this study is to identify the AOX2, PTAIL1, and IBR genes proven to play roles in the adventitious rooting in the two different local olive varieties and to examine the expression levels of these genes on the different kinds of auxin-treated cuttings. With this aim, the olive cuttings of Gemlik and Domat cultivars were treated with IBA, IBA-NAA, and NAA, and then samples were collected for the 3 stages of adventitious rooting and gene expression analysis were performed. Moreover, the sequences of olive IBR genes (OeIBR1, OeIBR3, and IBR10) and OePTAIL1, which is a transcription factor, were determined for the first time.

The conversion of IBA to IAA is one of the variables that determine AR. Although auxins such as IAA stimulate rooting in these processes, the high auxin levels in the early stages suppress rooting. Therefore, the genes IBR1, IBR3, and IBR10, which are assumed to play a role in converting IBA to IAA, were investigated in this project. Our project's findings show that applying NAA decreases gene expression. According to research on IBR genes in Arabidopsis gene expression databases, biotic and abiotic stress treatments have varied effects on the expression of the IBR1, IBR3, and IBR10 genes (Frick & Strader, 2018). These findings show that different IBR genes can replace others depending on the environment (temperature, humidity, UV light, or physical injury).

As a result of PCR and sequence analysis studies, transcript sequences of OeAOX2, OeIBR3 and OeIBR10 genes of both cultivars were obtained. The obtained consensus sequences were confirmed by blast analysis and a phylogenetic tree was drawn. OeIBR3, IBR10 and OeAOX2 sequences obtained by the study were grouped with IBR genes belonging to other olive genome in the phylogenetic tree. The closest group to the group with olive sequences includes species such as *Dorcoceras hygrometricum*, *Striga asiatica*, *Handroanthus impetiginosus*, *Sesamum indicum*, *erythranthe guttata* and *Salvia splendens*.

AR formation has an important role in vegetative propagation and some of the olive varieties are difficult to propagate vegetatively. In this study, gene expression and transcript sequence analyses of genes that affect adventitious root formation were performed after two different auxin treatments on the two local olive varieties, which are easy-to-root (Gemlik)

and hard-to-root (Domat). Performing functional studies on the genes examined in the study will also reveal the roles of the relevant genes in vegetative reproduction by cuttings.



## REFERENCES

- Agulló-Antón, M. Á., Ferrández-Ayela, A., Fernández-García, N., Nicolás, C., Albacete, A., Pérez-Alfocea, F., Sánchez-Bravo, J., Pérez-Pérez, J. M., & Acosta, M. (2014). 'Early steps of adventitious rooting: Morphology, hormonal profiling and carbohydrate turnover in carnation stem cuttings.' *Physiologia Plantarum*, 150(3), 446–462. <https://doi.org/10.1111/ppl.12114>
- Ali, A., & Abbasi, N. (2009). 'Effect of different concentrations of auxins on In vitro rooting of olive cultivar "Moraiolo."' In *Article in Pakistan Journal of Botany*. <https://www.researchgate.net/publication/266093180>
- Arnholdt-Schmitt, B., Costa, J. H., & de Melo, D. F. (2006). 'AOX - a functional marker for efficient cell reprogramming under stress?' *Trends in Plant Science*, 11(6), 281–287. <https://doi.org/10.1016/j.tplants.2006.05.001>
- Ayoub, S. J., & Qrunfleh, M. M. (2006). 'Anatomical Aspects of Rooting "Nabali" and "Raseei" Olive Semi-Hardwood Stem Cuttings.' In *Jordan Journal of Agricultural Sciences* (Vol. 2, Issue 1).
- Aziz Kurd, A., Khan, S., Hussain Shah, B., & Ahmed Khetran, M. (2010). 'EFFECT OF INDOLE BUTYRIC ACID (IBA) ON ROOTING OF OLIVE STEM CUTTINGS.' In *Pakistan J. Agric. Res* (Vol. 23, Issue 4).
- Botanicae, N., Agrobotanici, H., Pop, T. I., Pamfil, D., & Bellini, C. (n.d.). '*Auxin Control in the Formation of Adventitious Roots*.' [www.notulaebotanicae.ro](http://www.notulaebotanicae.ro)
- da Costa, C. T., de Almeida, M. R., Ruedell, C. M., Schwambach, J., Maraschin, F. S., & Fett-Neto, A. G. (2013). 'When stress and development go hand in hand: Main hormonal controls of adventitious rooting in cuttings.' In *Frontiers in Plant Science* (Vol. 4, Issue MAY). Frontiers Research Foundation. <https://doi.org/10.3389/fpls.2013.00133>
- De Klerk, G.-J., Keppel, M., Brugge, J. Ter, & Meekes, H. (1995). 'Timing of the phases in adventitious root formation in apple microcuttings.' In *Journal of Experimental Botany* (Vol. 46, Issue 289). <http://jxb.oxfordjournals.org/>
- Denaxa, N. K., Vemmos, S. N., & Roussos, P. A. (n.d.). '*The Effect of IBA, NAA and Carbohydrates on Rooting Capacity of Leafy Cuttings in Three Olive Cultivars (Olea europaea L.)*.'



- Druege, U., Franken, P., & Hajirezaei, M. R. (2016). 'Plant hormone homeostasis, signaling, and function during adventitious root formation in cuttings.' In *Frontiers in Plant Science* (Vol. 7, Issue MAR2016). Frontiers Media S.A. <https://doi.org/10.3389/fpls.2016.00381>
- Druege, U., Hilo, A., Pérez-Pérez, J. M., Klopotek, Y., Acosta, M., Shahinnia, F., Zerche, S., Franken, P., & Hajirezaei, M. R. (2019). 'Molecular and physiological control of adventitious rooting in cuttings: Phytohormone action meets resource allocation.' *Annals of Botany*, 123(6), 929–949. <https://doi.org/10.1093/aob/mcy234>
- Edgar, R. C. (2004). MUSCLE: 'Multiple sequence alignment with high accuracy and high throughput.' *Nucleic Acids Research*, 32(5), 1792–1797. <https://doi.org/10.1093/nar/gkh340>
- Epstein, E., & Lavee, S. (1984). 'Conversion of Indole-3-butyric Acid to Indole-3-acetic Acid by Cuttings of Grapevine (*Vitis vinifera*) and Olive (*Olea europea*) 1.' In *Plant & Cell Physiol* (Vol. 25, Issue 5).
- Fernandes Serrano, J., & Serrano Amaral, M. E. (n.d.). 'Effect of Different Hormone Treatments on Rooting of *Olea europaea* cv. *Galega vulgar* Cuttings.'
- Frick, E. M., & Strader, L. C. (2018). 'Roles for IBA-derived auxin in plant development.' In *Journal of Experimental Botany* (Vol. 69, Issue 2, pp. 169–177). Oxford University Press. <https://doi.org/10.1093/jxb/erx298>
- Haq, I. U., Ahmad, T., Hafiz, A., & Abbasi, N. A. (2009). 'INFLUENCE OF MICROCUTTING SIZES AND IBA CONCENTRATIONS ON IN VITRO ROOTING OF OLIVE cv. "DOLCE AGOGIA."' In *Pak. J. Bot* (Vol. 41, Issue 3).
- Hedayati, V., Mousavi, A., Razavi, K., Cultrera, N., Alagna, F., Mariotti, R., Hosseini-Mazinani, M., & Baldoni, L. (2015a). 'Polymorphisms in the AOX2 gene are associated with the rooting ability of olive cuttings.' *Plant Cell Reports*, 34(7), 1151–1164. <https://doi.org/10.1007/s00299-015-1774-0>
- Hedayati, V., Mousavi, A., Razavi, K., Cultrera, N., Alagna, F., Mariotti, R., Hosseini-Mazinani, M., & Baldoni, L. (2015b). 'Polymorphisms in the AOX2 gene are associated with the rooting ability of olive cuttings.' *Plant Cell Reports*, 34(7), 1151–1164. <https://doi.org/10.1007/s00299-015-1774-0>
- Hürkan, K., Sezer, F., Özbilen, A., & Taşkın, K. M. (2018). 'Identification of reference genes for real-time quantitative polymerase chain reaction based gene expression studies on

- various Olive (*Olea europaea* L.) tissues.’ *Journal of Horticultural Science and Biotechnology*, 93(6), 644–651. <https://doi.org/10.1080/14620316.2018.1427005>
- İsfendiyaroğlu, M. (2016). ‘ROOT REGENERATION IN CUTTINGS OF *OLEA EUROPAEA* L.: EFFECT OF AUXIN AND AUXIN SENSITIVE PHASE’ (Vol. 45, Issue 2).
- İsfendiyaroğlu, M., & Özeker, E. (2008). ‘ROOTING OF *OLEA EUROPAEA* “DOMAT” CUTTINGS BY AUXIN AND SALICYLIC ACID TREATMENTS.’ In *Pak. J. Bot* (Vol. 40, Issue 3).
- İljazi, R., Ismaili, H., & Salillari, A. (2014). International Journal of Green and Herbal Chemistry Section B: Herbal Chemistry ‘Study on some doses of IBA concentration in the rooting of olive (*Olea europaea* L.).’ In *Section B* (Vol. 3, Issue 3). [www.ijghc.com](http://www.ijghc.com)
- Itoh, J. I., Nonomura, K. I., Ikeda, K., Yamaki, S., Inukai, Y., Yamagishi, H., Kitano, H., & Nagato, Y. (2005). ‘Rice plant development: From zygote to spikelet.’ In *Plant and Cell Physiology* (Vol. 46, Issue 1, pp. 23–47). <https://doi.org/10.1093/pcp/pci501>
- Kearse, M., Moir, R., Wilson, A., Stones-Havas, S., Cheung, M., Sturrock, S., Buxton, S., Cooper, A., Markowitz, S., Duran, C., Thierer, T., Ashton, B., Meintjes, P., & Drummond, A. (2012). ‘Geneious Basic: An integrated and extendable desktop software platform for the organization and analysis of sequence data.’ *Bioinformatics*, 28(12), 1647–1649. <https://doi.org/10.1093/bioinformatics/bts199>
- Korasick, D. A., Enders, T. A., & Strader, L. C. (2013). ‘Auxin biosynthesis and storage forms.’ In *Journal of Experimental Botany* (Vol. 64, Issue 9, pp. 2541–2555). <https://doi.org/10.1093/jxb/ert080>
- Kreiser, M., Giblin, C., Murphy, R., Fiesel, P., Braun, L., Johnson, G., Wyse, D., & Cohen, J. D. (2016). ‘Conversion of Indole-3-Butyric Acid to Indole-3-Acetic Acid in Shoot Tissue of Hazelnut (*Corylus*) and Elm (*Ulmus*).’ *Journal of Plant Growth Regulation*, 35(3), 710–721. <https://doi.org/10.1007/s00344-016-9574-5>
- Lakehal, A., & Bellini, C. (2019). ‘Control of adventitious root formation: insights into synergistic and antagonistic hormonal interactions.’ *Physiologia Plantarum*, 165(1), 90–100. <https://doi.org/10.1111/ppl.12823>
- Legué, V., Rigal, A., & Bhalerao, R. P. (2014). ‘Adventitious root formation in tree species: Involvement of transcription factors.’ In *Physiologia Plantarum* (Vol. 151, Issue 2, pp. 192–198). Blackwell Publishing Ltd. <https://doi.org/10.1111/ppl.12197>

- Li, S. W., Xue, L., Xu, S., Feng, H., & An, L. (2009). 'Mediators, genes and signaling in adventitious rooting.' *Botanical Review*, 75(2), 230–247. <https://doi.org/10.1007/s12229-009-9029-9>
- Noceda, C., Peixe, A., & Arnholdt-Schmitt, B. (2022). 'Selection of Reference Genes for Transcription Studies Considering Co-Regulation and Average Transcriptional Stability: Case Study on Adventitious Root Induction in Olive (*Olea europaea* L.)' Microshoots. *Agronomy*, 12(12). <https://doi.org/10.3390/agronomy12123201>
- Olive Propagation Manual*. (n.d.).
- Pacurar, D. I., Perrone, I., & Bellini, C. (2014). 'Auxin is a central player in the hormone cross-talks that control adventitious rooting.' In *Physiologia Plantarum* (Vol. 151, Issue 1, pp. 83–96). Blackwell Publishing Ltd. <https://doi.org/10.1111/ppl.12171>
- Porfírio, S., Calado, M. L., Noceda, C., Cabrita, M. J., da Silva, M. G., Azadi, P., & Peixe, A. (2016). 'Tracking biochemical changes during adventitious root formation in olive (*Olea europaea* L.)' *Scientia Horticulturae*, 204, 41–53. <https://doi.org/10.1016/j.scienta.2016.03.029>
- Porfírio, S., Gomes da Silva, M. D. R., Cabrita, M. J., Azadi, P., & Peixe, A. (2016). 'Reviewing current knowledge on olive (*Olea europaea* L.) adventitious root formation.' In *Scientia Horticulturae* (Vol. 198, pp. 207–226). Elsevier B.V. <https://doi.org/10.1016/j.scienta.2015.11.034>
- Rigal, A., Yordanov, Y. S., Perrone, I., Karlberg, A., Tisserant, E., Bellini, C., Busov, V. B., Martin, F., Kohler, A., Bhalerao, R., & Legué, V. (2012a). 'The AINTEGUMENTA LIKE1 homeotic transcription factor PtAIL1 controls the formation of adventitious root primordia in poplar.' *Plant Physiology*, 160(4), 1996–2006. <https://doi.org/10.1104/pp.112.204453>
- Santos MacEdo, E., Cardoso, H. G., Hernández, A., Peixe, A. A., Polidoros, A., Ferreira, A., Cordeiro, A., & Arnholdt-Schmitt, B. (2009). 'Physiologic responses and gene diversity indicate olive alternative oxidase as a potential source for markers involved in efficient adventitious root induction.' *Physiologia Plantarum*, 137(4), 532–552. <https://doi.org/10.1111/j.1399-3054.2009.01302.x>
- Santos Macedo, E., Sircar, D., Cardoso, H. G., Peixe, A., & Arnholdt-Schmitt, B. (2012). 'Involvement of alternative oxidase (AOX) in adventitious rooting of *Olea europaea* L. microshoots is linked to adaptive phenylpropanoid and lignin metabolism.' *Plant Cell Reports*, 31(9), 1581–1590. <https://doi.org/10.1007/s00299-012-1272-6>

- Steffens, B., & Rasmussen, A. (2016). 'The physiology of adventitious roots.' *Plant physiology*, 170(2), 603-617.
- Unver, T., Wu, Z., Sterck, L., Turktas, M., Lohaus, R., Li, Z., Yang, M., He, L., Deng, T., Escalante, F. J., Llorens, C., Roig, F. J., Parmaksiz, I., Dundar, E., Xie, F., Zhang, B., Ipek, A., Uranbey, S., Erayman, M., ... Van de Peer, Y. (2017). 'Genome of wild olive and the evolution of oil biosynthesis.' *Proceedings of the National Academy of Sciences of the United States of America*, 114(44), E9413–E9422. <https://doi.org/10.1073/pnas.1708621114>
- Van Der Krieken, W. M., Breteler, H., & Visser, M. H. M. (1992). 'The Effect of the Conversion of Indolebutyric Acid into Indoleacetic Acid on Root Formation on Microcuttings of Malus.' In *Plant CellPhysiol* (Vol. 33, Issue 6).
- Velada, I., Grzebelus, D., Lousa, D., Soares, C. M., Macedo, E. S., Peixe, A., Arnholdt-Schmitt, B., & Cardoso, H. G. (2018). 'AOX1-subfamily gene members in olea europaea cv. "Galega vulgar"—gene characterization and expression of transcripts during IBA-induced in vitro adventitious rooting.' *International Journal of Molecular Sciences*, 19(2). <https://doi.org/10.3390/ijms19020597>
- Vidoz, M. L., Loreti, E., Mensuali, A., Alpi, A., & Perata, P. (2010). 'Hormonal interplay during adventitious root formation in flooded tomato plants.' *Plant Journal*, 63(4), 551–562. <https://doi.org/10.1111/j.1365-313X.2010.04262.x>
- Went, F. W., & Thimann, K. V. (1937). 'Phytohormones.' *Phytohormones*.
- Zolman, B. K., Martinez, N., Millius, A., Adham, A. R., & Bartel, B. (2008a). 'Identification and characterization of Arabidopsis indole-3-butyric acid response mutants defective in novel peroxisomal enzymes.' *Genetics*, 180(1), 237–251. <https://doi.org/10.1534/genetics.108.090399>
- Zolman, B. K., Martinez, N., Millius, A., Adham, A. R., & Bartel, B. (2008b). 'Identification and characterization of Arabidopsis indole-3-butyric acid response mutants defective in novel peroxisomal enzymes.' *Genetics*, 180(1), 237–251. <https://doi.org/10.1534/genetics.108.090399>
- Zolman, B. K., Nyberg, M., & Bartel, B. (2007). 'IBR3, a novel peroxisomal acyl-CoA dehydrogenase-like protein required for indole-3-butyric acid response.' *Plant Molecular Biology*, 64(1–2), 59–72. <https://doi.org/10.1007/s11103-007-9134-2>

## APPENDIX

<b>Homogeneous Subsets</b>			
RGE			
		N	Subset for alpha = 0.05
Time			1
Tukey HSD <sup>a,b</sup>	7th day	4	,99061337
	24h	11	1,92345479
	15th day	4	2,00542165
	Sig.		,704

Means for groups in homogeneous subsets are displayed.

a. Uses Harmonic Mean Sample Size = 5,077.

b. The group sizes are unequal. The harmonic mean of the group sizes is used. Type I error levels are not guaranteed.

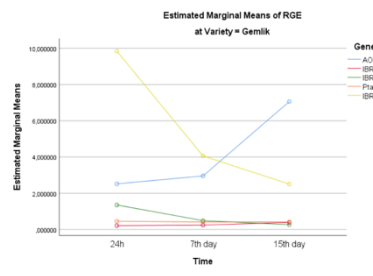
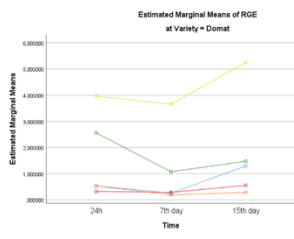
Appendix 1: Results of Tukey HSD homogeneity test.

Dependent Variable: RGE

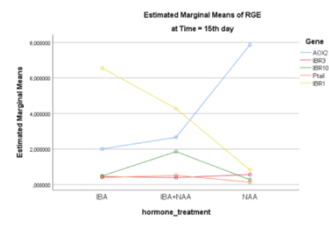
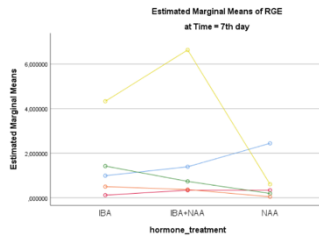
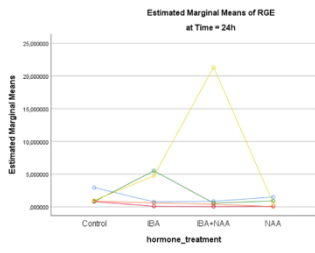
Source	Type III Sum of Squares	df	Mean Square	F	Sig.
Corrected Model	4140,160 <sup>a</sup>	99	41,820	44,002	,000
Intercept	680,504	1	680,504	716,017	,000
Gene	503,293	4	125,823	132,390	,000
hormone_treatment	132,796	3	44,265	46,575	,000
Variety	24,955	1	24,955	26,257	,000
Time	47,536	2	23,768	25,008	,000
Gene * hormone_treatment	976,049	12	81,337	85,582	,000
Gene * Variety	129,691	4	32,423	34,115	,000
Gene * Time	281,249	8	35,156	36,991	,000
hormone_treatment * Variety	43,439	3	14,480	15,235	,000
hormone_treatment * Time	97,800	4	24,450	25,726	,000
Variety * Time	13,486	2	6,743	7,095	,001
Gene * hormone_treatment * Variety	298,141	12	24,845	26,142	,000
Gene * hormone_treatment * Time	599,832	16	37,489	39,446	,000
Gene * Variety * Time	226,130	8	28,266	29,741	,000
hormone_treatment * Variety * Time	52,203	4	13,051	13,732	,000
Gene * hormone_treatment * Variety * Time	149,348	16	9,334	9,821	,000
Error	133,056	140	,950		
Total	5212,701	240			
Corrected Total	4273,216	239			

Appendix 2: Results of nested ANOVA.

Time \* Gene \* Variety



hormone\_treatment \* Gene \* Time



### Appendix 3: Results of nested ANOVA graph